A STUDY ON THE GEOACOUSTIC PROPERTIES OF MARINE SEDIMENTS

Thesis submitted

in partial fulfilment of the requirements

for the degree of Doctor of Philosophy

in Physical Oceanography under the

Faculty of Marine Sciences

by

PRADEEP KUMAR. T

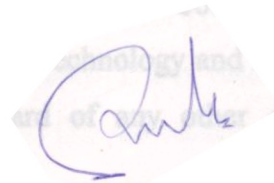**Naval Physical and Oceanographic Laboratory**
Cochin 682 021

to

Cochin University of Science and Technology
Cochin 682 022

December 1999

DECLARATION

I hereby declare that the thesis entitled "A Study on the Geoacoustic Properties of Marine Sediments" has not previously formed the basis for the award of any degree, diploma or associateship in any University.

Cochin –21
December 1999

PRADEEP KUMAR. T
Scientist 'D',
Naval Physical and Oceanographic Laboratory.

CERTIFICATE

I hereby declare that the thesis entitled "A Study on the Geoacoustic Properties of Marine Sediments" is an authentic record of research work carried out by Mr. Pradeep Kumar. T under my supervision and guidance in the Naval Physical and Oceanographic Laboratory, Cochin for the Ph.D degree of Cochin University of Science and Technology and no part of it has previously formed the basis for the award of any other degree in any university.

Cochin
December 1999

Dr. Basil Mathew
(Research Supervisor)

ACKNOWLEDGEMENTS

CONTENTS

PREFACE

Seabed plays an important role in underwater acoustics, as most of the sound transmission takes place through it, especially in shallow waters and in many cases in deepwater as well. As the bottom is more variable in its acoustic properties, inasmuch as it may vary in composition from hard rock to soft mud. The seabed has many of the effects on sound propagation, as does the sea surface. It reflects, refracts and scatters sound and the bottom interacting processes are more complex compared to those at the sea surface. Proper understanding of these processes is possible only by systematic study of the geoacoustic properties of sediments.

In recent years, marine geoacoustics has become a research area of intensely increasing interest. The research area can be divided into two basic fields: research-using acoustics to probe the ocean bottom and research aimed at determining how the ocean bottom affects sound propagation in the ocean. The phenomenon of sound transmission through marine sediments is of extreme interest to researchers in both fields. The geoacoustic properties of the seafloor, compressional and shear wave speeds, its attenuation, together with the knowledge of the material bulk density and its variation as a function of depth are the main parameters needed to study the problems in underwater acoustics.

The most important physical properties of sediments that influence sound propagation are mean grain size, porosity, saturated bulk density and mineral grain density. These properties differ from environment to environment, as they are dependent on depositional characteristics of the sediments and mineral constituents in the sample. Detailed seafloor surveys are becoming increasingly important for the siting of offshore structures. Siting of platforms, cables and pipelines requires information on sediment physical properties. These informations on sediment physical properties are also useful in studies related to ocean engineering and structural geology.

A considerable amount of work has been carried out on the geological, biological and chemical aspects of the sediments of the Indian Ocean. A review on the studies on physical and geoacoustic properties of sediments indicates that few information is available on the physical and acoustical properties of sediments from Pacific and Atlantic oceans while practically no study exist for the Indian Ocean. Hence, a study on the geoacoustic properties of marine sediments is undertaken.

Seasonal variability of both the wind and the currents is much stronger in the Arabian Sea than in Bay of Bengal and the summer peak is stronger than the winter peak. In certain parts of the Indian Ocean, temperature variations can penetrate to depths far below the thermocline because of seasonal variability of warm and cold currents, as well as downwelling and upwelling. The upwelling and sinking processes in the Arabian Sea is much stronger than in Bay of Bengal. The heat flow across the water/sediment interface could result in the variation of the physical and geoacoustic properties of sediments. The present study is restricted to the eastern Arabian Sea and the seasonal variations in geoacoustic properties of sediments at selected locations are also included in the study.

The thesis is divided into seven chapters with further subdivisions. The first chapter reviews the present knowledge on physical and geoacoustic properties of sediments, their measurements, its variations, empirical relationships and a brief description about the objective of the present study.

The second chapter contains a review of theoretical studies and the basis of the theories opted for prediction of sound speed and attenuation in sediments. The effect of variation of temperature in bottom water on sound speed and attenuation of sediments are also discussed.

Third chapter discusses the seasonal variability of temperature, salinity, density and sound speed for selected areas off the west coast of India with emphasis on the characteristics of water at the sea bottom interface.

The fourth Chapter deals with the details of the development of instrumentation and calibration methods for measuring sound speed of compressional wave of marine sediments in the laboratory.

The fifth chapter contains details of the predicted compressional wave sound speed and attenuation of sediments along with comparison between the predicted and measured sound speeds in sediments. Regression relationships among physical and geoacoustic properties of sediments are developed.

The sixth chapter deals with the details of seasonal variation of sound speed and attenuation of marine sediments based on the oceanographic conditions of the water at the bottom. The results of the laboratory measurement of sound speed at different temperatures are also given.

The seventh, and the last, chapter summarises all the important results and conclusions drawn from the present study with future scope of the work.

LIST OF FIGURES

CHAPTER 1

INTRODUCTION

The use of sound waves in water for the transmission of intelligence has been of interest to man to a variety of purposes for his use and exploration of the seas. Sound is used in military and rescue operations and a number of commercial activities like dredging, fisheries and navigation. Knowledge of geoacoustic and geotechnical parameters of the seafloor is important in many engineering applications, which include evaluation of offshore foundation sites for drilling towers and other structures. In the field of ocean exploration and exploitation of georesources, knowledge of physical properties of sediments is necessary to estimate geotechnical properties of the sea bottom. Seabed sediment is a highly complex material, having properties that are site specific and time specific due to the action of natural weathering forces. Site specific geotechnical studies are essential for offshore activities and valuable information can be obtained from the correlation between geophysical and geotechnical properties

In most shallow-water environments and in many deep-water cases, as well, the seabed is a dominant factor controlling under water acoustic propagation. In shallow-waters seafloor sediments are generally quite inhomogeneous both vertically and laterally, and can vary from very soft mud to compact sands over short distances depending on the geological history of the area. The upper several meters of the sedimented seafloor contain the largest gradients in physical and acoustic properties of the sediment-water system. The sea bottom has many of the same effects on sound propagation, as does the sea surface. It reflects and scatters sound and the return of sound from the seabed is vastly more complex than from the sea surface for several reasons. The bottom is more variable in its acoustic properties, inasmuch as it may vary in composition from hard rock to soft mud. It is often layered, with a density and sound speed that change gradually or abruptly with depth. Sound can readily enter a sedimentary bottom and be reflected back to the sea by sub-bottom layers, or be refracted back by steep sound speed gradients in sediments. For these reasons the loss of intensity suffered by sound interacting the seabed is less easily predictable than the loss at the sea surface.

1

The propagation of sound in the ocean is inevitably accompanied by fluctuations in the amplitude and phase of an acoustic signal received at large distances from the source. The fluctuations are manifestations not only of changing patterns of interaction with the bottom and surface, particularly important in shallow-water propagation, but also passages of the wave through time-varying inhomogenities in the ocean medium. The variability in acoustic propagation can be considered to arise from variations in the index of refraction, or sound speed, of the medium, which in turn, are induced by a variety of ocean processes, covering a wide range of temporal and spatial scales.

Fluctuations in the water column parameters affect not only the propagation of sound in the water column, but also the manner in which sound interacts with the sea bottom. Less obvious is the fact that these fluctuations can also modify the properties of the sea bottom (Ali, 1993). Yet this is precisely the conclusion of recent investigations by Rajan and Frisk (1992). Using data obtained at different seasons but at the same location in the Gulf of Mexico, Rajan and Frisk investigated the seasonal variation of the sediment compressional wave speed profile due to temperature variability in the water column. It was hypothesized that heat flow from the bottom of the water column into the sediment affects the sediment pore water temperature, thereby influencing the temperature structure, and thus the compressional wave speed, in sediments. Since this heat flux varies with season, the effect on sediment compressional wave speed should also change seasonally. In the shallower depths (<30 m) of the Gulf of Mexico, seasonal fluctuations in the ocean bottom temperature as great as 15°C have been observed. Rajan and Frisk (1991,1992) investigated the heat flux across the water/sediment interface, and using Biot model for the sediments, assessed its effects on the compressional wave speed in sediment layers. They showed that the compressional wave speed varies approximately linearly with pore water temperature, independent of both the porosity and sediment type. Applying an inversion technique to the two data sets from the Gulf of Mexico, the effect of variation in water column temperature on sediment compressional speed was demonstrated. The experimental results indicate that the influence of the water column is felt to substantially greater depths in the sediments than predicted by the theory. As a final point, Rajan and Frisk

(1992) noted that the temperature-induced variations in the bottom compressional speeds can have important effects on the prediction of the pressure field in the water column (especially at higher frequencies), and also on source localization schemes like matched-field processing.

The most important physical properties of sediments that influence sound propagation are mean grain size, porosity, saturated bulk density, and mineral grain density. These properties differ from environment to environment, as they are dependent on depositional characteristics of the sediments and mineral constituents in the sample. The most important geoacoustic parameters that directly govern the effects of acoustic and seismic processes at the seafloor are density, sound speed (compressional wave, shear wave) and attenuation (compressional wave and shear wave) in marine sediments. The variations in the geoacoustic properties as a function of depth are essential inputs to the development of geoacoustic models. A "geoacoustic model" is defined as a model of the sea floor with emphasis on measured, extrapolated, and predicted values of those properties important in underwater acoustics and those aspects of geophysics involving sound transmission (Hamilton, 1980). In general, a geoacoustic model details the true thickness and properties of sediment and rock layers of the sea floor. A complete model includes water mass data, a detailed bathymetric chart, and profiles of the sea floor (to obtain bottom topography).

Until recently, the motivation behind studies of the relationship among acoustic and physical properties of the sediment has been to enable predictions of acoustic characteristics given the more commonly available physical property measurements. Recent engineering and signal processing developments permit measurements of the floor and sub sea floor acoustic impedance from a ship while underway (Bachman, 1985). Now, the interest is developing in the inverse problem. A variety of inverse methods have been proposed in the literature for obtaining these quantities from measurements of the acoustic field in the water column.

One of the most important problems in underwater acoustics is the determination of geoacoustic properties of the ocean bottom. Experimental and

theoretical work has shown that it is possible to study the geoacoustic properties of sediments by remote sensing techniques. Such techniques have been developed using inversion of both acoustic and seismic data (Rajan et al., 1987, 1992; Akal et al., 1992, Null et al., 1996). In deep water bottom interacting rays can be isolated from other elements of the field, such as surface-reflected rays. The bottom reflectivity can then be estimated and the corresponding bottom properties inferred from the data.

Techniques developed for remote sensing of the uppermost sediments (25 to 50 m below the sea floor) utilize broad-band sources (small explosives) and an array or single geophone deployed on the sea floor (Akal et al., 1992). To obtain estimates of the bottom properties as a function of depth, both refracted compressional and shear waves as well as interface waves are analyzed. Inversion of the data is carried out using modified versions of the inversion techniques developed by earthquake seismologists and geophysicists to study dispersed Rayleigh-waves and refracted waves. Chapman et al. (1986) estimated the acoustic parameters of the top-most layer of sediments from the phase-shift information contained in post-critical water bottom reflection arrivals.

1.1. Sound Speed in Sea Water

Measurements of speed of sound in seawater were the subject of the earliest investigations of sound propagation - or calculated using empirical formulae if temperature, salinity, and hydrostatic pressure (or depth) are known. Sound speed in seawater increases with temperature, salinity, and depth. The variation of sound speed with temperature is non-linear. The rate of variation of sound speed at 5°C and 30°C are 4.1 m/s and 2.1 m/s respectively. A variation of salinity by 1 PSU and depth by 100 m lead to a change in sound speed of 1.2 m/s and 1.6 m/s, respectively (Brekhovskikh and Lysanov, 1982).

Empirical relations for sound speed are derived from the analysis of controlled laboratory measurements on water samples. Wilson (1960) published empirical equations of sound speed in seawater as a function of temperature, salinity and pressure. Later improved results were published by Del Grosso and Mader (1972), Del

4

Grosso (1974), and Chen and Millero (1977). The Chen and Millero expression is the international standard for sound speed computations (Fofonoff and Millard, 1984). However, recent travel time measurements in the Pacific Ocean are reported to be inconsistent with travel times predicted from the international standard, but consistent with those predicted from Del Grosso's algorithm (Spiesberger and Metzger, 1991).

In practical applications where hydrographic data are involved, there is an additional requirement of pressure-to-depth conversion using a suitable formula (Leroy, 1968; Fofonoff and Millard, 1984). Leroy (1969) and Medwin (1975) published equations for sound speed as a function of temperature, salinity, and depth. Mackenzie (1981) published a more general nine-term equation valid for depths up to 8000m. This equation, which takes the Del Grosso and Mader equation as the "truth" has a standard error estimate of 0.07 m/s and is accurate enough for practical computations of sound speed in seawater. Sound speed in sea water is given by (Mackenzie, 1981):

$$
\begin{aligned}
C &= 1448.96 + 4.591T - 5.304 \times 10^{-2} T^2 + 2.374 \times 10^{-4} T^3 \\
&+ 1.340(S - 35) + 1.630 \times 10^{-2} D + 1.675 \times 10^{-7} D^2 \\
&- 1.025 \times 10^{-2} T(S - 35) - 7.139 \times 10^{-13} TD^3
\end{aligned}
\tag{1.1}
$$

where C is the sound speed (m/s), T is the temperature (°C), S is the salinity (PSU), and D is the depth (m). In this study Mackenzie's equation for sound speed computations is followed.

Advances in electronics have made possible precise measurements of sound speed in the laboratory by various kinds of methods (Urick, 1982). Sound speed can be measured *in situ* using special instruments-velocimeters that are now commercially available. The error of measurements by modern velocimeters is about 0.1 m/s. The accuracy of calculations by most complete empirical formulae is about the same.

1.2. Ocean Bottom Topography

The sea floor can be divided into three major topological regions: the continental margins, the ocean-basin and the mid-ocean ridge system.

1.2.1. Continental Margins

These include the continental shelf, the continental slope, and the continental rise. Continental shelf is the seaward extension of the landmass, and its outer limit is defined by the shelf edge, or breaks, beyond which there is usually a sharp change in gradient as the continental slope is encountered. The continental rise lies at the base of this slope. In many parts of the world both the continental slope and rise is cut by submarine canyons. These are steep-sided, V-shaped valleys, which are extremely important features from the point of view of the transport of material from the continents to the oceans since they act as conduits for the passage of terrigenous sediment from the shelves to deep-sea regions by processes such as turbidity flows. Trenches are found at the edges of all the major oceans, but are concentrated mainly in the Pacific, where they form an interrupted ring around the edges of some of the ocean basins. The trenches are long (up to ~4500 km in length), narrow (usually <100 km wide) features that form the deepest parts of the oceans and are often associated with island arcs. Both features are related to the tectonic generation of the oceans. The trenches are important in the oceanic sedimentary regime because they can act as traps for material carried down the continental shelf. In the absence of trenches, however, much of the bottom-transported material is carried away from the continental rise into the deep sea.

1.2.2. Ocean–Basin Floor

Ocean-basin floor lies beyond the continental margins. Abyssal plains cover a major part of the deep-sea floor in the Atlantic, Indian and northeast Pacific Ocean. These plains are generally flat, almost feature-less expanses of sea bottom composed of thick (>1000m) layers of sediment, and have been formed by the transport of material from continental margins by turbidity currents, which spread their loads out on the deep-sea floor to form thick turbidite sequences. Thus, large amounts of sediment

transported from the continental margins are laid down in these abyssal plains. The plains are found in all the major oceans, but because the Pacific is partially ringed by a trench belt that acts as a sediment trap, they are more common in the Atlantic and Indian oceans. Because the Pacific has fewer abyssal plains than the other major oceans, abyssal hills are more common here, covering up to ~80% of the deep-sea floor in some areas. Seamounts are volcanic hills rising above the sea floor, which may be present either as individual features or chains. Seamounts are especially abundant in the Pacific Ocean.

1.2.3. Mid-Ocean Ridge System

Mid-ocean ridge system is one of the major topographic features on the surface of the sea floor. It is an essentially continuous feature, which extends through the Atlantic, Antarctic, Indian and Pacific Oceans for more than ~ 60 000 km, and the 'mountains' forming it rise to over 3000 m above the seabed in the crestal areas. The topography of the ridge system is complicated by a series of large semi-parallel fracture zones, which cut across it in many areas. It is usual to divide the ridge system into crestal and flank regions. The flanks lead away from ocean basins, with a general increase in height as the crestal areas are approached. In the Mid-Atlantic Ridge the crestal regions have an extremely rugged topography with a central rift valley (1-2 km deep) that is surrounded by Rift Mountains.

1.3. Continental Shelf Sediments of the West Coast of India

Continental shelves are the submerged portions of the continents under the sea. Several rivers, large and small and drainage streams deposit large amounts of sediments every year, thus converting these shelves into large sedimentary basins. Surficial sediments of the western continental shelf and slope of India can be divided into terrigenous, biogenic, and chemogenic sediments. Terrigenous sediments mostly occur as sands (including heavy minerals) in the nearshore (up to 10-12 m water depth). This is followed by a zone of silty clays on the inner shelf between Saurashtra and Quilon. Relict sandy sediments carpet the outer shelf and are predominantly biogenic between Saurashtra and Mangalore and admixture of abundant terrigenous and biogenic

7

constituents between Mangalore and Quilon. Biogenic sediments are again predominant on the continental shelf between Quilon and Cape Comorin. The continental slope sediments are clayey silts with abundant carbonate content. Chemogennic sediments are phosphorites and authigenic green clays (Purnachandra Rao, 1997).

The continental shelf near Karachi widens from about 100-160 km southwest of the Gulf of Kutch. North of Bombay the shelf broadens to a maximum width of about 300 km. Off Bombay the shelf is about 220 km wide, and it narrows down towards south. The shelf width is about 60 km near 10°N. Near Cape Comorin the shelf is again about 100 km wide. From there it bends northeastward, narrowing to about 25 km. The shelf receives a very large portion of its supplies of sedimentary materials from the Indus in the north and from the Narmada and Tapthi in the Bombay region. Several small rivers, and drainage channels further south contribute their share.

A characteristic feature of the shelf is the occurrence of clastic sediment zone along the inner continental shelf from Saurashtra to Cochin. The sediments are silty clays and this zone is widest on the continental shelf off Narmada and Tapti and narrows down to the south. It is 40 km wide off Saurashtra, 175 km off Tarapur, 80 km off Bombay, 40 km off Ratnagiri, 45 km off Goa and Bhatkal and 25 km off Cochin. This zone extends up to 60 m water depth off the major rivers and narrows down to 25 m depth in the south-western part. The organic carbon content ranges from 1 to 4% in the nearshore sediments (Paropakari, 1979). The carbonate content is about 8-10% and rarely exceeds 20%.

The continental shelf between Quilon and Cape Comorin does not contain a clay zone unlike the rest of the inner shelf between Saurashtra and Quilon. It consists of biogenic carbonate sands. Off the Kerala coast, seasonal mud banks are a characteristic feature between Alleppey and Quilon but are absent further south between Quilon and Cape Comorin. One of the likely reasons for this is that the rivers draining between Alleppey and Quilon supply a large sediment flux to the shelf compared to the rivers between Quilon and Cape Comorin that supply less sediment to the shelf. Another reason is that south of Quilon, the shelf is narrow (with steep gradient) or wide with flat

shallow bottom (the Wadge Bank). Just south of Quilon the coastal orientation changes from 340° NW to 280° NW. The southwest monsoon waves approach from around 200° SW direction which make a more oblique angle to the coast at Neendakara rocky headland, there by creating a longshore transport southward leading to the removal of sediments brought by earlier cycles. Moreover, alongshore currents show a seasonal reversal in the southern part. The no-clay zone in the southwestern shelf may therefore be due to hydrodynamic factors influenced by the coastal configuration.

1.4. Physical Properties of Sediments

The most important physical properties of marine sediments, that influence sound propagation, are such as porosity, bulk density, sediment grain density and mean grain size.

1.4.1. Porosity and saturated bulk density

The values and variations of density and porosity at the surface and with depth in marine sediments are of importance in basic and applied studies of the earth. Density of various layers of oceanic crust is important in the propagation of shear and compressional waves, and other elastic waves. Values of densities are required in all mathematical models of sound interacting with sea floor.

Marine sediment may be defined as a deposit of different mineral particles whose pore space is filled by seawater. For saturated sediments, the porosity is the ratio of the volume of the porous space to the total volume of the sediment mass and the bulk density is given by weight of the sample per unit volume. Laboratory values of saturated bulk densities, bulk densities of mineral grains, porosities, and interrelationships between these properties were discussed by several authors (Hamilton *et al.*, 1956, 1970a; Nafe and Drake, 1957; Sutton *et al.*, 1957; Shumway, 1960b). Akal (1972) presented a relationship using the data from more than 400 sediment core samples taken from various physiographic regions of the Pacific, and Atlantic Oceans, and the Norwegian, Mediterranean and Black Seas.

9

The saturated bulk density (wet density) of a unit volume of gas-free sediments has two components: mineral grains and water within pore spaces. The relationship among these constituents and porosity is

$$\rho_{sat} = n\rho_w + (1-n)\rho_s \qquad (1.2)$$

where ρ_{sat} = saturated bulk density (or wet density)

n = fractional porosity

ρ_w = density of pore water

ρ_s = bulk density of mineral solids (or grain density).

Theoretically this linearity only exists if the dry densities of the mineral particles are the same for all marine sediments. The density of the sediment would then be the same as the density of the solid material at zero porosity, and the same as the density of the water at 100% porosity. To check this linearity, Akal (1972) plotted the relative density $(\rho = \rho_{sat}/\rho_w)$ as a function of porosity for the sediment samples and a regression line has fitted. The fitted regression line is a straight line and is represented by

$$\rho = 2.604 - 1.606n, (\sigma = 0.036) \qquad (1.3)$$

where ρ is the relative bulk density and n is the porosity.

The porosity of sediments in the sea floor (*in situ*) is very slightly greater than in laboratory because of the effect of hydrostatic pressure in reducing the volume of mineral grains (Hamilton, 1971b). Mathews, (1980) confirm that there is usually a progressive reduction in porosity with depth below the deep-sea floor. Bachman and Hamilton (1976) in their study concluded that, in various sediment types (Arabian Sea), there is less reduction of porosity with depth in the first 100m in deep water sediments than previously supposed: 8%-9% in pelagic clay, and calcareous and terrigenous sediments, and 4%-5% in siliceous sediments. This increase is so small that it can be disregarded: it amounts to less than 0.001 percent for any reasonable mineral or

porosity at depth 9500 m. Although true porosities do not require corrections from laboratory to *in situ* values, most published laboratory values require corrections to obtain true porosities.

The variation of porosity with depth can be estimated using the regression equations of Hamilton (1976d). Hamiltons regression equations are:

$n = 0.720 - 0.816z + 0.361 z^2$ (terrigeneous)

$n = 0.720 - 0.987z + 0.830 z^2$ (calcareous)

$n = 0.814 - 0.813z - 0.164 z^2$ (pelagic clay)

$n = 0.900 - 0.016z - 3.854 z^2$ (radiolarian ooze)

$n = 0.861 - 0.549z - 0.492 z^2$ (diatomaceous ooze)   (1.4)

where the depth z is in kilometers.

Mohan (1985) derived an equation for estimating compaction of shale for a well of Bombay offshore basin. The equation to compute porosity with depth for Bombay high is given by

$$n(z) = \frac{P}{1 + 0.0025z}$$ (1.5)

where P is the porosity in decimal fraction and z is the depth in meters.

Hamilton (1980) estimated density of various marine sediments versus depth from *in situ* porosities in the sea floor. In terrigenous sediments and in calcareous sediment the variation is more or less the same in the fist top 300 m (1.52 g/cm^3 to 1.85 g/cm^3); below 300 m rapid variation of density with depth is noticed in calcareous sediment compared to terrigenous sediments (Hamilton, 1980).

In the laboratory, bulk densities were determined (Hamilton and Bachman, 1982) by the weight-volume method. The bulk densities of the mineral solids were determined by a pycnometer method. Porosities were determined after drying sediment

11

samples in an oven at (110± 5°C) and corrections were made to allow for the amount of dried salts in the dried mineral residues (Hamilton, 1971b).

When seawater is evaporated from sediments during laboratory measurements dried salt remains with the dried mineral residues. A "salt correction" should be made to eliminate the false increment to the weight of dried minerals; otherwise, porosity, water content, and bulk grain density values are incorrect (Hamilton, 1974). Methods of making a salt correction were detailed by Hamilton (1971b).

The salt correction to porosity is small but should be made when laboratory procedures are to be precise, especially when the porosities are to be used in computations of elastic constants. The correction amounts to an increment to porosity varying, according to porosity, from 0.5 to 1.0 percent. Hamilton (1971b) suggested that the porosity with salt to be multiplied by 1.012 to get salt-free or true porosity. This empirical correction can be applied with little or no significant difference from the results of more elaborate computations. He has given correction multiplier for seawater salinity varying from 33 PSU to 35 PSU. In this study, a salt correction is applied to the laboratory measured porosity values following 'Volume-of-sea-water method' of Hamilton (1971b).

1.4.2. Density of Pore-water

The density of pore-water (seawater) varies with changes in temperature, salinity and pressure. Pore-water density, ρ_w decreases as temperature increases and increases as salinity and pressure increase. The variations are usually expressed as those in sigma-t [$\sigma_t = (\rho_w - 1000)$ kg/m^3]. For a given salt-free porosity and bulk density of minerals, the only variable factor between laboratory and *in situ* density is the density of pore water. At a given salinity, the density variations are due to the effects of temperature and pressure.

In computations involving pore-water and bottom-water, salinities are approximately the same. The values for the laboratory density of seawater can be

12

obtained from Sigma-t tables (e.g., NAVOCEANO, 1966). For marine sediments, Hamilton (1974) suggested a laboratory value at 23°C of 1.024 g/cm^3 would be within 0.002 g/cm^3 of any other density at reasonable "room temperatures." Hamilton (1974) recommended this value for laboratory computations. In this study the pore water density is computed using the International Equation of State of Sea Water (Millero and Poisson, 1981, Pond and Pikcard, 1986).

1.4.3. Density of Mineral Solids

Bulk density of the mineral solids in sediments varies widely because the mineral species present depend on minerology and nearness of source areas for terrigeneous components, on pelagic particles deposited from water, and on diagenetic changes in minerology in the sea floor. Hamilton (1974) reported that in the open Pacific to the south, the deep-sea clays have average grain density values between 2.61 and 2.75 g/cm^3. Akal (1972) reported the density of the solid particles (ρ_s) in the marine sediments as 2.66. In a similar study, Nafe and Drake (1963), and Urick (1982) reported the value of ρ_s as 2.68. Murty and Muni (1987) reported the value of ρ_s as 2.71 for the sediments off Cochin.

1.4.4. Mean Grain Size

The relationship between acoustic properties of marine sediments and mean grain size (Mϕ) is useful in estimating sound speed and attenuation where the grain size is known. Mean grain sizes are estimated in the logarithmic phi scale (Mϕ = -log$_2$ of grain diameter in mm). Mean grain size (Mϕ) is determined in the laboratory by grain size analysis. Grain size analysis is carried out by wet sieving with a dispersing agent to separate the sand fraction (> 0.062 mm). The pipette method is used for size analyses for silt and clay fraction. The results of these analyses, the mean grain sizes are determined by averaging the 16th, 50th, and 84th percentiles (Folk and Ward, 1957); when the 84th percentile would have involved undue extrapolation, the 25th, 50th, and 75th percentiles were used.

Above method (wet sieving and pipette method) is followed in this study for grain size analysis and Folk and Ward (1957) method is followed for mean grain size estimation.

Studies on the grain size distribution and carbonate content of the sediments of the western shelf of India are carried out by Nair and Pylee (1968). Hashmi *et al.*, (1978) conducted grain size and coarse fraction studies of sediments between Vengurla and Mangalore based on grab samples of sediments collected from the continental shelf of the area. The continental shelf in the study area has an average width of 80 km and the depth of the shelf break varies between 90 and 120m. To a depth of 50 m the shelf is smooth featureless and covered dominantly by the fine sediments (clayey silt/silty clay). Beyond the depth of 50 m, small scale (<5 m) prominence and undulations appear and sediments also become coarse (silty/clayey sand to sand). The major portion of the area has mean grain size between 2 Mϕ and 4 Mϕ, in the fine sand size. The dominating mean size range in the inner shelf is between 4 Mϕ and 8 Mϕ corresponding to the silt size. Murty and Muni, (1987) made a study on the physical properties of sediments of the backwaters and adjoining continental shelf off Cochin. They reported that mean grain size, porosity and bulk density influence the sound speed in sediments than do other physical properties.

1.5. Geoacoustic Properties of Sediments

The upper several meters of the sedimented sea floor contain the largest gradients in physical and acoustic properties in the sediment-water system. The geoacoustic properties of the sea floor, compressional and shear wave speeds, their attenuation, together with the knowledge of the material bulk density, and their variation as a function of depth are the main parameters needed to study the problems in underwater acoustics.

For high frequency (>10 kHz) acoustic applications, geoacoustic properties of the upper tens of centimeters must be known (Richardson, 1986), where as for low frequency applications surficial geoacoustic properties provide the initial conditions

used for prediction of depth gradients of sediment physical properties (Hamilton, 1980). Accurate values of surficial sediment geoacoustic properties (including variability) are therefore required for geoacoustic models covering the wide range of frequencies of interest to those studying underwater acoustics, marine sedimentology, geophysics, and marine geotechnology.

1.5.1. Compressional Wave (Sound) Speed

The basic equation for the speed V_p of a compressional wave is

$$V_p = [(\kappa + \frac{4}{3}\mu)/\rho]^{\frac{1}{2}} \tag{1.6}$$

where κ is incompressibility or bulk modulus, μ is the shear (rigidity) modulus, and ρ is the saturated bulk density. When the medium lacks rigidity, above equation becomes

$$V_p = (\kappa/\rho)^{\frac{1}{2}}$$

or

$$V_p = (\frac{1}{\beta\rho})^{\frac{1}{2}} \tag{1.7}$$

where β is compressibility and equals $(1/\kappa)$.

The speed of sound in sediment is closely related to its porosity and therefore its density. At the seabed, high porosity/low density sediments, such as mud, have compressional wave speeds only slightly less (up to 3%) than that of the overlying water; low porosity/high density sediments, such as hard sands, have speed 10-20% greater than that of the overlying water. These higher speeds are due to the presence of rigidity and frame bulk modulus in the mineral structure of the sediments (Hamilton, 1971a). The low sound speed effect in high porosity mud or silty clays is the result of a balance between water and mineral compressibilities (or bulk moduli) and densities,

15

plus low rigidities and low mineral frame bulk moduli (Hamilton, 1971a; Hamilton and Bachman, 1982). This low sound speed phenomenon was noted in laboratory studies, and has been confirmed by measurements in the sea floor (Tucholke and Shirley, 1979; Hamilton, 1956; Schreiber, 1968). The lowest speeds measured in the higher porosity sediments are usually no more than 3% less than in seawater at the same temperature and pressure.

When the sediment surface sound speed is less than that in the bottom water, and there is a positive sound speed gradient, a sound channel can be formed in the surficial sediments which should be present in most deep seafloors and in some shallow areas (Hamilton, 1970a). The depths of these sound channels in deep water normally vary between 15 and 60m.

Hamilton (1970b) carried out *in situ* measurements of sound speed by means of probes placed in sea bottom by divers. He measured sound speed in core samples. He reported that sound speed in coarse sand with porosity 39% to be 1836 m/s, while a silty clay of porosity 76% had a speed of 1519 m/s, compared to the speed in water of about 1560 m/s.

Hamilton and Bachman (1982) presented data on geoacoustic properties from 340 sediment samples collected on continental shelf and slope. They measured sound speed, density, porosity, grain density, and grain sizes of sediments and computed velocity ratio and impedance. Regression equations are provided for important empirical relationships between properties. They concluded that sound speed and density are about the same for a given sediment type in the same environment in any ocean, if porosities are the same. With the knowledge of the mean grain size of mineral grains or average porosity of sediment, the average sound speed can be predicted within 1% or 2% in most environments.

Murty and Muni (1987) derived regression relations among a few physical properties of the sediments of the backwaters and adjoining continental shelf off

Cochin. They reported that the sound speed is better correlated with porosity, bulk density, and phi mean than with other physical properties.

In his study Smith (1986) concluded that the geotechnical characteristics of the seabed and seismo-acoustics are intertwined and indivisible. Attempts to utilize seismic measurements to predict geotechnical quantities have not found universal favor among design engineers through the lack of acceptance of strain amplitude and rates employed. Davis and Bennel (1986) have shown that these can be easily obtained by the strain rate and strain level correction curves produced by the resonant column apparatus.

Vertical variability was generally greater than horizontal variability for all properties measured. Sediment geoacoustic properties of most coastal marine sediments are controlled by the interaction of biological and hydrodynamic processes (Richardson *et al.* 1983). Biological processes tend to dominate in finer sediments, where as hydrodynamic processes control sediment geoacoustic properties in sandy substrates. Richardson *et al.* (1983) noticed lower compressional wave speed and higher attenuation in medium sand than the coarser sand. Hamilton (1972a,b) also reported similar results. The speed of compressional waves in sediments can be measured at shallow depths below the bottom by acoustic probes *in situ* and by core measurements in the laboratory. At deeper depths, a variety of geophysical techniques involving travel time measurements can be employed, including using conventional sonobuoys and explosives shots for work over deep water (Hamilton *et al.*, 1974, 1977).

Hamilton (1979b) studied the compressional wave speed gradients in sediments using a variety of data collected by different methods such as *in situ*, seismic refraction and reflection experiments, and by laboratory or shipboard measurements on long cores.

Below the seabed as the increasing pressure of the overburden sediment grains reduces the porosity is forced into closer contact and the sound speed increases. Smith (1986) has shown that this increase cannot be accounted for by consolidation alone

(i.e., by a reduction in porosity). The main cause of the sound speed gradients is the increase in the stiffness of the sediment frame with depth in the sediment column. Such a stiffness increase can be attributed to many factors among which effective stress, chemical bonding, and even geological time itself loom large.

This increase in sound speed with depth is very rapid compared to the speed gradient in the overlying water; it is found to lie in the range 0.5 to 2.0 s^{-1} (Nafe and Drake, 1963). In isothermal water the corresponding value is $0.017s^{-1}$. Hamilton (1979) discusses the causes of sound speed gradients in marine sediments in detail. For silt clays and turbidites it was concluded that, to 500m depth in the sea floor, the pressure-induced porosity reductions and effects on sediment mineral frame due to overburden pressure accounted for about 66% of the gradient. The other factors were sound increases due to heat flow and consequent temperature increases with depth (about 17%) of the gradient), pore water pressure increases (about 2%) and increases in rigidity caused by lithification (about 15%). Sound speed gradients in a thick sediment layer are usually positive and may be linear, but more often are parabolic, and decrease with depth in sediments (Hamilton, 1979, 1980). It is convenient for purposes of comparison and to compute sediment layer thicknesses, to express these gradients as positive, and linear.

Tucholke and Shirley (1979) reported six *in situ* measurements of sound speed and sound speed gradients to about 12 m in pelagic sediments and turbidites in the North Atlantic. They used a velocimeter attached to a piston corer. The measured sound speed gradients ranged from 0.5 to 1.1 /s.

Murty and Naithani (1996) studied the influence of sound speed gradients on bottom reflection loss (BRL). They reported that the effect is noticed only beyond critical angle in the case of sand-silt-clays. However the effect is noticed all grazing angle for silty clays or clayey silts. The BRL decreases with increase of gradients; while it increases with increase of frequency.

The relationships between mean grain size data and sound speed are important because grain size analysis can be made of dried sediment in which density, porosity, and sound speed measurements cannot be made. Additionally, there is much data on grain size in geologic literature that can be used as indices to acoustic properties. Sound speed increases with increasing mean grain size and decreasing amounts of clay size material (Hamilton and Bachman, 1982). Sediment mean grain size, or clay size percentages affect sound speed only through other elastic properties such as density and porosity (Hamilton 1970b). Mineral grain shape may influence sediment structural rigidity and there by affect sound speed in minor ways (Hamilton, 1971). Examination of the regression equations of Hamilton and Bachman (1982) indicated that mean grain size and percent clay size are as good or even slightly better than porosity or density relation to sound speed.

Anderson (1974) made regression analysis studies to determine the statistical correlation of sound speed and physical properties measured in the laboratory on sediments from 82 cores collected in the Atlantic, Pacific, and Indian Oceans, and Mediteranean Sea. He noticed that mean grain size (Mφ), and porosity are the two parameters showing the highest significant correlation with sound speed. He grouped the data by different oceans or physiographic provinces and water depths to determine the effect of these parameters on sound speed- porosity and sound speed-grain size relationships. He observed that for a given grain size, the sound speed is higher in the Atlantic Ocean than in the Pacific Ocean. For a given porosity, the sound speed is higher in the oceanic rise provinces than elsewhere. However, all of the data except those from the oceanic rise province are well represented by one second degree equation (Anderson, 1974) with porosity as the independent variable for predicting sound speed.

In recent years geoacoustic properties of the near bottom sediment, such as compressional and shear speed and attenuation, have been studied extensively. Presently this knowledge is being gained through rather elaborate direct and/or remote measurements of sediment parameters. However, recently Akal and Stoll (1995) developed an expendable penetrometer that can remotely measure some of these

parameters from a moving ship or aircraft based on existing XBT technology and able to sense deceleration upon impact with the seafloor. By a complete analysis of the impact signature, including both the initial plastic penetration and the subsequent damped oscillation, they classified the sediment type and estimated the shear strength, and geoacoustic properties. Bowman *et al.*, (1995) compred the results of eXpendable Doppler Penetrometer (XDP) developed by US Navy and quasi-static cone penetrometers incorporating an element to sense pore water pressure ("piezocones") to collect seafloor informations. Data collected using both tools showed comparable results.

Best *et al.*, (1998) developed a new instrument for rapid acquisition of seafloor geophysical and geotechnical data. The instrument can measure compressional wave speed and attenuation down to 1 m sub-bottom depth in sands and gravels at frequencies up to 10 kHz, and the speeds of horizontally and vertically polarised shear waves at the surface at about 120 Hz.

Literature review indicate that researchers conducted a number of theoretical studies on compressional wave sound speed and compressional wave attenuation in marine sediments and the details are included in Chapter 2.

1.5.2. Shear Wave (Sound) Speed

Shear waves are important in underwater sound propagation because compressional waves can be partially converted to shear waves or Stoneley waves on reflection at boundaries, and the energy is rapidly attenuated (Urick, 1982). It has been shown that shear wave speed and rigidity are important properties for more sophisticated mathematical models involving sound interactions with the sea floor (Vidmar and Foreman, 1979).

At the seabed, sediments have extremely low shear wave speed. The review by Hamilton (1976c) showed that at a depth of one meter below the sea bed marine sands, and silt-clays have shear wave speed in the range 5-150 m/s. However, the increase

with depth or compaction is rapid, increasing to about 200 m/s at 10 m and to about 400 m/s at a depth of 100 m. The speed of shear waves in the first layer of the sediments and in lower layers of sedimentary rocks can be approximately predicted by the relations between compressional and shear waves from the studies (Hamilton, 1979a, 1980). For sand sediments, shear wave speed can be approximated by the relations between compressional and shear wave velocities of Hamilton (1979a). Hamilton (1976c) derived regression equation for the estimation of *in situ* shear wave speed with depth in fine sands, and the equation is given by

$$V_s = 128D^{0.28} \qquad\qquad (1.8)$$

Where D is depth in m, and V_s is the shear wave speed in m/s.

The usefulness of the shear wave in civil engineering is basically to define the shear modulus and its directional variations, particularly with depth, so that the performance of any proposed structure can be predicted (Smith, 1986). The studies indicated that for a near-surface material (sand, ooze or over-consolidated clay) there is a very rapid increase in the sound speed over the first few tens of meters of depth in the homogeneous (presumed) media.

As the magnitude of the shear wave speed is related to the stiffness of the sediment frame, the cause of the gradients must somehow be wrapped up in the factors which control the bonding of the frame. The effective stress is the dominant factor in the near surface sediments providing large gradients at such depths. In contrast to the compressional wave there is no clear division of the various sediments into groups obeying the same sort of sound speed gradient. For most of the sediments, some power law obtains but the exponent can be quite variable from about 0.25 to 0.50; this means to have no relation to the type of material. Ogushwitz's (1985) predictions give linear gradient ranges from 2.8 /s at the sediment water interface to 0.9 /s for sands at 500 meters and 2.4 /s to 0.7 /s for clays over the same range. Smith (1986) reported the results of directional linear gradients of shear wave speed for over-consolidated clays:

21

$$V_s = 122 + 9.21z \text{ (parallel to bedding)}$$

$$V_s = 84 + 16z \text{ (perpendicular to bedding)} \qquad (1.9)$$

The first of these is similar to Hamilton's equation for shallow depth silt-clays and turbidites:

$$V_s = 116 + 4.65z \qquad (1.10)$$

Clearly, the empirical equations for shear wave speed variations with depth are extremely variable, particularly for the near-bottom sediments where it is most important for both geotechnical and seismo-acoustic propagation studies. At depths, the study shows, most sediment have similar gradients.

Unfortunately, data on shear wave speed and shear wave attenuation in sediments of Indian Ocean is not available and hence not considered in this study.

1.5.3. Compressional Wave Attenuation

The attenuation of compressional waves in sediments and rocks has been measured by a wide variety of methods, ranging from *in situ* probes in sediments to resonance technique and inversion technique. Such measurements extend over a wide frequency range. Hamiltom (1974b) has compiled data from many sources over a wide range of frequency, and shown that the attenuation coefficient tends to increase approximately as the first power of the frequency, accordingly, attenuation coefficient α in dB/meter can be written

$$\alpha = kf^1 \qquad (1.11)$$

where k is a constant for the sediment type, and f is the frequency in kHz. The predicted values of attenuation of compressional waves for the sediment surface in models are usually based on published relationships between attenuation and sediment porosity or

mean grain size (Hamilton, 1972,1974). Stoll (1977) casts doubt as to whether this linear variation extends downward to very low frequency range. At very low frequency range, another source of sound energy loss (frame loss) may become dominant over the loss due to viscosity. The details are discussed in Chapter 2.

Like sound speed, attenuation is strongly related to porosity in sediments. Richardson (1985) studied the variability of surficial sediment geoacoustic properties and reported that highly porous mud found in low energy environments showed the lowest range of values in physical and acoustic properties. Mixtures of sand and shell found in higher energy environments that exhibited the highest range of values. Compressional wave attenuation consistently exhibited the highest variability followed by mean grain size, porosity, and compressional wave speed.

Because of compaction, attenuation of compressional waves decreases rapidly with depth in natural sedimentary materials. While there is wide variability with sediment type at shallow depths, where most measurements exist, the rapid decrease of k with depth is evident. At a depth of 2 km, the attenuation in a sedimentary column is only about one-tenth of its value at the surface.

Very little data are available to determine compressional wave attenuation as a function of depth in the sea floor, (Hamilton, 1976a, 1980). In silty clays there is distinctly different variation of attenuation with depth in the seafloor. The data indicate that attenuation increases with depth from the sediment surface to some depth where pressure effect becomes dominant over reduction in porosity. In surface sands, attenuation coefficient varies between about 0.25 and 0.6 (Hamilton 1972b, 1976a). It appears that attenuation in sands decreases with about the −1/6 power of overburden pressure. More details and discussions on compressional wave attenuation are included in the Chapter 2.

1.5.4. Shear Wave Attenuation

When compressional sound wave get reflected at some impedance mismatch within the sea floor, some of the energy is converted to shear wave and the converted

energy is rapidly attenuated. The attenuation of shear waves is a required input for many mathematical models of sound interaction with the sea floor. Hamilton (1976b) reviewed the subject of the attenuation of shear waves in sediments.

One of the best *in situ* studies of shear waves in natural, saturated sediments was that of Kudo and Shima and the details are reported by Hamilton (1980). They found that in sands, silt, and mudstones, the attenuation of shear waves have a dependence of f^1 at frequencies of 15-90 Hz. McDonal *et al.* (1958) found a first order dependence of shear wave attenuation on frequency in the frequency range of 20-125 Hz. Stoll (1977) measured the attenuation of shear waves in sands and silt in the laboratory at low frequencies (43-391 Hz) and found that attenuation is not dependent on the first power of frequency.

Very little information is available on the variation of shear wave attenuation with pressure or depth in sediments. Hamilton (1980) reviewed various studies carried out on the variation of shear wave attenuation with depth. He reported that attenuation of shear and compressional waves varied about the same under increasing normal, effective pressures: attenuation decreased with about the $-1/6$ power of overburden pressure. There are no data on the effects of pressure on shear wave attenuation in higher porosity silt-clays. It is concluded that, in the absence of data, and in view of the review work, it can be assumed for modelling purposes that shear-wave attenuation varies with depth in the sea floor proportionally with compressional wave attenuation.

In this study shear wave attenuation in marine sediments are not included due to the non-availability of data.

1.6. Objectives of the present study

A considerable amount of work has been carried out on the geological, biological, and chemical aspects of sediments of the Indian Ocean. The review on the topic physical and geoacoustic properties of the sediments of Indian Ocean indicates that within the country, there have not been much studies on various aspects of

geoacoustic properties of sediments off the west coast of India. Hamilton *et al.*, (1974, 1977) determined sound speed in deeper layers of the Bengal Fan in the Indian Ocean by constructing sound speed versus travel time curves from sonobuoy data. Murty and Muni (1987) studied the physical properties of sediments of the backwaters and continental shelf off Cochin. Pradeep Kumar and Murty (1993) studied the seasonal variation of compressional wave speed at the sea bottom interface. Pradeep Kumar (1997) reported seasonal variation of compressional wave attenuation in sediments at the sea bottom interface off Cochin.

Venkateswarlu et al. (1989) identified acoustic reflectors at 25 to 75 m below the sea bottom for the area off Gopalpur (Orissa). They also gave the sediment distribution of the area. Khadge (1992) studied the physical and geotechnical properties of two sediment cores collected from the Central Indian Ocean basin. Das *et al.* (1993) determined various physical parameters of sediments collected from the shelf area of the Bay of Bengal off Narsapur to study the profiles of porosity, bulk density, water content, shear strength etc. Murty and Pradeep Kumar (1989) made a study on the compressional wave speed in sediments based on laboratory measurements. Review on the geoacoustic properties of sediments indicated that no detailed study is undertaken till now to bring out the interrelationships between physical and acoustic properties of sediments off the Indian Coast. With this background, a study on the geoacoustic properties of marine sediments off the west coast of India is undertaken.

In this study, sediments varying from coarse sand to very fine clay noticed on the continental shelf off the west coast of India are considered. To understand the seasonal variation of geoacoustic properties of sediment due to the variability in bottom water characteristics, six areas between Quilon and Bombay are selected. The study is carried out based on the monthly variation of temperature, salinity, density, and sound speed in the bottom water and its influence on the sediment at the selected areas.

In Chapter 2 the details of theoretical background for the prediction of sound speed and attenuation in sediments are included. The effect of variation in

oceanographic conditions of the sea bottom water on sound speed and attenuation in sediment with season is also included in Chapter 2.

Chapter 3 contains the details of seasonal variation of temperature, salinity, density and sound speed at selected areas in the shelf off the west coast of India.

The details of the development of a velocimeter to measure sound speed in marine sediments and its calibration are included in Chapter 4. The details of correction for laboratory sound speeds to *in situ* values are also discussed.

Prediction of compressional wave speed and attenuation in marine sediments is included in Chapter 5 and comparison of the predicted sound speeds in sediments with laboratory sound speeds is presented. The details of new empirical relationships among geoacoustic properties and physical properties of marine sediments are also included in Chapter 5.

In Chapter 6, details of laboratory measured sound speeds in marine sediments at different temperatures are given. A study on the seasonal variation of sound speed and attenuation in marine sediments is carried out and a discussion based on the temperature variability at the sea bottom is also included. Summary of all important results and conclusions is included in Chapter 7.

CHAPTER 2

SOUND SPEED AND ATTENUATION IN MARINE SEDIMENTS

In this Chapter, a review of theoretical studies and the basis of the theories opted for prediction of sound speed and attenuation in sediments in the present study are included. Discussion on the effect of variation of bottom water temperature on sound speed and attenuation in sediments is presented.

2.1. Sound speed in sediments

The sedimentary material found in the seafloor includes high-porosity suspensions of colloidal clay particles at one end to low-porosity porous solids at the other. Many particles, particularly those of clay and silty clay size, are in suspension, while those of sand size are in contact with another. Each particle has an irregular shape. Although certain minerals predominate in sediments, each sediment sample has a unique mineral grain composition. As the acoustic properties of sediments are determined by such properties, any general theory for acoustic wave propagation in sediments must consider these variables.

Earlier studies on the variation of sound speed in marine sediments can be divided into two basic types: theoretical and empirical. Theoretical models have some basis in a physical model and the model parameters are specified *priori*. Empirical equations assume no a *priori* model, and the dependent parameters are only determined by reference to some explicit data set. Alternatively, different equations may be proposed for different physical properties connecting sound speed (Hamilton, 1980, Bachman, (1985).

For the derivation of geoacoustic properties from the structural parameters of marine sediments, essentially two different approaches have been applied. The earlier approach (Urick, 1948; McCann and McCann, 1969) is based on the assumption that fine-grained unconsolidated marine sediments can be described as suspensions, and, for the compressional wave speed, uses the formula of Wood (1941) for the effective compressibility of suspensions. Theoretical studies (Wyllie *et al.*, 1956; Wood, 1941) have examined one or more equations, based on some physical model that relate

velocity to the porosity. These theoretical models have often suffered from a lack of general applicability. For example, the Wood equation is valid for particles in suspension. The bulk compression is computed as the weighted mean compressibility of the solid and fluid fractions and thus is only valid for sound speed estimation when the bulk material has no strength. The time average equation (Wyllie *et al.*, 1956) is approximately valid for mixtures of fluid media, and thus is only valid for low-porosity materials. The main draw back of this concept is that the sediment does not have rigidity. This is an unreasonable assumption, for shear waves are observed even in very soft high-porosity mud (Hamilton, 1972).

The more comprehensive approach (Stoll and Bryan, 1970; Stoll, 1977; Hovem and Ingram, 1979; Stoll, 1985; McCann and McCann, 1985) applies theory of acoustics of porous media. The description of unconsolidated marine sediments with Biot theory (Biot, 1956a,b) appears to be more realistic than former approach because it accounts for the occurrence of shear waves. An overview of some of the theoretical developments related to the sound speed and attenuation in marine sediments is presented below.

2.1.1. Wood Model

Wood (1941) considered a medium (sediment) composed of grains, some of which are in contact and some of which are not. The pore space is filled with water. At higher porosities fewer of the grains are in contact. As the porosity decreases, more and more grains come in contact forming a rigid matrix. Any given medium may thus be considered to be composed of pockets of slurries (particles in suspension) and rigid grain matrices. The fraction of slurry depends directly on the porosity. The travel time across any given volume of the medium will then be the sum of the travel times across the individual slurry and rigid particles that make up that volume. Based on this simple model, Wood (1941) proposed an equation for sound speed (V_p) in slurry:

$$\frac{1}{\rho V_p^2} = \frac{n}{\rho_f V_f^2} + \frac{(1-n)}{\rho_r V_r^2}$$ (2.1)

where ρ is the bulk density, defined by $\rho = n\rho_w + (1-n) \rho_r$, n is the porosity, V_f is the speed of sound in the fluid medium, V_r is the speed of sound solid medium, V_p is the speed of sound in the porous medium, ρ_r is the density of solid medium and ρ_f is the density of fluid medium. The Wood equation is approximately valid only at high porosities.

2.1.2. Wyllie *et al.* Time Average Model

Wyllie *et al.* (1956) studied mixtures of rigid media, and proposed that sound speed was well represented by the average travel time equation

$$\frac{1}{V_p} = \frac{n}{V_f} + \frac{(1-n)}{V_r} \qquad (2.2)$$

The parameters are as defined previously. The Wyllie or time average equation is approximately valid at low porosities (less than 30%), where media can be considered as approximately rigid.

2.1.3. Nafe and Drake Model

Nafe and Drake (1957) compared the Wood model to the behavior of compressed springs in series. The Wood model breaks down at low porosities because the increased grain to grain contact stiffens the lattice to the extent that the behavior is more akin to springs in parallel. They derived the relation,

$$V_p^2 = nV_f^2 + (1-n)^m V_r^2 \rho_r / \rho \qquad (2.3)$$

The exponent m is a constant to be determined with experimental data. Nafe and Drake found a good fit to their experimental data using m = 4 and 5. Boyce (1981) found a value of m as high as 9 required to fit his data. Nobes *et al.* used a value of 2ρ for m.

Alternately the exponent is allowed to vary with porosity as $m = a + bn$. The values of $a = 5.3 \pm 0.2$ and $b = -3.5 \pm 0.3$ yielded best fitting model to their data.

2.1.4. Nobes *et al.* Model

Nobes *et al.* (1989) proposed a time averaged model for the variation of sound velocity with porosity and obtained an equation which is a simple combination of Wood and Wyllie equations. Here, instead of assuming the two media as the fluid and solid fractions, the sediments are assumed to be mixtures of slurry and rigid components. The amount of slurry depends directly on the amount of porosity. By taking the weighted mean of the Wood and Wyllie equations, an equation is obtained that is representative of the physical models described above.

$$\frac{1}{V_p} = \frac{n}{V_w} + \frac{(1-n)}{V_l} \qquad (2.4)$$

where V_w represents the Wood's sound speed and V_l the fine average sound speed of Wyllie *et al.* Good agreement between results obtained using the equation and experimental data has been reported.

A cursory look at the above equations show that all the models depend on V_r. Nafe and Drake used a constant value of 6000 m/s for V_r. Tosaya and Nur (1982) developed an empirical equation to represent the sound speed in grains, V_r (in km/s), where f_c is the clay fraction.

$$V_r = 5.8 - 2.4 f_c \qquad (2.5)$$

If the lithology are accurately known, Nobes *et al.*, (1989) given a better suggestion and the equation can be generalized as

$$\frac{1}{V_r} = \sum_j \frac{f_j}{V_j}, \qquad (2.6)$$

where f_j is the fraction of the medium composed of the jth component, which has sound speed V_j.

2.1.5. Biot theory

Biot (1956a, 1956b) considered a saturated sediment to consist of a porous assemblage of sediment grains (the "skeletal frame"), whose interconnected pores are filled with water or gas (the "pore fluid"). Biot devised a theoretical model of the acoustic behavior of such a material. The Biot model treats both the individual and coupled behavior of the frame and pore fluid. Energy loss is considered to be caused by the inelasticity of the skeletal frame and by the viscosity of the pore fluid as it moves relative to the frame. The model predicts that sound speed and attenuation in sediment will depend on frequency, elastic properties of the sediment grains and pore fluid, porosity, mean grain size, permeability, and effective stress.

The practical application of Biot's theory was rather limited until Stoll and Bryan (1970) and Stoll (1974,1977) applied the theory to the discussion of sound speed and attenuation as a function of frequency in marine sediments. The modified form of Biot theory by Stoll is presently known as Biot-Stoll theory. In the Biot-Stoll theory the loss terms are included to the elastic parameters of the solid frame and thereby account losses due to grain-to-grain contacts as well as fluid loss. Compressional and shear waves travelling through this structure are attenuated by two physical mechanisms: frictional grain to grain contact sliding and viscous dissipation caused by relative motion between the grains and the interstitial fluid.

The Biot-Stoll theory predicts three kinds of body waves in a fluid-saturated porous medium. One of the compressional waves and a shear wave are the traditional body waves of elastic media. The 'second' compressional wave is highly attenuated and for most of the geophysical applications is not important. However, recent demonstrations of its existence provide a striking success for the Biot-Stoll model.

31

Ogushwitz (1985a,b) has shown that Biot-Stoll theory can be used to model marine acoustic sound speed and attenuation data for artificial and natural materials with porosities ranging from 2% to 100%.

The mathematical formulation of the Biot-Stoll theory is given below.

Let u be the displacement of the frame, U be displacement of the pore fluid relative to the frame, and n be porosity. Then the dilatation of a volume element attached to the frame is given by

$$e = div(u) \tag{2.7}$$

and the volume of fluid that has flowed into or out of that element is given by

$$\zeta = n * div(u - U) \tag{2.8}$$

Biot nominated the following equations to be constitutive equations for a porous, saturated, isotropic medium

$$\tau_{ij} = 2\mu e_{ij} + \delta_{ij}[(H - 2\mu)e - C\zeta], \tag{2.9}$$

$$P = M\zeta - Ce, \tag{2.10}$$

.

where τ_{ij} and e_{ij} are the stress and strain components respectively of an element of volume attached to the skeletal frame, P is the pore fluid pressure, H, C, M, and μ are real constants, and δ_{ij} is the Kronecker delta.

By assuming that the sediment porosity remains constant under the small strains typical of acoustic waves, Stoll showed that the constants of the Biot theory could be identified with measurable physical properties in the following way:

$$H = \frac{(K_r - K_b)^2}{(D - K_b)} + K_b + \frac{4}{3}\mu, \qquad (2.11)$$

$$C = \frac{K_r(K_r - K_b)}{(D - K_b)}, \qquad (2.12)$$

$$M = \frac{K_r^2}{(D - K_b)} \qquad (2.13)$$

where

$$D = K_r[1 + n(K_r / K_f - 1) \qquad (2.14)$$

Here, K_r and K_f are the bulk moduli of the sediment grains and pore fluid respectively, and K_b and μ are bulk and shear moduli of the skeletal frame respectively. To incorporate the inelasticity of the frame into the model, Stoll permitted H, C, M, and μ to be complex. In particular, he concentrated the inelastic effects in the skeletal frame moduli K_b and μ.

Biot (1956a, 1956b) derived wave equations for dilatational and shear waves from the constitutive equations, the equations of motion, and the equations of flow through a porous medium. In particular, the compressional wave equations are

$$\nabla^2(He - C\zeta) = \frac{d^2}{dt^2}(\rho e - \rho_w\zeta) \qquad (2.15)$$

$$\nabla^2(Ce - M\zeta) = \frac{d^2}{dt^2}(\rho_w e - m\zeta) - \frac{\eta F}{k}\frac{d\zeta}{dt} \qquad (2.16)$$

33

Here ρ_w is the fluid density, ρ is the total density of the volume element, η is the fluid viscosity, and k is the dynamic permeability of the skeletal frame. Note that

$$\rho = n\rho_w + (1-n)\rho_r \qquad (2.17)$$

where ρ is the density of the solid grains. The parameter m is given by

$$m = a'(\rho_w / n), a' \geq 1 \qquad (2.18)$$

The coefficient a', which is called the "structure factor," accounts for the apparent increase in fluid inertia caused by the tortuosity of the pores. The frequency dependence of η/k (the viscous resistance to fluid flow) is accounted for by a complex correction factor F which is given by

$$F(\kappa) = \frac{\kappa T(\kappa)}{4[1 + 2iT(\kappa)/\kappa]} \qquad (2.19)$$

where $T(\kappa)$ is given by the complex Kelvin function

$$T(\kappa) = \frac{ber'(\kappa) + i bei'(\kappa)}{ber(\kappa) + i bei(\kappa)} \qquad (2.20)$$

where

$$\kappa = a(\omega \rho_w / \eta)^{\frac{1}{2}} \qquad (2.21)$$

is non dimensional and depends on the pore-size parameter, a the fluid density ρ_w, the viscosity η and the angular frequency ω.

34

If one assumes solutions of the form

$$e = A_1 \exp[i(\omega t - lx)], \qquad\qquad (2.22)$$

$$\zeta = A_2 \exp[i(\omega t - lx)], \qquad\qquad (2.23)$$

then Eqs.(2.15) yield the compressional wave dispersion relation

$$
\begin{vmatrix}
Hl^2 - \rho\omega^2 & \rho_w\omega^2 - Cl^2 \\[2em]
Cl^2 - \rho_w\omega^2 & m\omega^2 - Ml^2 - iF\omega\eta/k
\end{vmatrix} = 0 \qquad\qquad (2.24)
$$

For shear waves, one obtains the analogous dispersion relation,

$$
\begin{vmatrix}
\rho\omega^2 - \mu l^2 & \rho_f\omega^2 \\[2em]
\rho\omega^2 & m\omega^2 - i\omega\eta F/k
\end{vmatrix} = 0 \qquad\qquad (2.25)
$$

The dispersion relation of Eq. (2.24) has two distinct complex roots of the form, $l \equiv l_r + il_i$. The wave speed for each root is given by ω/l_r and the attenuation by l_i (Np/m). One solution corresponds to a relatively slow wave with high attenuation, the so-called Biot "slow wave" while the other root corresponds to the usual, higher speed, acoustic wave. The attenuation of this wave is very high and the second wave has therefore limited practical importance except that is directly connected to the viscous loss of the first wave (Hovem, 1980). Johnson and Plona (1982) and Chotiros (1995)

35

verified the existence of the compressional waves of the "second kind" predicted by the Biot theory.

Eq. (2.25) indicates that only one kind of shear wave can propagate. It also shows that this wave may suffer some dispersion because the solid and fluid components can move out of phase with one another causing viscous dispersion. However, this is not considered in this study.

The theory predicts that attenuation, when dominated by viscous flow losses in the pore space of the sediment, will vary as the second power of frequency for low frequencies and will vary as the square root of frequency for high frequencies. Frictional loss mechanisms, in contrast, exhibit a linear dependence of attenuation.(The ratio of the cross-sectional length scale of the pore space in the sediments to the wavelength of the acoustic wave determines the boundary between high and low frequencies).

Biot-Stoll theory of wave propagation in porous, saturated material is complicated, with more than ten parameters affecting dispersion relation. Some of the parameters are directly measurable or known *a priori* (e.g., grain density, saturated bulk density, porosity, and fluid density). However, the parameters that are directly related to the grain geometry and nature of the grain contacts are not well known (e.g., pore size parameter, mass factor, and elastic moduli of the frame) and their values are usually inferred from empirical data. Ogushwitz (1985) and Holland and Brunson (1988) in their studies discussed different methods (empirical and theoretical) to predict these parameters for natural sediment materials.

Murty and Pradeep Kumar (1989,1990) studied the applicability of sound speed models of Wood, Wyllie *et al.*, Nafe and Drake, Nobes *et al.*, and Biot-Stoll for predicting sound speeds in sediments of two environments - backwaters and continental shelf off Cochin. They compared the laboratory measured sound speeds with predicted values of each model. Biot-Stoll model showed good agreement for the entire range of sediments. Nobes *et al.* model fitted well with the laboratory data for carbonate rich sediments. Wood's equation also agreed well with the sediments from backwaters

indicating that these sediments behave like suspensions and lack rigidity. In this study, Biot-Stoll model is considered for the prediction of sound speed in sediments. The details are discussed in Chapter 5.

2.2 Attenuation in sediments

When sound energy passes through saturated sediment, energy is lost through a number of mechanisms. Some of these such as friction between mineral grains and the relative movement of the mineral frame and pore fluid are fundamental to the material and are usually referred to as intrinsic attenuation. In the seabed itself other factors play a part in the absorption process. Gas bubbles, shells, boulders, and other inhomogeneties can produce losses through scatterring. Energy conversion between compressional, shear and interface waves and multiple inter-bed reflections also introduce significant attenuation. The total of all losses is called "effective" attenuation and it is that to be considered in any practical situation.

An approach developed by Stoll (1956a, 1956b) assumes that two key mechanisms control the dynamic response of fluid-saturated sediments under insonification. One mechanism produces energy loss through intergranular friction at the contact area between particles of the frame and the other through the viscosity of the pore fluid. The effects of viscosity manifest themselves in two different ways depending on the permeability of the sedimentary material. They differ from those associated with intergranular friction in that the overall motion of the fluid relative to the skeletal frame of the sediment is predicted to result in a frequency-dependent damping.

Considering all these effects are real, the overall intrinsic damping in sediments will involve all the three mechanisms just described namely, friction, overall fluid motion, and local fluid motion. The first mechanism would lead to attenuation proportional to the first power of frequency. The two losses associated with the fluid are believed to produce attenuation that varies at f^1, f^2, or $f^{1/2}$, depending on the frequency range involved. Attenuation should thus vary in a complex manner when all

the mechanisms are combined. This proposed nonlinear relation between frequency and attenuation is a subject of the debate among researchers.

Major obstacles to the wider acceptance by the acoustical community of Biot-Stoll approach to sound propagation in sediments have been the lack of data to adequately verify the model's predictions and relatively small magnitude of the effects involved compared with the scatter in attenuation measurements. Moreover, individual measurement programs are usually confined to a narrow frequency range, a linear dependence of attenuation and frequency has often appeared justified for the limited data obtained.

Literature survey shows that the theories fall into one of the two broad groups. One considers the medium as a continuum with viscoelastic properties representative of the bulk material as a whole. In the second category wave propagation is assumed to depend upon the properties of individual constituents of the material and on structural characteristics of the skeleton. In this approach acoustical properties of the sediments are related to its observable physical properties.

2.2.1. Viscoelastic models

a) The Hamilton viscoelastic model

In his model Hamilton (1974a) assumes that sediments can be represented by an isotropic two-phase system composed of sediment grains and water. The mechanics of attenuation are not specified but provision is made for velocity dispersion and a nonlinear dependence of attenuation and frequency.

The basic derivation of this model leads to an equation for both the shear and compressional attenuation which, with appropriate changes in notation, is

$$\frac{1}{Q} = \frac{aV}{\left(\pi f - \dfrac{a^2 V^2}{4\pi f}\right)} \tag{2.26}$$

38

where 1/Q is the specific attenuation factor, a is the attenuation coefficient, V is the wave velocity (V_p or V_s), and f is the frequency.

When energy losses are small, the term $a^2 V^2 / 4\pi f$ is negligible and we obtain

$$\frac{1}{Q} = \frac{aV}{\pi f} = \frac{2aV}{\omega} = \frac{\Delta}{\pi} = \tan\theta$$

(2.27)

Additionally,

$$\frac{1}{Q_p} = \tan\theta_p = \frac{\Delta_p}{\pi},$$

(2.28)

$$\frac{1}{Q_s} = \tan\vartheta_s \frac{\Delta_s}{\pi}.$$

(2.29)

$$\alpha_p = \frac{8.686\pi f}{Q_p V_p} dB/m$$

(2.30)

$$\alpha_s = \frac{8.686\pi f}{Q_s V_s} dB/m$$

(2.31)

where Δ is the logarithmic decrement (natural log of the ratio of the amplitudes of two successive cycles an exponentially decaying sine wave), θ is the loss angle, and $\alpha = 8.686a$) is the attenuation coefficient in decibels per unit length (dB/m). V_p is the compressional wave speed, V_s is the shear wave speed, and Q_p, and Q_s are the specific attenuation factors for compressional and shear waves.

The wave speed, specific attenuation factor, and logarithmic decrement are independent of frequency if the attenuation coefficient is proportional to the first power of frequency. Otherwise, if 1/Q is independent of frequency, α will be linearly related

to that parameter. In recent literature (Mitchell and Focke, 1980; Kibblewhite, 1989) it is reported that Q is independent of frequency only in very dry rocks or over a restricted bandwidth in wet rocks. It has been demonstrated that pore fluids control attenuation in porous sands and sandstones and that the sound speed and attenuation of elastic waves in these media are dependent on pressure and the degree of saturation involved.

b. Kelvin-Voigt model

The homogeneous viscoelastic model generally recognized in connection with rocks and sediments is the solid model of Kelvin-Voigt. This is often represented by springs and viscous dashpot in parallel, an arrangement that leads to a viscoelastic relationship in which stress is not directly proportional to strain, as it is in Hookean elasticity, but is proportional to time rate of change of strain as well. Such models are rarely used because of the mathematical complexity involved (Kibblewhite, 1989).

2.2.2. Physical sediment models

In porous, permeable sediments, three mechanisms are generally considered to account for most of the observed response to acoustic waves: scattering, frictional losses at grain-grain contacts, and viscous losses due to relative motion between pore fluid and sediment frame.

a. Suspension models

In this approach, sediment is considered as a composite medium consisting of an emulsion of solid particles in a continuous liquid phase. The theory assumes that the medium has no frame rigidity. While successful in some applications, the model is not applicable in fluid-saturated media in which the skeletal frame must be attributed with appreciable rigidity (Kibblewhite, 1989). Later, skeletal effects are included in describing the interactions between the two components of a saturated porous medium. He formulated a "closed system" in which no pore fluid motion is allowed to take place. This model predicts sound speed in sediments if the moduli of the sediment

components are known. Attenuation due to frame friction has to be assessed by experimental observations.

b. Biot-Stoll sediment model

This approach to sediment modeling was discussed earlier (section 2.1.5). The initial Biot model assumed a perfectly elastic sediment frame. Stoll allowed for losses due to frictional effects at grain-grain contacts. The Biot-Stoll theory, despite its limitations, remains one of the most promising approaches to this complex problem.

Discrepancies between the literature data and predictions using Biot-Stoll Model (BSM) lead to the assumption that in unconsolidated fine-grained marine sediments, an additional absorption mechanism occurs that is activated during the excitation by compressional waves that is not covered by the BSM. Leurer (1997) introduced such a mechanism into the BSM. The formulation of the Effective Grain Model (EGM) is based on the assumption that the description of the grain material by a normally assumed constant real bulk modulus is not adequate in the case, in which the sediment has a significant clay fraction and swelling clay minerals are present. The grain material is therefore treated as an effective medium with an anelastic response to stress waves, described by a complex frequency-dependent bulk modulus. The associated relaxation mechanism consists of the stress-induced motion of the interlayer water into the pore space and its reentry into the interlayer space of the crystallite. This process includes the fluid motion caused by the squeezing of the thin interlayer-water films and can therefore be regarded as a squirt-flow process (Mavko and Nur, 1975), a phenomenon that is generally characterized by locally restricted fluid flow.

Swelling clay minerals to various amounts, encountered in nearly all clay-bearing marine sediments. In the case that the clay fraction of the sediment consists totally of nonswelling clay minerals the EGM is insignificant and the original BSM applies. Including the EGM leads to a comparatively good fit to existing literature data and is in agreement with the observed linear frequency dependence of the attenuation coefficient in the range of a few kHz to about 1MHz. The limitation of the applied distribution

causes the EGM curves to gradually converge with the curves of the BSM at lower frequencies and with those of Biot model at higher frequencies. Although the EGM showed comparatively good fit to existing data, a reliable test of its capability can only be carried out by further experiments on physically well-described sediment samples.

c. Buckingham's Theory

Toksoz et al. (1979), Johnston et al. (1979), and Winkler and Nur (1982) experimentally identified some form of internal friction as being responsible for the characteristic attenuation exhibited by granular materials. Buckingham (1997) pointed out that the Biot- Stoll theory does not account for the *characteristic attenuation* in granular materials over an extended frequency range. The term *characteristic attenuation* was introduced by Buckingham (1997) to identify the component of attenuation that scales accurately as f^1 corresponding to a constant quality factor Q. In a series of publications he introduced a unified theory of sound propagation in saturated marine sediments on the basis of a linear wave equation. In his first publication, Buckingham (1997) included a new dissipation term representing internal losses arising from inter-particle contacts. In his paper Buckingham (1997) considered pore-fluid viscosity to be insignificant compared to inter-granular friction in saturated marine sediments. A new model of the mechanical properties of sediments is developed based on the idea of randomly packed rough mineral grains. When the mechanical model is coupled to the wave theory through a simple relationship between a frictional coefficient and the grain size, expressions are obtained that relate the acoustic properties (wave speed and attenuation) to the mechanical properties (grain size, density, and porosity). The resultant relationships between the acoustical and mechanical properties (e.g., sound speed and porosity) of marine sdiments are shown to follow the trends of published experimental data sets very closely.

In his second paper of the series, Buckingham (1998) considered the theory of compressional and shear waves in fluid-like marine sediments in which medium is treated as a fluid that supports a dissipative rigidity, which is capable of supporting shear. This behavior is distinct from that of a viscous fluid, for which the shear

equation is diffusion like in character, giving rise to critically damped disturbances rather than propagating waves. Buckingham (1998) compared the predicted values of attenuation coefficient for both compressional and shear waves. He claims that the attenuation coefficient for both the compressional and shear wave is proportional to the first power of frequency, in accord with published data. However, the data used by Buckingham (1998) for the comparison mostly represented measurements above 1 kHz and he extended the fitted power line to the lower frequency end. Stoll (1985) reported that in the frequency range from 10-500 Hz, many new *in situ* measurements from different geologic settings fall well below the data used to justify the assumption of first power dependency. It is true in the case of Buckingham's comparison study also. Below 1 kHz, few data points shown in his comparison study indicate more deviation from the fitted line. So, Buckingham's conclusions on attenuation coefficient for both compressional and shear waves that scales with the first poer of frequency is unacceptable in the case of entire frequency range. As the new theory needs more evaluation for predicting sound speed and attenuation in marine sediments this is not considered further in this study.

d. Relaxation time –attenuation model

Haumeder (1986) derived the relaxation time for a porous, fluid-filled material on the basis of the Biot theory. The porous material acts as a band-pass filter with respect to broad-band acoustic energy and the fraction of energy that is transferred into the interior of the porous material is used to drive the internal flow. For many frequencies this internal flow will follow the excitation by the pressure wave with a delay. Such a delay results in energy dissipation due to relaxation. Relaxation can be described best in terms of a characteristic response time, the so-called relaxation time, τ. The porous material acts as a band-pass filter with respect to broad-band acoustic energy, and the fraction of energy that is transferred in to the interior of the porous material is used to derive the internal flow. For many frequencies this internal flow will follow the excitation by the pressure wave with a delay. Such a delay results in energy dissipation due to relaxation. Relaxation can be described best in terms of a

characteristic response time, the so-called relaxation time, τ. Relaxation times are expressed entirely in terms of flow parameters, which give evidence that the underlying microscopic process is a flow process. With a knowledge of the relaxation time, the response of the attenuating medium can be completely characterized and hence the equation of Haumeder (1986) is opted for computing compressional wave attenuation in this study.

Haumeder (1986) derived equation for compressional wave attenuation coefficient,

$$\alpha = \frac{\omega}{V\sqrt{2}}\sqrt{-1 + \frac{1}{1+[\omega\tau + \frac{F_i}{F_r}]^2}\{[K\omega^2\tau^2 + \frac{F_i}{F_r}]\pm\sqrt{[1+\{\omega\tau+\frac{F_i}{F_r}\}^2][1+\{[\omega\tau+\frac{F_i}{F_r}]-K\omega\tau\}^2]}\}}$$

(2.32)

where

$$K = \frac{n\rho_f}{\rho},$$

(2.33)

and

$$F(\kappa) = F_r(\kappa) + F_i(\kappa)$$

(2.34)

$$\tau = \frac{\rho k}{n\eta}F_r.$$

(2.35)

where ρ is the bulk density, n is the porosity in decimal fraction and k is the coefficient of permeability of the porous frame with dimension (L^2). τ has the dimension of a time

44

and can be identified as a relaxation time. This typical response time of the porous material is entirely expressed in terms of parameters that are descriptive of the internal flow of the pore fluid through the frame, i.e., permeability k, fluid density, viscosity, and the real part of the frequency correction factor F_r. K is a dimensionless factor that is determined by the density ratio of the fluid and porous material. This factor introduces an altered frequency into the attenuation formula.

The above equation valid for all frequencies takes the form

$$\alpha = \frac{\omega}{V\sqrt{2}}\sqrt{-1 + \frac{1}{1+\omega^2\tau^2}\{K\omega^2\tau^2 \pm \sqrt{[1+\omega^2\tau^2\ ][1+\omega^2\tau^2\{1-K\}^2]}\}}$$

(2.36)

when $f \to 0$, $F_i/F_r \to 0$

For the case of a pure liquid ($n = 1$), K equals one and the above equation takes the form of the well-known formula for relaxation attenuation in a viscous fluid:

$$\alpha = \frac{\omega}{V\sqrt{2}}\sqrt{-1 + \frac{1}{1+\omega^2\tau^2}[\omega^2\tau^2 \pm \sqrt{[1+\omega^2\tau^2]}]}$$

(2.37)

This shows that the formula is capable of producing proper results in the limit n = 1. The derivation of complex correction factor is valid only for frequencies where the wave length is large comparted with the pore size. For sands, this puts the upper limit on frequencies at about 10^5 to 10^6 Hz (Haumeder, 1985).

2.2.3. Effect of temperature on sound speed and attenuation in marine sediments

Rajan and Frisk (1992) conducted a study on the variation of compressional wave speed in sediments due to the temperature variability in the water column of the shallow waters of Gulf of Mexico. They used temperature data collected at different

45

seasons and at the same location for the study. It was hypothesized that heat flow from the bottom of the water column into the sediment affects the sediment pore water temperature, there by influencing the temperature structure and thus the compressional wave speed in the sediments. Since this heat flux varies with season, the effect on sediment wave speed should also change seasonally.

In the shallower depths (< 30m) of the Gulf of Mexico, seasonal fluctuations in ocean bottom temperature as great as 15°C have been observed (Rajan and Frisk, 1992). They investigated the heat flux across the water/sediment interface and using Biot-Stoll model for the sediments, assessed its effects on the compressional wave speed in the sediment layers. They reported that the compressional wave speed varies approximately linearly with pore water temperature, independent of both the porosity and sediment type. The study showed that temperature induced variations in the bottom compressional speeds can have important effects on the prediction of the pressure field in the water column (especially at higher frequencies), and also on source localization schemes like matched-field processing.

Ali (1993) made a study on the oceanographic variability in shallow water acoustics and the dual role of the sea bottom. He reported that, while sea bottom plays a significant part in degrading a waterborne signal, it could also provide an additional seismic path for the propagation of sound – particularly at very low frequencies.

Due to the variability in oceanographic conditions, density of pore water (seawater at the ocean bottom) varies with the change in temperature and salinity of the bottom water. As the saturated bulk density of the sea floor sediment depends on the pore water density for a given porosity, density of the sediment also indicates corresponding variation. Shumway (1958) reported that in seawater of 35 PSU salinity, density changes by about 6% when temperature varied between 0°C and 100°C. In quartz, the variation in density is 0.36% when temperature varies between 20°C and 100°C, while in calcite density changes by 0.08% in the same temperature range. Accordingly, sound speed in sediment also varies with the change in oceanographic conditions of the bottom water.

A number of laboratory and *in situ* studies of sound speed in unconsolidated water saturated sediments have been reported in literature (Hamilton, 1963, 1970, 1972; Fu *et al.*, 1996, Best *et al.*, 1998). But very few sound speed measurements at different temperatures have been reported (Sutton *et al.*, 1957, Shumway, 1958, Leroy *et al.*, 1986).

Sutton *et al.* (1957) made sound speed measurements at different temperatures on two samples and the effect of temperature on compressibility was reported. Shumway (1958) measured sound speed as a function of temperature in different types of sediments using the resonant chamber technique. He concluded that temperature effect on these water-saturated sediments was approximately the same as that for water alone and is due to the large water compressibility dominating over the water-sediment mixture. The temperature effect on water compressibility is considerable whereas it is small for calcite and quartz.

Leroy *et al.* (1986) made laboratory measurements of sound speed against temperature variation. They reported a variation of about 150 m/s (1725 to 1875 m/s) in sound speed in sand for a temperature variation of 60°C (5 to 65°C).

Pradeep Kumar and Murty (1993) in their study, considered the effect of variation of temperature on pore water density and sediment density for computing sound speed in sediment using Biot-Stoll model. The data on the variability of the temperature at the sea bottom is obtained from the monthly hydrocast and mechanical bathythermograph (BT) data of 12 months collected from the same location, off Cochin. The temperature of the bottom water 1 meter above the sea floor is taken as the pore water temperature at the time of measurement.

Pradeep Kumar (1997) studied the seasonal variation of relaxation time and attenuation in sediment at the sea bottom interface based on Biot-Stoll and Haumender models. Biot-Stoll model is used for computing sound speed in marine sediments and

relaxation time- attenuation model (Haumender, 1986) is used for computing attenuation.

Pradeep Kumar (1997) in his study included the effect of variation of temperature on the viscosity of pore water to account for the variability in viscous loss. Viscosity of seawater decreases rapidly and non-linearly with temperature rise (Sverdrup et al., 1942; Dera, 1992). Increasing salinity raises the viscosity of seawater slightly. The relationship between viscosity and pressure is a more complex one, highly dependent on the temperature and salinity (Dera, 1992). The pressure rise at low temperatures slightly reduces the viscosity; but this reduction in viscosity is only slight. For estimating viscosity of pore water at the bottom temperature, the data given for different values of the temperature at salinity of 35 PSU by Sverdrup et al. (1942) are used. Effect of variation of salinity and pressure on viscosity is very small and hence neglected in this study. The viscosity of the sea bottom water is computed by fitting the following equation to the Sverdrup et al. data. The fitted equation (Pradeep Kumar, 1997) is

$$\eta_{t,35} = 0.0183534e^{-0.025748t} \qquad\qquad (2.38)$$

here $\eta_{t,35}$ is the viscosity of sea water at a temperature t, and salinity 35 PSU.

In this study, Haumender's (1986) equation is used to compute the variation in compressional wave attenuation due to the change in bottom water temperature and the above equation is used for estimating pore water viscosity. It is also hypothesized that heat flow from the bottom of the water column into the sediment affects the sediment pore water temperature, thereby influencing the temperature structure, pore water viscosity and thus the compressional wave speed and attenuation in the sediments. Details of the study are included in Chapter 6.

CHAPTER 3

SEASONAL VARIATION OF TEMPERATURE, SALINITY, DENSITY, AND SOUND SPEED IN WATER AT THE SEA BOTTOM - OFF THE WEST COAST OF INDIA

In this chapter the details of the seasonal variation of temperature, salinity, density and sound speed at selected areas off the west coast of India are included. The variability of temperature and sound speed at the sea bottom interface is also discussed.

3.1. Introduction

The spatial and temporal variations of the temperature and salinity in the ocean are controlled by a number of physical processes in the atmosphere and oceans. In certain parts of the World Ocean, temperature variations can penetrate to depths far below the thermocline because of seasonal variability of warm and cold currents, as well as downwelling (sinking) and upwelling. In the zones of strong currents (Kuroshio, California Currents), the total amplitude of annual variation of temperature may reach 2 to 3°C even at depths of 500 to 600 m (Monin et al., 1977). In the east Australian current region, the seasonal variations can be observed to depths greater than 1000 m. Elliott et al., (1991) discussed the monthly distributions of surface and bottom temperatures in the northwest European shelf seas as a part of modeling of the thermal structure of shallow seas. In the shallower depths (< 30 m) of the Gulf of Mexico, seasonal fluctuations in the ocean bottom temperature as great as 15°C have been reported (Rajan and Frisk, 1992).

In the Arabian Sea and Bay of Bengal, the seasonal variations of the currents are caused by the summer and winter monsoons. Seasonal reversing winds associated with the summer and winter monsoons and the resultant circulation have profound influence in modifying the temperature distribution in the Arabian Sea and Bay of Bengal. It is reported that seasonal variability of both the wind and the currents is much stronger in the Arabian Sea than in the Bay of Bengal and the summer peak is stronger than the winter peak. The monsoon effects can be traced north of 10°S, to a depth of 400 m in the western part of the Indian Ocean, and to 100 m in its central and eastern parts (Duing, 1970).

In the Arabian Sea, the sea surface temperature (SST) exhibits a bimodal pattern in the annual cycle with warming during pre-monsoon and post-monsoon months and cooling during winter and summer (Colborn, 1975) and its amplitude exhibits both spatial and temporal variations. In the eastern Arabian Sea the SST maximum (>30°C) generally occurs during April-May (Joseph, 1990) while SST as low as 20-22°C is noticed near the coast during July-September (Pillai et al., 1980) especially in the coastal region.

Upwelling off the southwest coast of India was reported during summer monsoon (Ramasastry and Myrland, 1959, Banse, 1959; Ramamirtham and Jayaraman, 1960). The annual cycle of temperature/density distribution suggests the occurrence of upwelling from March-August off the southwest coast of India and sinking between November and February (Sharma, 1966, 1968,1978; Pillai et al., 1980; Mathew, 1983). Ramamurty (1963), Patil et al., (1964) and Noble (1966) studied the variability in temperature-salinity structure off the Karnataka coast for selected seasons. Hareeshkumar (1994) studied the thermohaline variability in the upper layers off the west coast of India on an annual cycle.

The salinity of seawater is a more conservative characteristic, and its seasonal variations are much less conspicuous in the open ocean. The salinity variations in the surface layers of the eastern Arabian Sea is controlled by evaporation, the inflow of high saline waters from northern Arabian Sea, low saline waters from Bay of Bengal/Equatorial Indian Ocean and river discharges (Darbyshire, 1967; Wyrtki, 1971; Johannessen et al., 1981; Pankajakshan and Ramaraju, 1987). The Arabian Sea has high surface salinity values up to 36.5 PSU, while in the Bay of Bengal the salinity decreases from about 34 PSU at about 5°N to 29 PSU or less in the north (Pickard and Emery, 1985; Shetye et al., 1991). However, close to the coastal regions of the Arabian Sea, it exhibits large seasonal variation due to the effect of fresh water influx from rivers, intrusion of Bay of Bengal water and evaporation.

Most of the studies on the temperature and salinity in the Arabian Sea are mainly confined to the upper layers of the water column. Studies on the bottom temperature and salinity are not available. The bottom temperature and its seasonal variation have lot of

influence in modifying the acoustic properties of sediments. Hence an attempt is made to bring out certain aspects of the seasonal variability of temperature, salinity, density and sound speed in the continental shelf along the west coast of India. Six areas selected for the study (Fig.3.1) are listed below.

i)   Off Quilon,

ii)   Off Cochin,

iii)   Off Kasaragod,

iv)   Off Karwar,

v)   Off Ratnagiri, and

vi)   Off Bombay.

At each study areas, two stations are selected in such a way that the maximum depth at these stations are 50m and 100m. These stations are denoted by SD50 and SD100 respectively.

3.2. Data

The data sets utlised in this study are obtained from the National Oceanographic Data Centre (NODC), Washington, Indian National Oceanographic Data Centre (INODC), Goa, and Pelagic Fisheries Project. A detailed quality check was carried out (Levitus, 1982) to these data sets and only the good profiles are accepted. The density of the sea water is computed using the International Equation of State of Sea Water (Millero and Poisson, 1981, Pond and Pickard, 1986) and sound speed is computed using Mackenzie's (1981) equation. Computational details are discussed in chapter I.

In order to obtain the broad scale features of the temperature, salinity, density and sound speed variations off the west coast of India, their monthly means at the two locations (SD50 and SD100) on the continental shelf off Quilon, Cochin, Kasaragod, Karwar, Ratnagiri and Bombay are presented in Figs. 3.2 to 3.13. The variability of
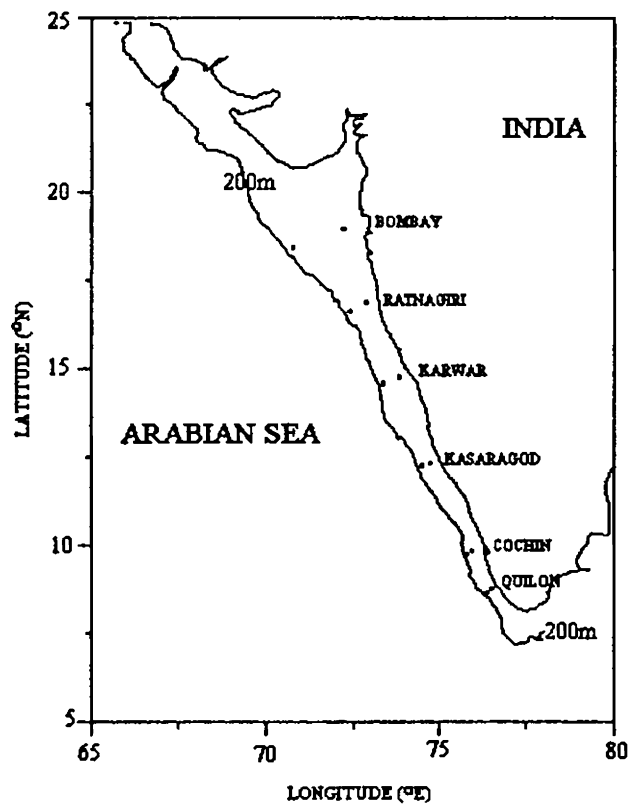
Fig. 3.1. Station location at the study area

temperature, salinity, density and sound speed in bottom water at the bottom layer (for both locations) are shown in Figs. 3.14 to 3.16.

3.3. Off Quilon

The thermal structure at both the locations (SD50 and SD100) shows significant ascending and descending motions over an annual cycle (Figs. 3.2 & 3.3) which is mainly due to the occurrence of upwelling and sinking (Ramasastry and Myrland, 1959). At SD50, the entire water column is warmer ($>27\,°C$) during the period of sinking (January-February) and colder during July ($<24\,°C$). The maximum SST ($>30\,°C$) in April-May is associated with the pre-monsoon heating (Hastenrath & Lamb, 1979). The lowering of bottom water temperature is significant from April to July (>27 to $<19\,°C$). On an annual cycle the surface layer cools by $6\,°C$ ($30\,°C$ in April to $24\,°C$ in July) while a variation of $9\,°C$ (>27 to $<19\,°C$) is noticed at the bottom layer. However the salinity distribution shows a different pattern. The influx of low saline Bay of Bengal water during winter (<34 PSU) and the fresh water discharge during summer monsoon season (<33.5 PSU) causes the occurrence of low saline water at the surface during most part of the year. However, the influence of freshwater is limited to the surface layer while the effect of Bay of Bengal water can be noticed up to 50m depth. As a result high saline waters of Arabian Sea origin is evident at the bottom during major part of the year (April to November). The density (σ_t) and sound speeds follow mainly the thermal cycle and shows an annual variation of 1.5 kg/m^3 (21 kg/m^3 in February to 22.5 kg/m^3 in August) and 12 m/s (1544 m/s in April to 1532 m/s in August) at the surface respectively. The corresponding variation at the bottom (Figs. 3.2, 3.14 and 3.16) is 3 kg/m^3 in density (22 kg/m^3 in March to 25 kg/m^3 in July) and 23 m/s in sound speed (1543 m/s in January to 1520 m/s in July).

At SD100 the upward movement of isotherms is evident from January onwards and continues till July (Fig. 3.3). Here the occurrence of maximum SST coincides with the period of maximum ($30\,°C$ in April) solar heating and minimum ($24\,°C$ in July) during the south west monsoon season (Hastenrath & Lamb, 1979). However, at the bottom, the

Fig.3.2. Monthly distribution of (a) Temperature (°C), (b) Salinity (PSU), (c) Density (Sigma-t), and (d) Sound speed (m/s) Study Area: Off Quioln, at SD50.

Fig. 3.3. Monthly distribution of (a) Temperature (°C), (b) Salinity (PSU), (c) Density (Sigma-t), and (d) Sound speed (m/s) Study Area: Off Quion, at SD100.

maximum is noticed during the period of sinking (27 °C in December-January) and minimum during the peak of upwelling (17 °C in July). This resulted an annual variation of 6 °C at the surface and 10 °C at the bottom. The salinity structure at the bottom is quite different from that of at SD50, as values >35 PSU are noticed throughout the year. This is due to the fact that the influence of Bay of Bengal water mass is mostly confined to the top 60m. At this location also the density and sound speed follows temperature. The density show an annual variation of 1.5 kg/m^3 (21.5 kg/m^3 in February–April to ~23 kg/m^3 in August) at the surface and bottom layer (~23 kg/m^3 in February to 25 kg/m^3 during July-August). However, sound speed shows an annual variation of 12 m/s at the surface (1544 m/s during March-April to 1532 m/s in July) and 27 m/s (1515 m/s in July to 1542 m/s in December) at the bottom (Figs. 3.3 & 315).

3.4. Off Cochin

At SD50 the maximum SST (>31 °C) occur during March-April and minimum during August-September (<26 °C). The warming, due to premonsoon heating and cooling, due to the process of upwelling resulted an annual variation of more than 5 °C at the surface (Figs. 3.4). However, close to the bottom, the temperature is maximum (~28 °C) is noticed during January-March when sinking dominates. The minimum (<20 °C) in August coincides with the period of upwelling. The upward movement of isotherms starts by April and continues upto August. The reverse process, downward movement starts after the withdrawal of summer monsoon (September) and continues upto December. The salinity is minimum in the surface layers during November-January (<33 PSU) when the influx of Bay of Bengal water is significant. During major part of the year (March to November) salinity at the bottom exceeds 35 PSU when the Arabian Sea water mass is present. The variations in density clearly resemble that of temperature except in winter, when it lowers significantly due to the effect of low salinity waters of Bay of Bengal origin. The sound speed in the surface layer reaches maximum during March-April (>1546 m/s) and minimum during August-September (<1535 m/s) whereas in the bottom layers the maximum and minimum occur during February–March (1542 m/s) and August-September (<1522 m/s) respectively (Figs. 3.4 & 3.14). At this location also the
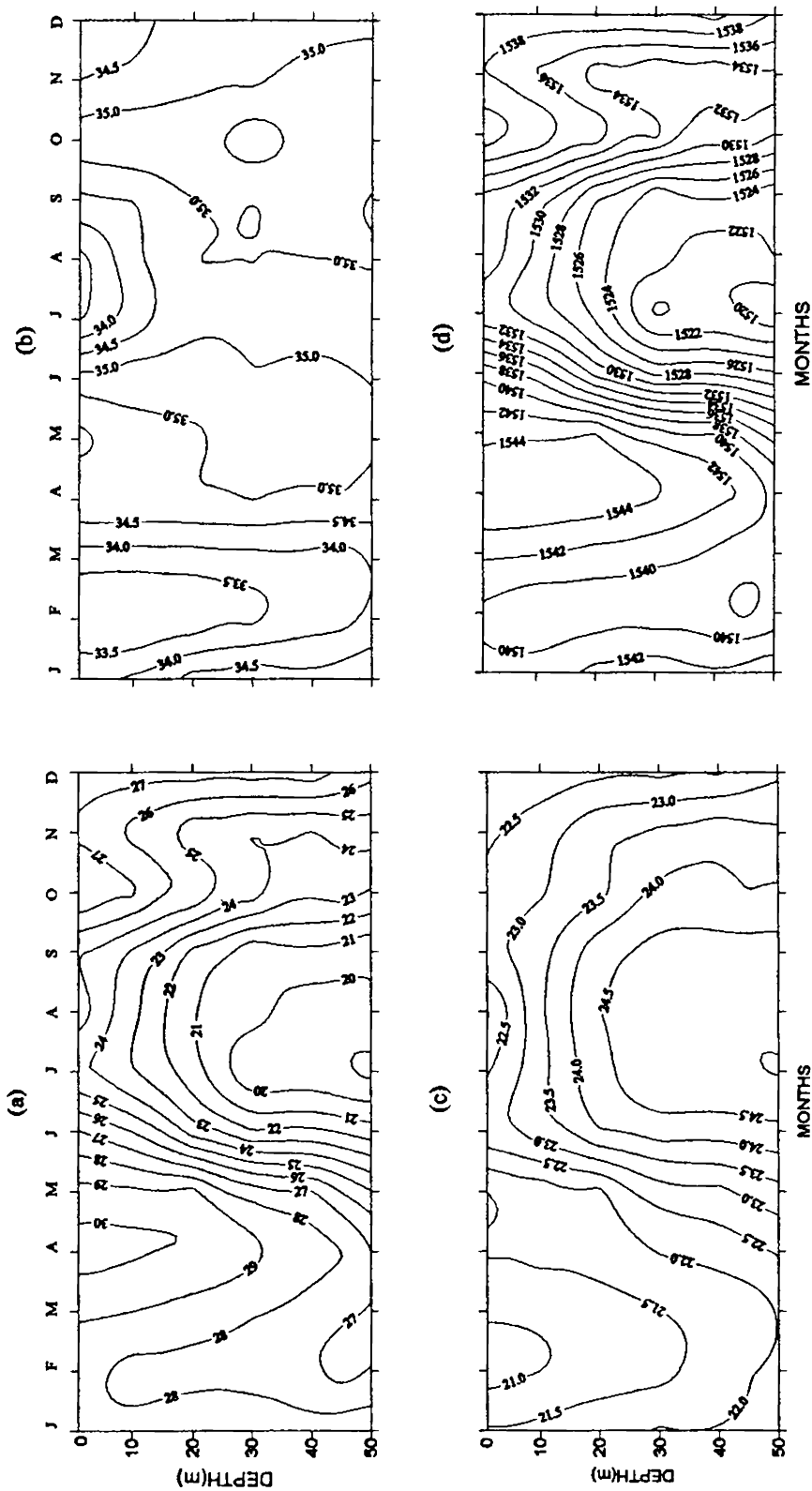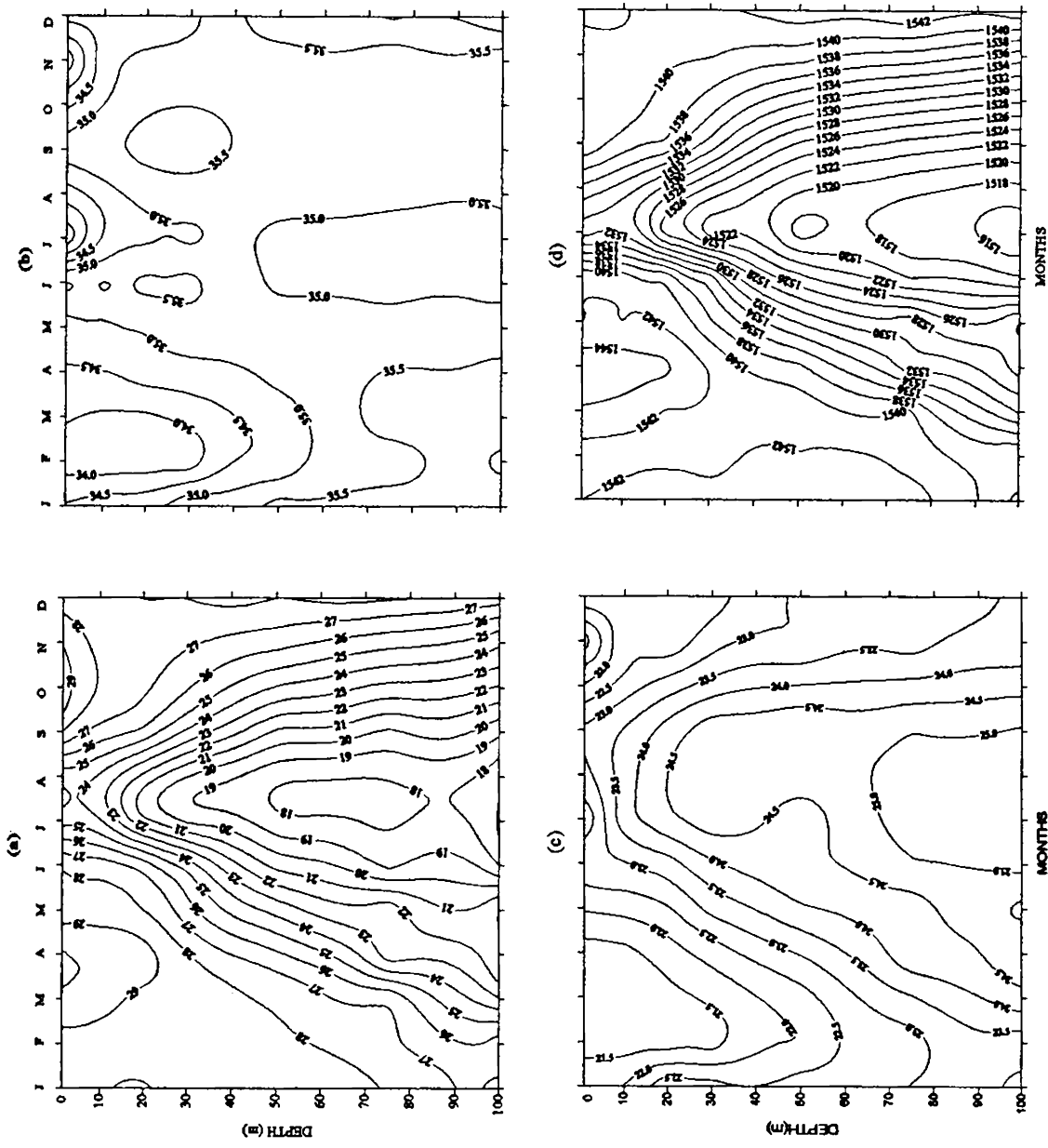
Fig.3.4. Monthly distribution of (a) Temperature (°C), (b) Salinity (PSU), and (c) Density (Sigma-t), and (d) Sound speed (m/s). Study Area: Off Cochin, at SD50.

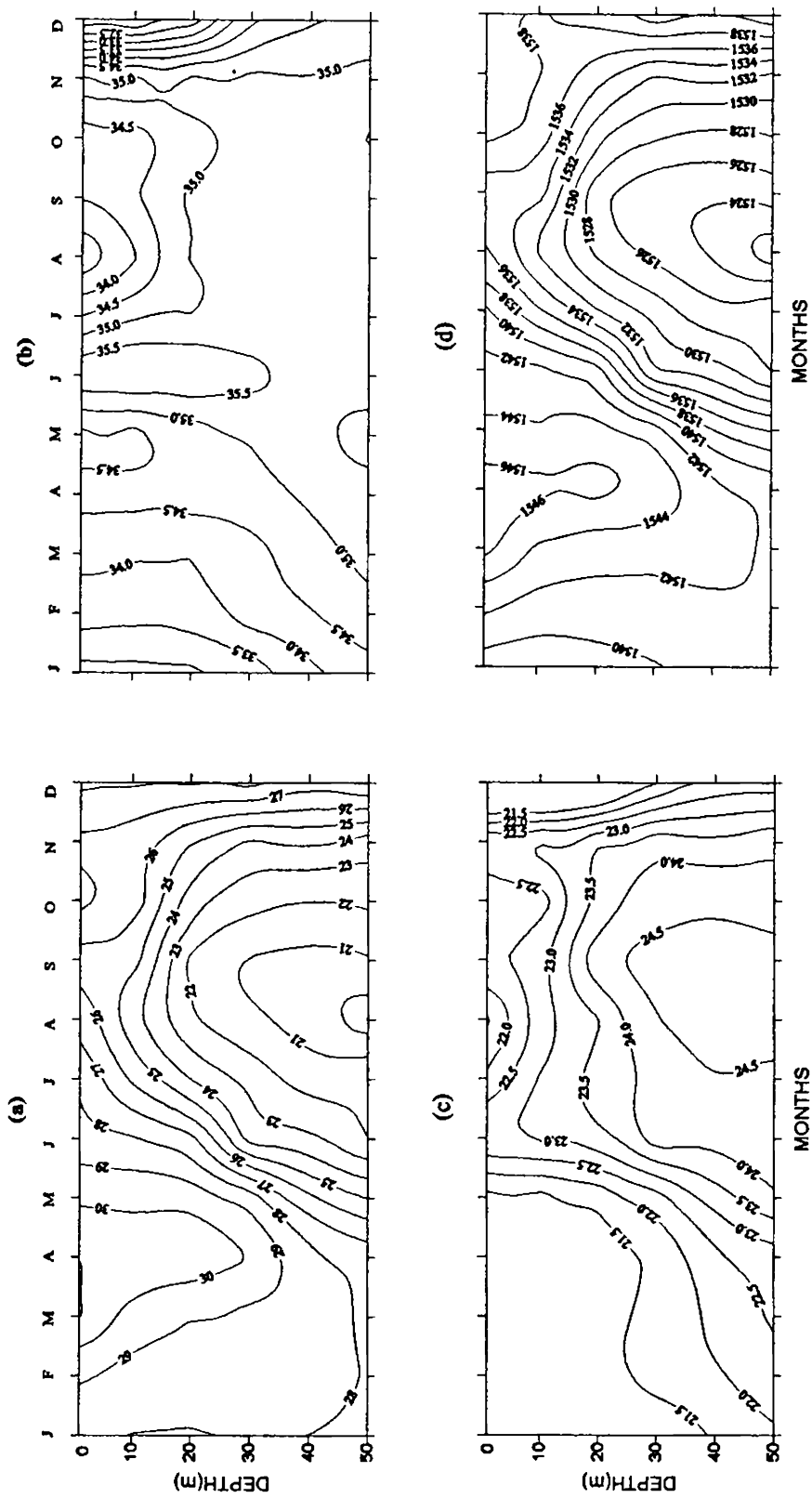Fig. 3.5. Monthly distribution of (a) Temperature (°C), (b) Salinity (PSU), (c) Density (Sigma-t) and (d) Sound Speed (m/s). Study Area: Off Cochin, at SD100.

density and sound speeds exhibits maximum annual range at the bottom (>2.5 kg/m^3 and 20 m/s) than at the surface (0.5 kg/m^3 and 11 m/s).

At SD100 (Fig. 3.5) the pattern of variations in the thermal structure is similar to that of at SD50. Here the upward movement of isotherms starts early (by February) at deeper levels and continues till August. The reverse process commences from September-October. The pre-monsoon heating is also evident in the surface layers during March to May (30 °C). Close to the bottom the annual variation of temperature exceeds 9 °C with the maximum (27 °C) during January-February and minimum (18 °C) during August-September (Fig. 3.15). The vertical salinity structure shows lesser variation (between 34 and 35.5 PSU) compared to SD50 the influence of Bay of Bengal water and fresh water influx are less pronounced at this location. The distribution pattern of density and sound speed follow that of temperature with an annual variation of 1 kg/m^3 and 10m/s at the surface and 2 kg/m^3 and 26 m/s at the bottom respectively.

3.5. Off Kasaragod

The evolution of thermal structure off Kasaragod at SD50 (Fig. 3.6) shows similarities with those off Cochin with SST maximum (>30 °C) and minimum (<26 °C) in March-May and September respectively. The process of upwelling and sinking are well pronounced at this station also. Lowering of temperature in the bottom layers (Fig. 3.14) starts by April and continues upto September. Afterwards warming is noticed (October to March). At the bottom the temperature decreases from ~29 °C in March to 20 °C in September resulting in a variation of 9 °C. The surface salinity structure is complex in the annual cycle with minimum during winter (<34.5 PSU) and August/September (<33 PSU) corresponding to the periods of Bay of Bengal water influx and fresh water influx respectively. High salinity waters (>36 PSU) observed in May corresponds to the Arabian Sea High Salinity Watermass (ASHSW) and occupied the bottom layers (Prasannakumar *et al.*, 1999) during the major part of the year. The surface sound speed also shows high values during pre-monsoon heating regime. Values over 1546 m/s in May and lesser than 1534 m/s in September results an annual variation of 12 m/s in the surface layer. The

Fig.3.6. Monthly distribution of (a) Temperature (°C), (b) Salinity (PSU), (c) Density (Sigma-t), and (d) Sound speed (m/s). Study Area: Off Kararagod, at SD50.
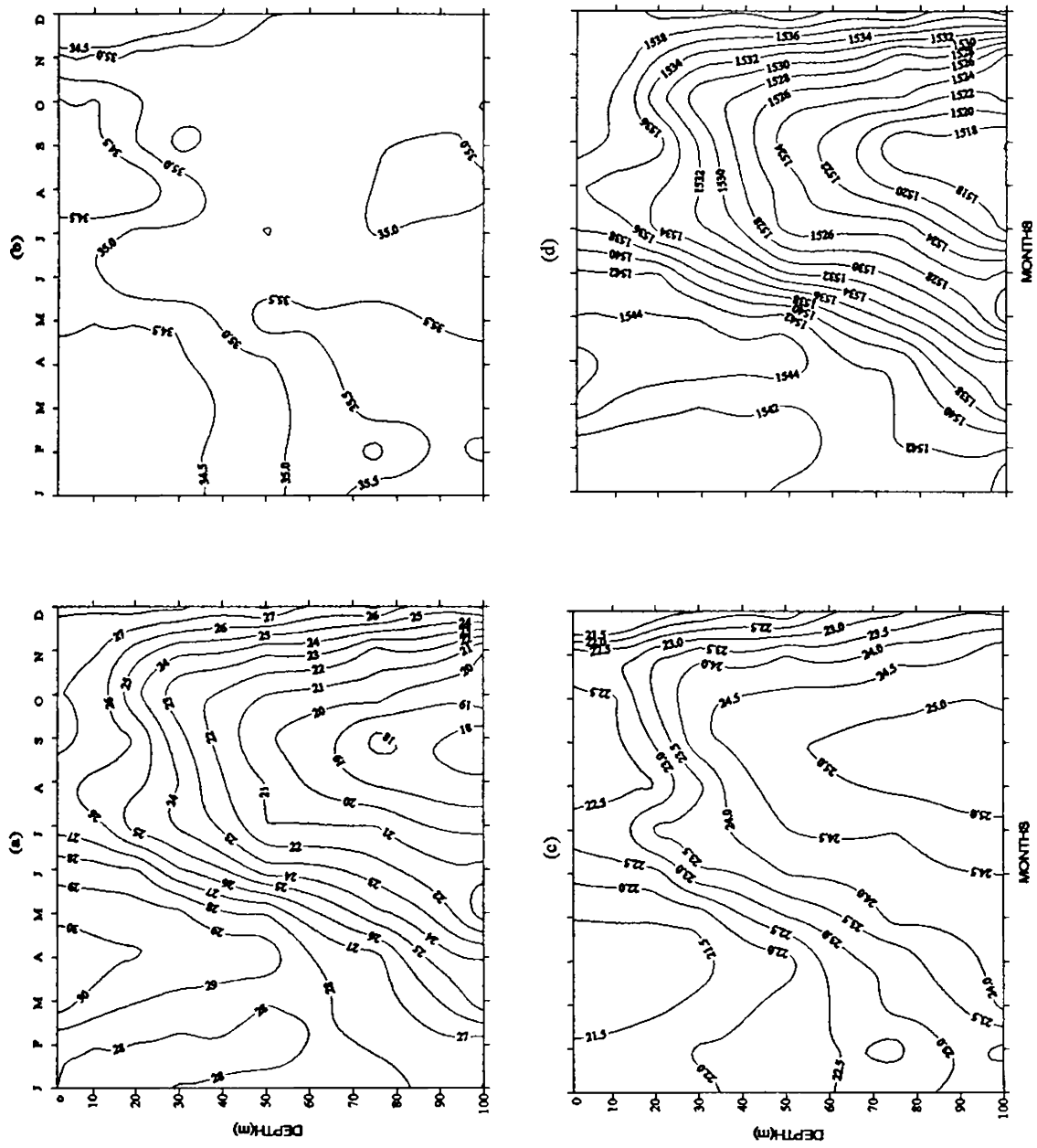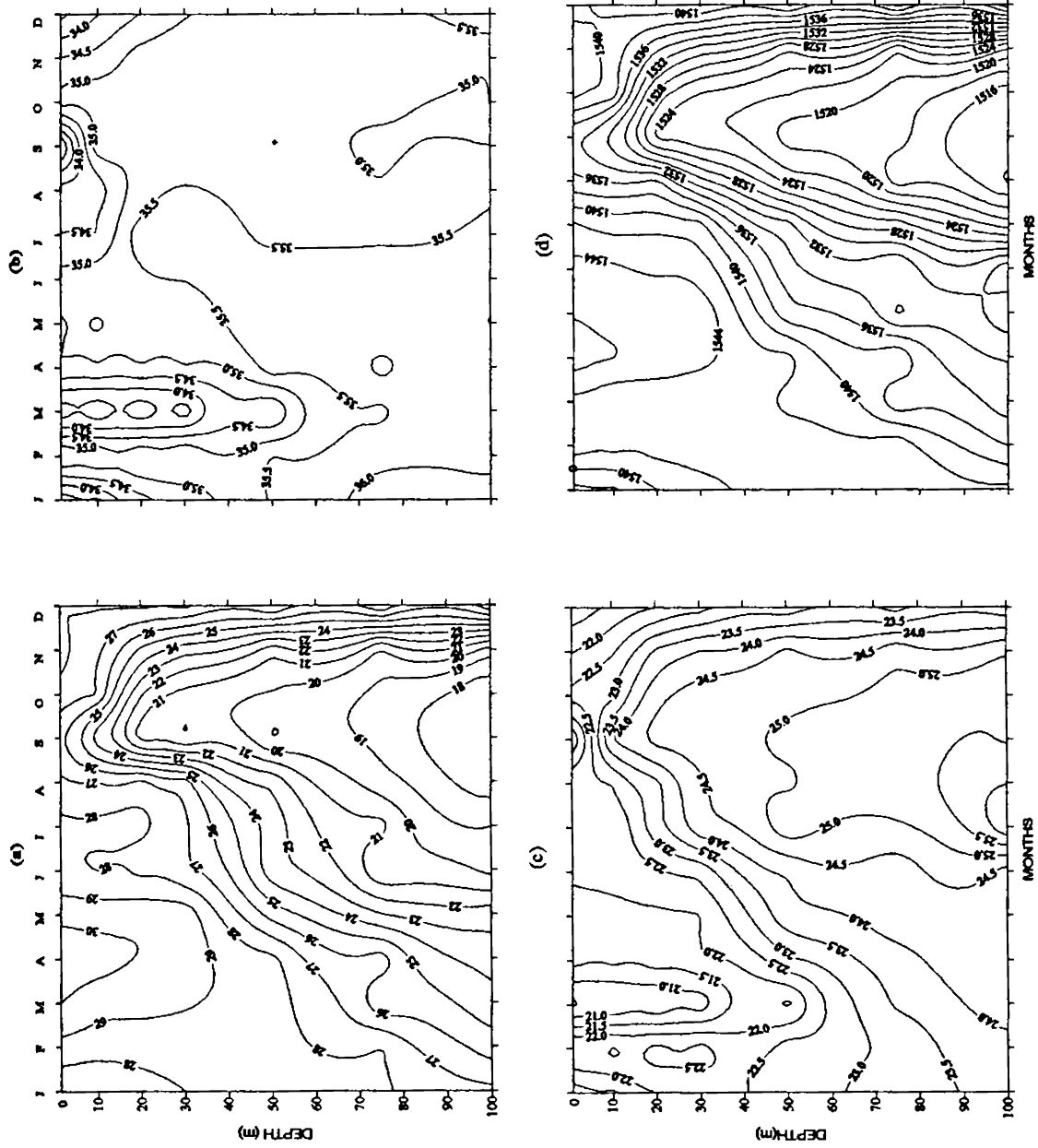
Fig. 3.7. Monthly distribution of (a) Temperature (°C), (b) Salinity (PSU), (c) Density (Sigma-t) and (d) Sound Speed (m/s).
Study Area: Kasaragod, at SD100.

density at the bottom increases from 22 to 25 kg/m³ (January to September) results an annual variation of 3 kg/m³. The sound speed in the bottom water decreases from 1542 m/s to 1522 m/s (variation of 20 m/s) between January and September (Figs. 3.6 & 3.14).

AT SD100 (Fig. 3.7) the ascending motion of isotherms is evident from January and continues upto September. The reverse process, sinking starts in October and continues upto December. The maximum SST (>30 °C) is noticed during the pre-monsoon heating regime. However, at the bottom the maximum temperature (>27 °C) is noticed during December-January. The minimum temperature (<18 °C) occurs during the monsoon season as observed at the other stations. This results in an annual variation of temperature of 9 °C at the bottom (Fig.3.15). As in SD50 the salinity structure is much complex in the surface layer. Here, the salinity is influenced by low saline Bay of Bengal water during winter, high saline Arabian Sea water during pre-monsoon period and fresh water discharge during summer monsoon season. At the bottom only the ASHSW is present throughout the year. As in the other locations the maximum annual variations of density and sound speed are noticed (Figs. 3.6, 3.15 & 3.16) at the bottom (2.5 kg/m³ and 28 m/s) than at the surface (1.5 kg/m³ and 12 m/s).

3.6. Off Karwar

At SD50, the maximum SST occur just before the onset of summer monsoon (30 °C in May) and the minimum (<26 °C) in October which coincide with the peak upwelling period (Fig.3.8). The upward movement of isotherms starts in April and continues upto October and sinking dominates afterwards. In the annual cycle, the SST varies by 5 °C while the bottom temperature varies by 8 °C. The surface salinity variations are similar to those at the other locations, with low saline waters (<34 PSU) in winter and southwest monsoon season and high saline water (>36 PSU) during May-June. One of the notable result is that the bottom salinity variation is more off Karwar (34.5 PSU to 36 PSU) compared to the southern locations. The sound speed is maximum (1546 m/s) at the surface during May-June and minimum (<1536 m/s) during October. The upwelling and sinking process considerably changes the bottom density and sound speed structure. This

Fig. 3.8. Monthly distribution of (a) Temperature (°C), (b) Salinity (PSU), (c) Density (Sigma-t) and (d) Sound Speed (m/s) Study Area: Off Karwar, at SD50.
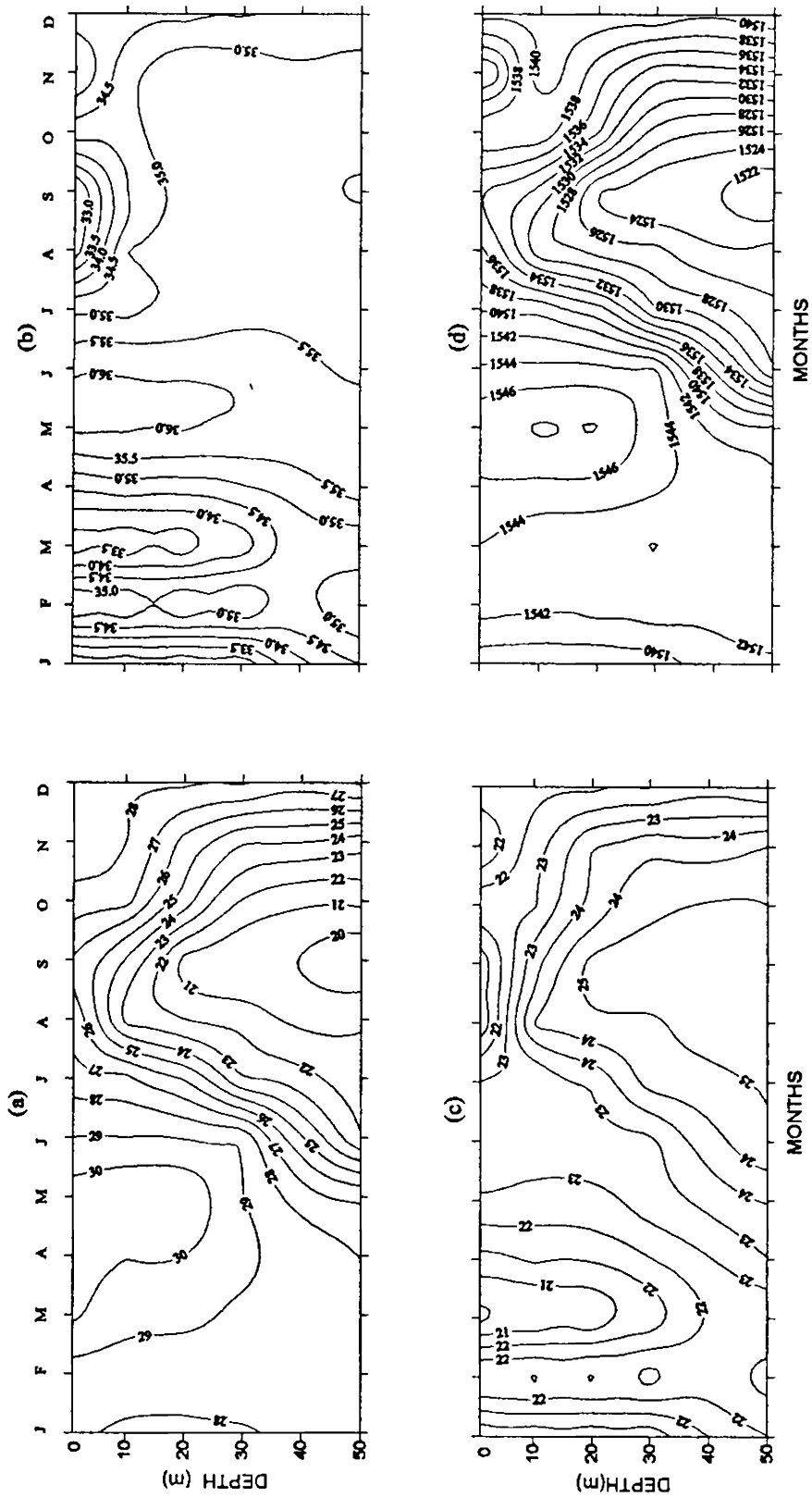
Fig. 3.9. Monthly distribution of (a) Temperature (°C), (b) Salinity (PSU), (c) Density (Sigma-t), and Sound Speed (m/s). Study Area: Off Karwar, at SD100.

indicated a fluctuations of 2.5 kg/m^3 (between 22.5 and 25 kg/m^3) in density and 20 m/s (between 1542 and 1522 m/s) in sound speed.

At SD100 the pattern of changes in temperature, salinity, density, and sound speed (Fig.3.9) is similar to that of at SD50. The upward movement of isotherms is evident from March onwards at deeper levels and continues till October, and from November onwards sinking dominates. Due to the effect of vertical motion, considerable variation of temperature occur at the bottom (9 °C) while SST variation is limited to 3 °C. The variation of bottom salinity is marginal (between 35 and 36 PSU) as only the ASHSW is present. The annual variations is conspicuous of sound speed and density are very less at the surface than at the bottom (0.5 kg/m^3 and 8m/s at the surface, and 2 kg/m^3 and 24 m/s at the bottom).

3.7. Off Ratnagiri

Off Ratnagiri (at SD50), the temperature, salinity, density and sound speed variations at the surface and subsurface levels are significantly smaller that those off the southern stations (Fig. 3.10). The upward movement of isotherms starts by May and continues till November. The SST maximum (30 °C) occurs in May while the minimum (<28 °C) occurs in October resulting in an annual variation of less than 2 °C. At the bottom the annual variation of temperature is less than 6 °C. The effects of influx of low saline water (~34.5 PSU) is limited from January to March and to the upper 20m. At the surface the variation of sound speed is marginal (between 1546 and 1540 m/s). At the bottom the variation of sound speed (Fig.3.14) is more than 15 m/s with maximum (1543 m/s) occur in April and minimum (1528 m/s) in October.

At SD100 (Fig. 3.11) the sea surface features does not vary much from that of SD50. The SST is maximum (~29 °C) in May and minimum during winter (<28 °C). At the subsurface depths the upward movement of isotherms is noticed from January onwards and continues till November. The minimum bottom temperature occur in November (<19 °C) which coincides with the sound speed minimum of 1520 m/s. The
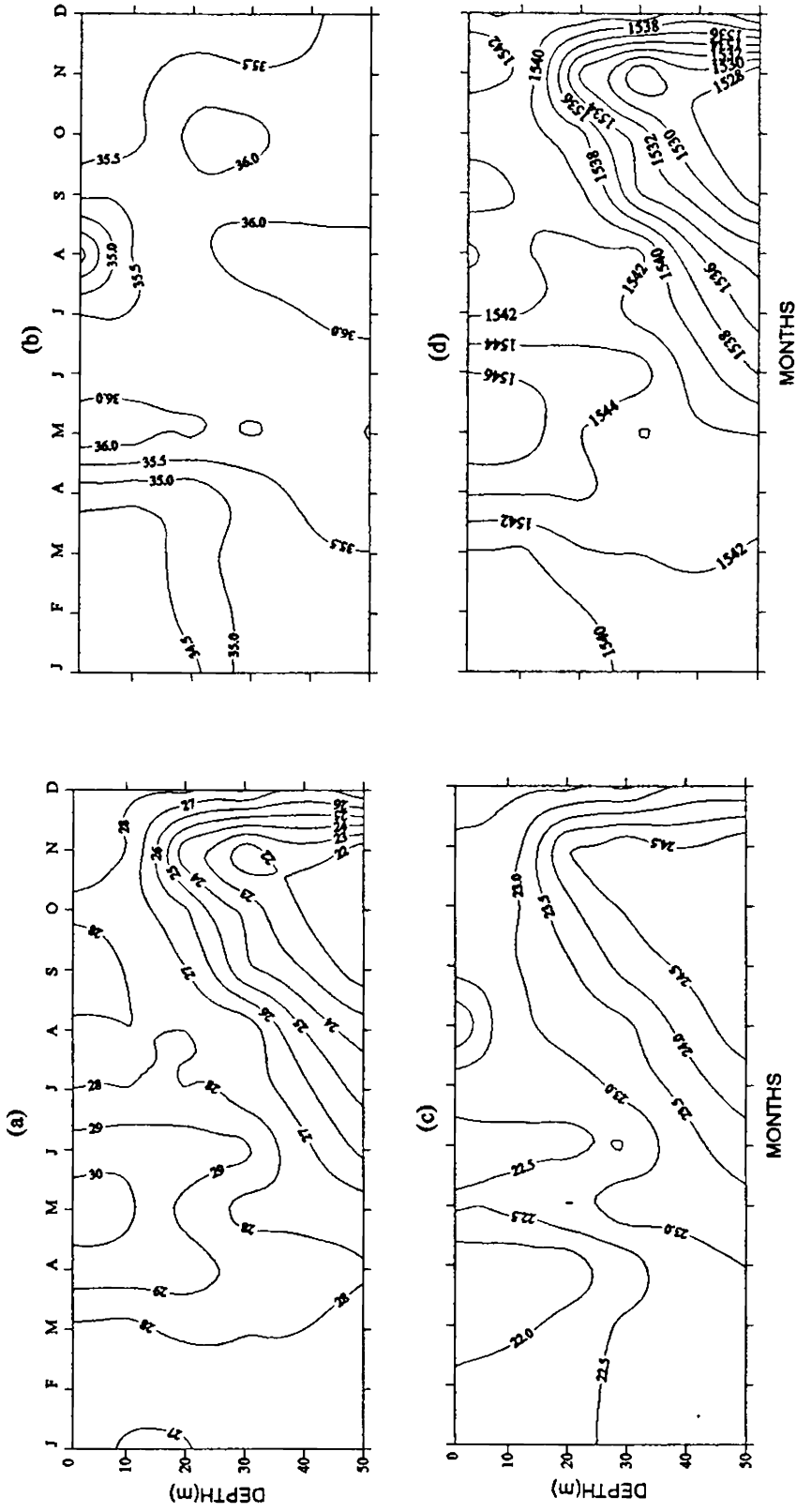
Fig. 3.10. Monthly distribution of (a) Temperature (°C), Salinity (PSU), (c) Density (Sigma-t) and (d) Sound Speed (m/s). Study Area: Off Ratnagiri, at SD50.
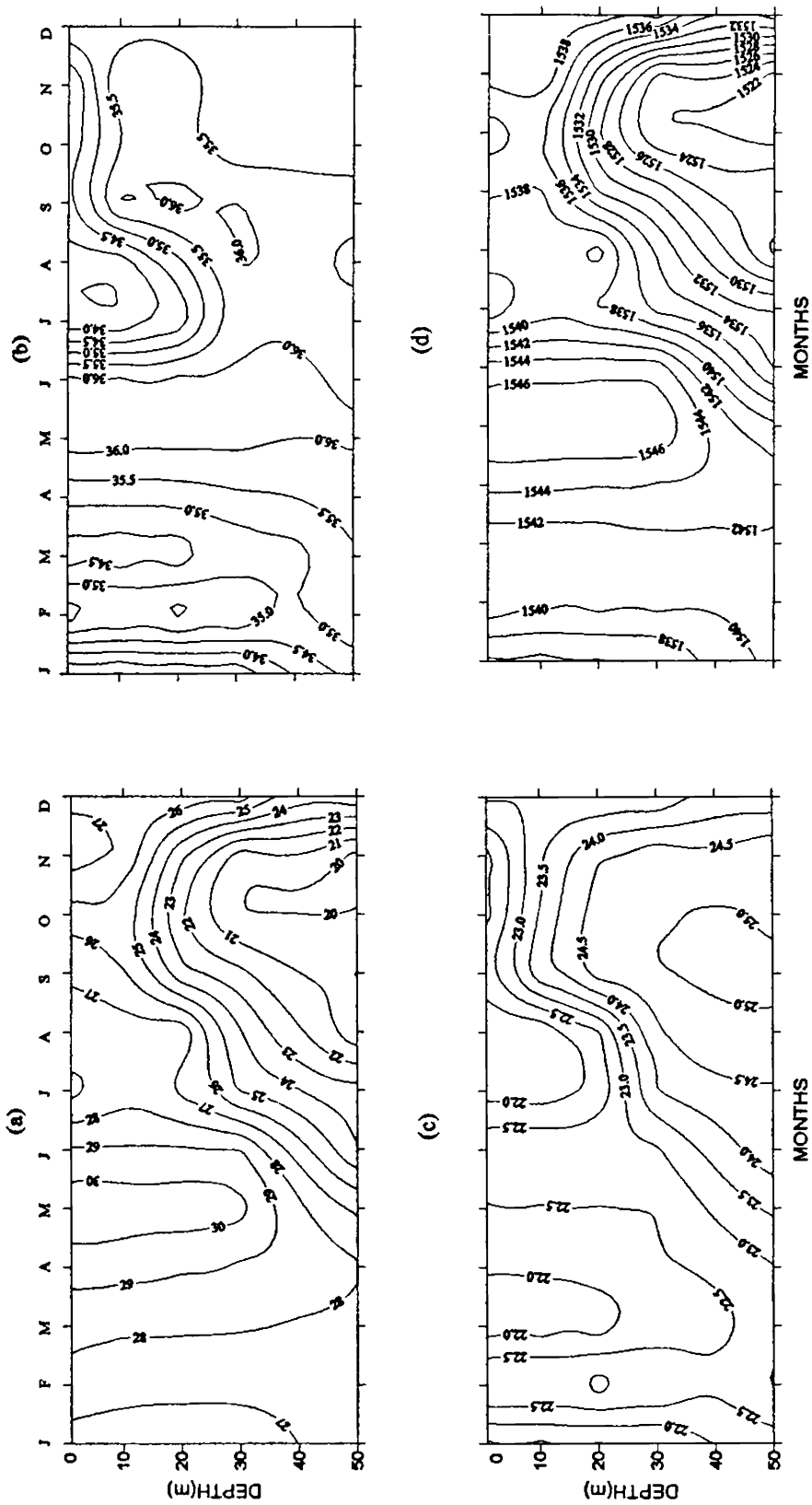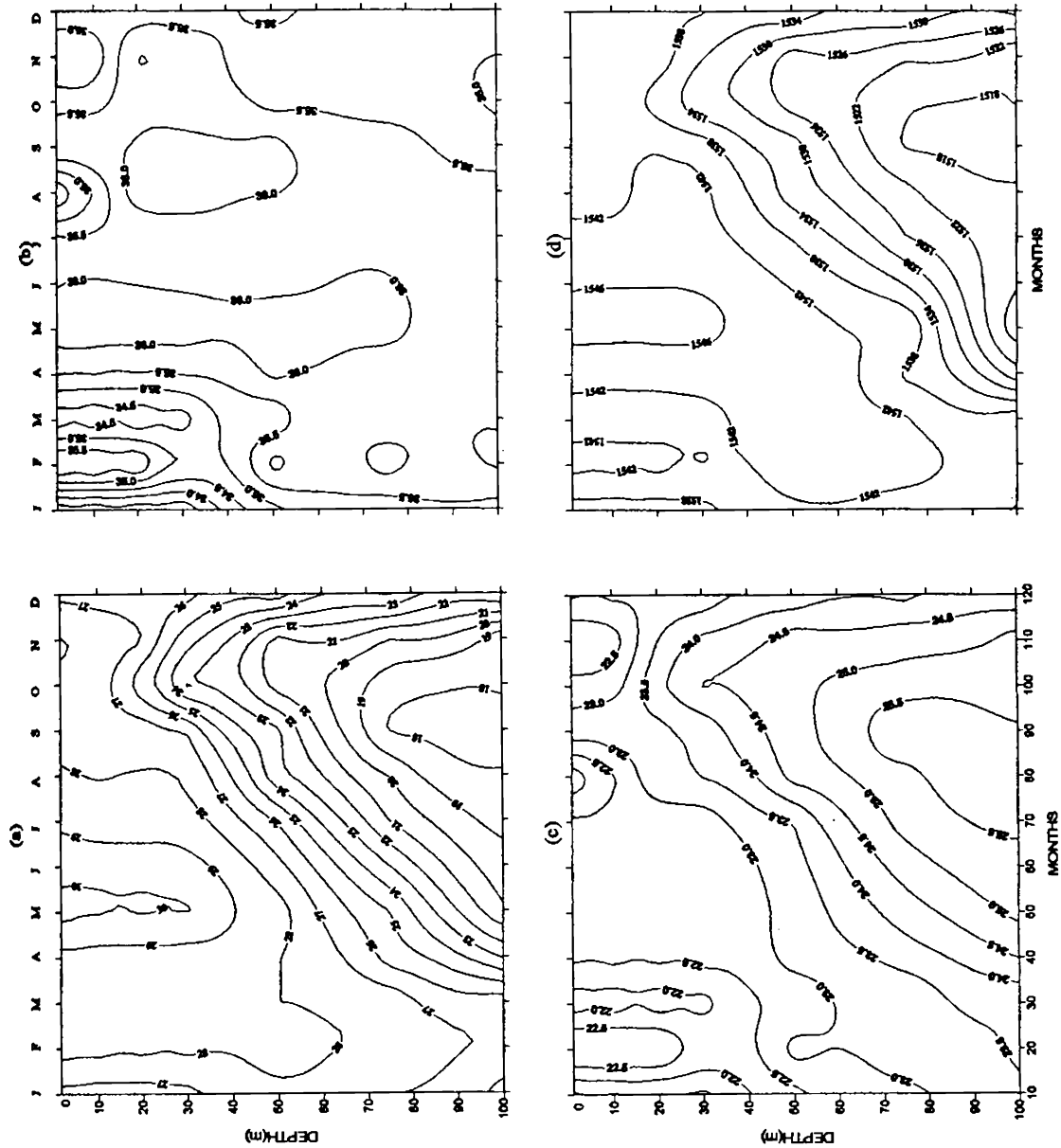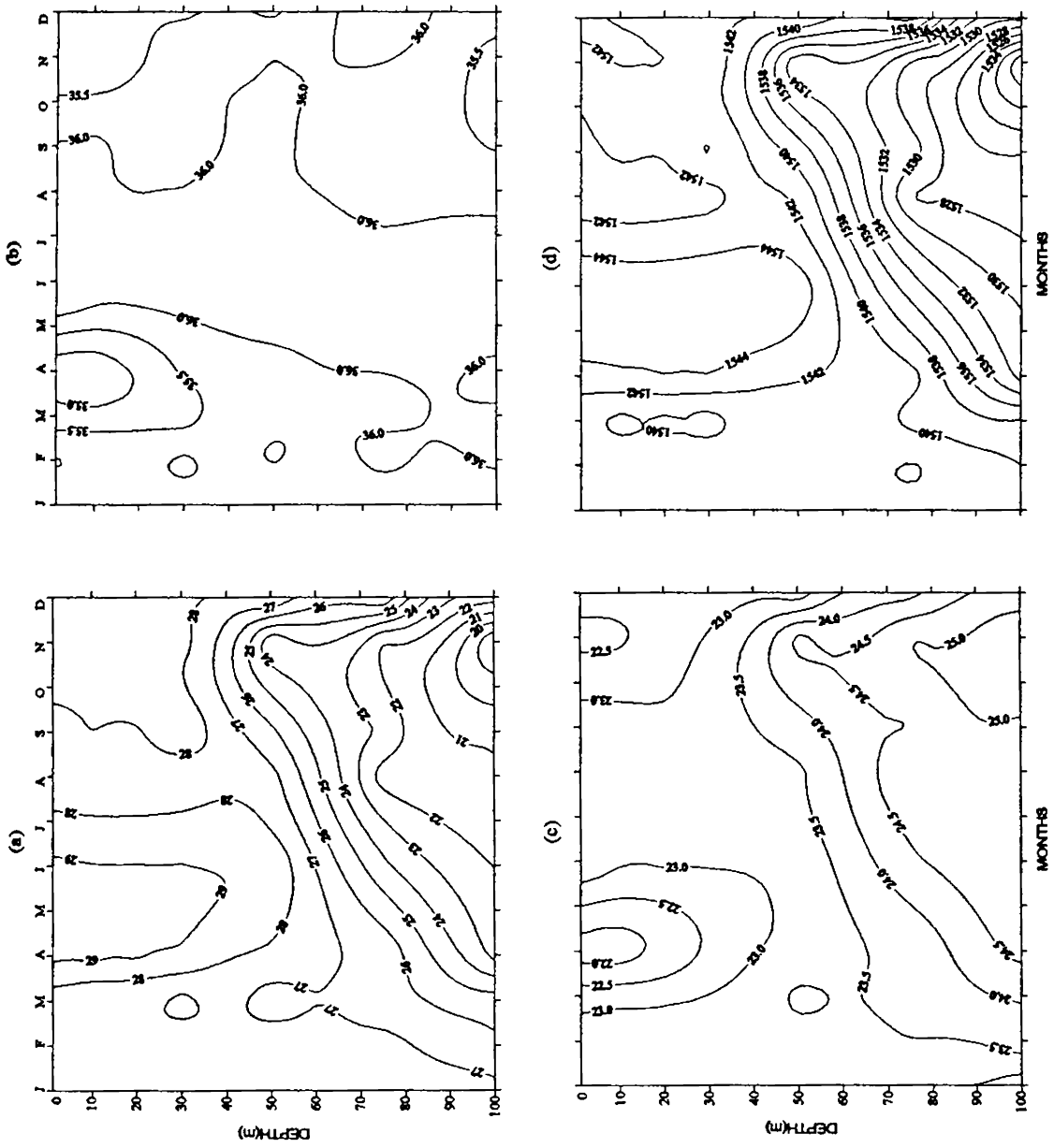
Fig. 3.11. Monthly distribution of (a) Temperature (°C), (b) Salinity (PSU), (c) Density (Sigma-t), and (d) Sound Speed (m/s)
Study Area: Off Ratnagiri, at SD100.

annual variation of temperature at the bottom is 8 °C while that of sound speed is 20 m/s (Fig.3.15). Here, density varies from < 23 kg/m^3 in January to 25 kg/m^3 during October-November resulting an annual range of 2 kg/m^3 (Fig. 3.16).

3.8. Off Bombay

At SD50, SST shows an annual variation of 3 °C with maximum occur during May to June (29 °C) and minimum during winter (26 °C in February). Here, the upward movement of isotherm is limited and occurs between July and September (Fig. 3.12). As the upwelling is very weak its effects are not prominent in the surface layers. The downward movement commences from November onwards. At the bottom (Fig. 3.14) the annual variation in temperature is less than 3 °C with maximum during July (27 °C) and minimum during October-November (24 °C). The entire water column is having more than 35.5 PSU salinity which indicates the presence of ASHSW. As a result of lower temperature and salinity variation, the density and sound speed also exhibits similar variation (0.5 kg/m^3 and 5 m/s at the surface and ~1 kg/m^3 and 8 m/s at the bottom).

At SD100, the upward movement of isotherms is evident from July onwards and continues till November (Fig. 3.13). The pre-monsoon and post-monsoon heating is clearly evident at the surface layer while marked cooling is noticed during winter. This results an annual temperature variation of 4 °C at the surface and 6 °C at the bottom. As in SD50, the entire water column is occupied by ASHSW. The annual variation in density and sound speed at the surface is 0.5 kg/m^3 (23 kg/m^3 during April-June to 23.5 kg/m^3 in July) and 8m/s (1536 m/s in February to 1544 m/s in May-June). At the bottom the variations are 1.5 kg/m^3 in density (24 kg/m^3 in July 25.5 kg/m^3 in November) and 13m/s in sound speeds (1537m/s in July and 1524m/s in November).

The observed annual variation in temperature, salinity, density and sound speed in the bottom water at the study areas SD50 and SD100 are shown in Table 3.1
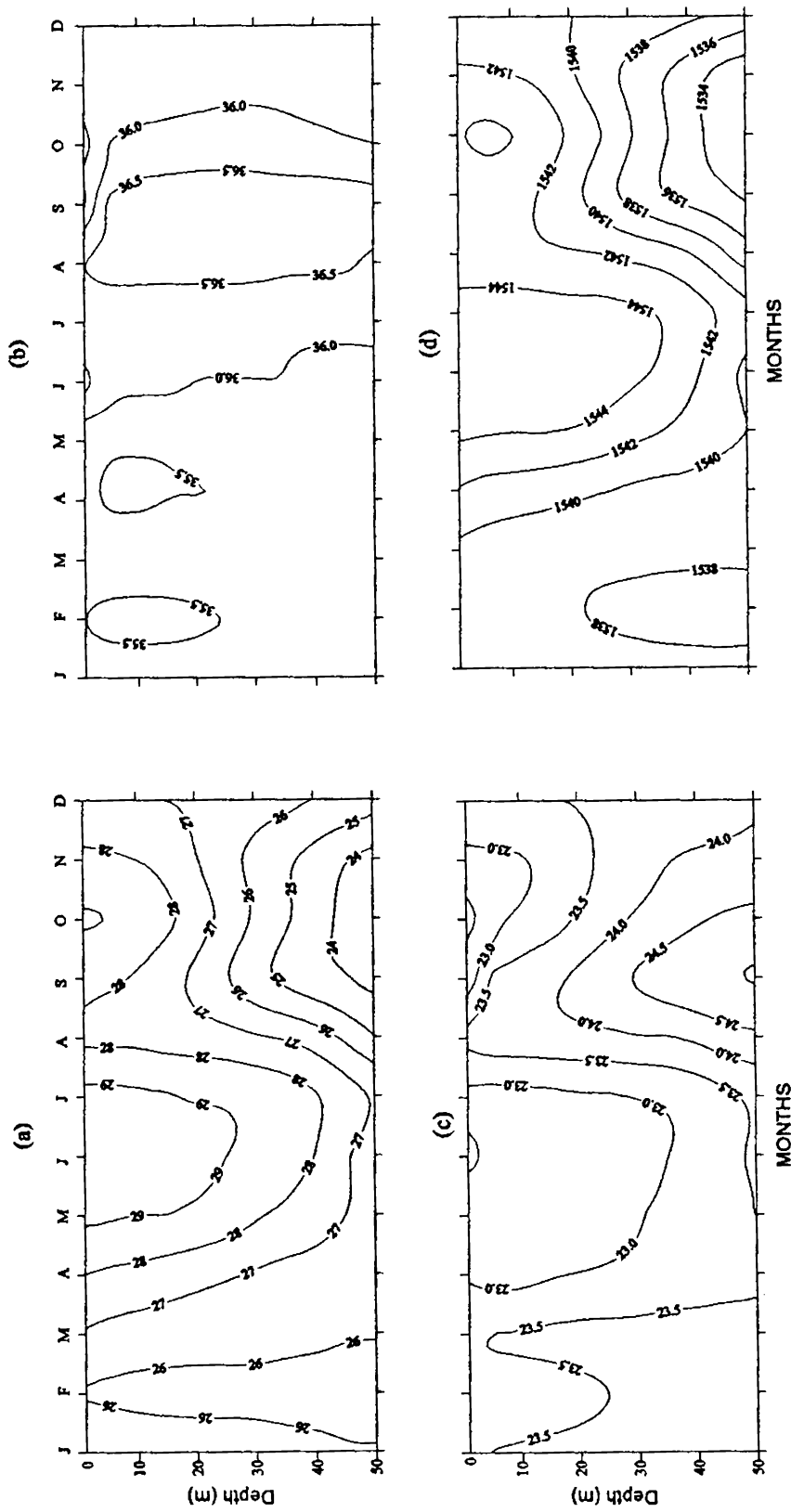
Fig. 3.12. Monthly distribution of (a) Temperature (°C), (b) Salinity (PSU), (c) Density (Sigma-t) and (d) Sound Speed (m/s). Study Area: Off Bombay, at SD50.
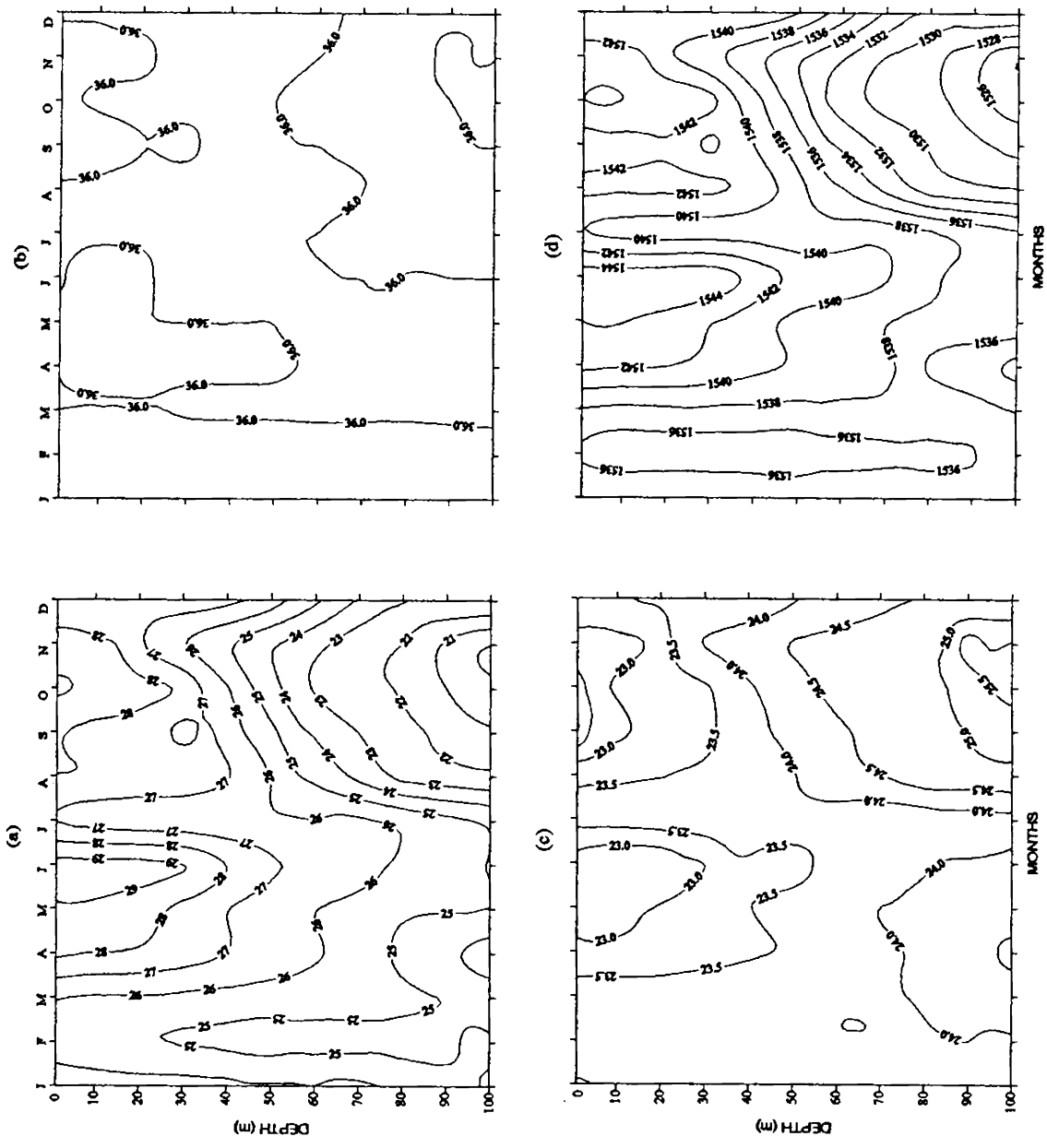
Fig.3.13. Monthly distribution of (a) Temperature (°C), (b) Salinity (PSU), (c) Density (Sigma-t), and (d) Sound Speed (m/s).
Study Area: Off Bombay, at SD100.
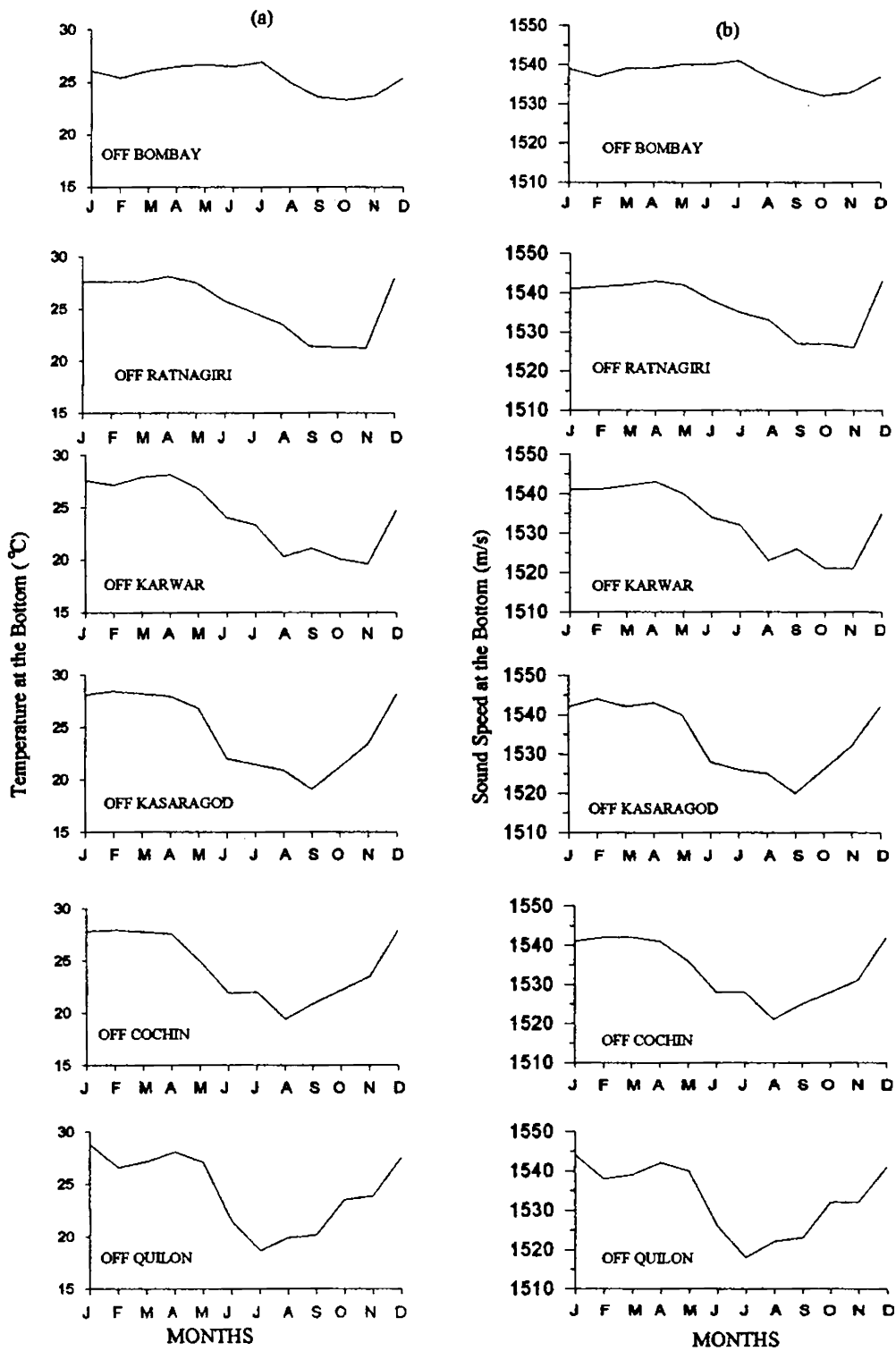
Fig.3.14. Seasonal variation of (a) temperature and (b) sound speed at the bottom, at SD50.
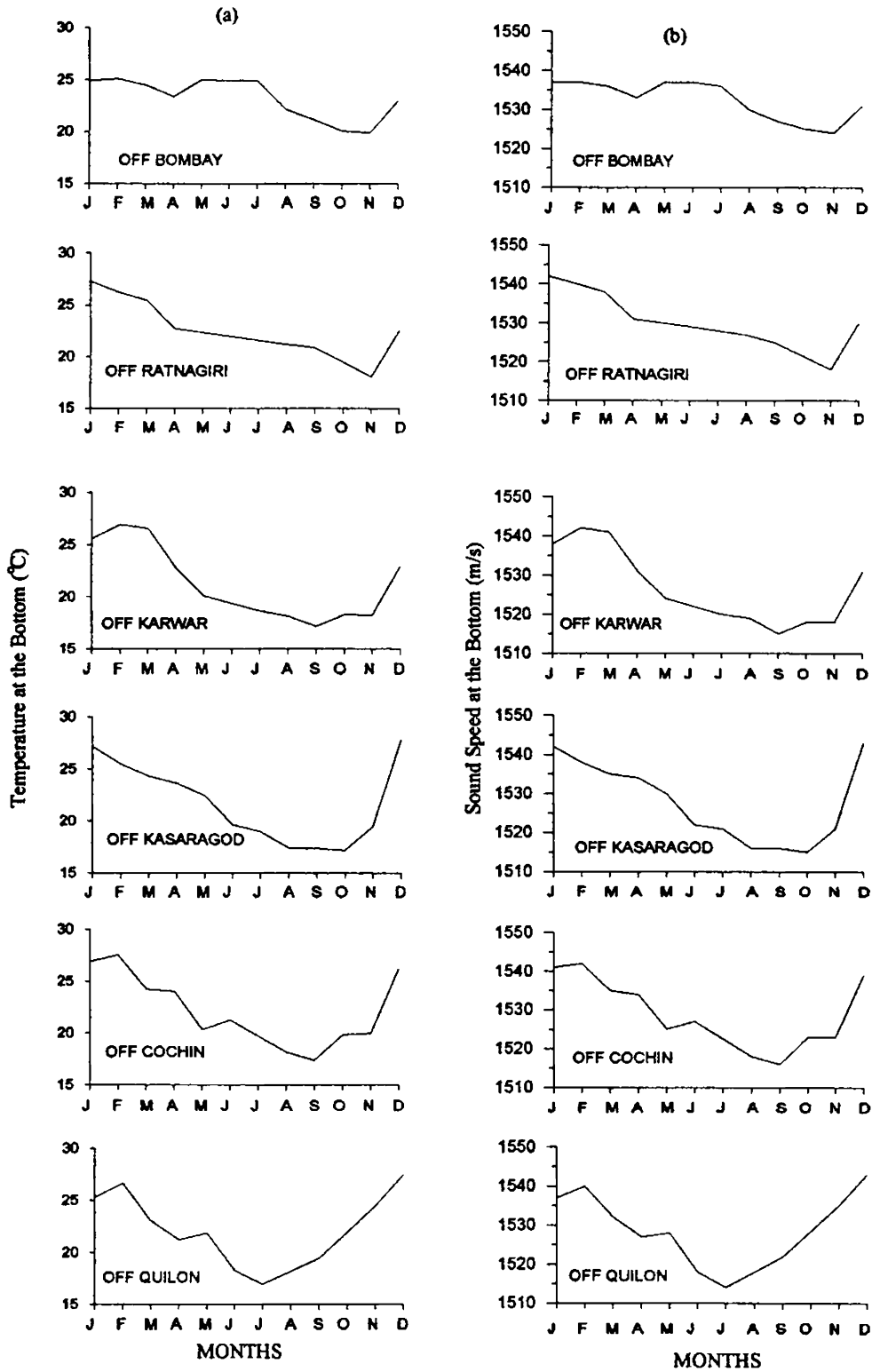
Fig.3.15. Seasonal variation of (a) temperature and (b) sound speed at the bottom, at SD100.
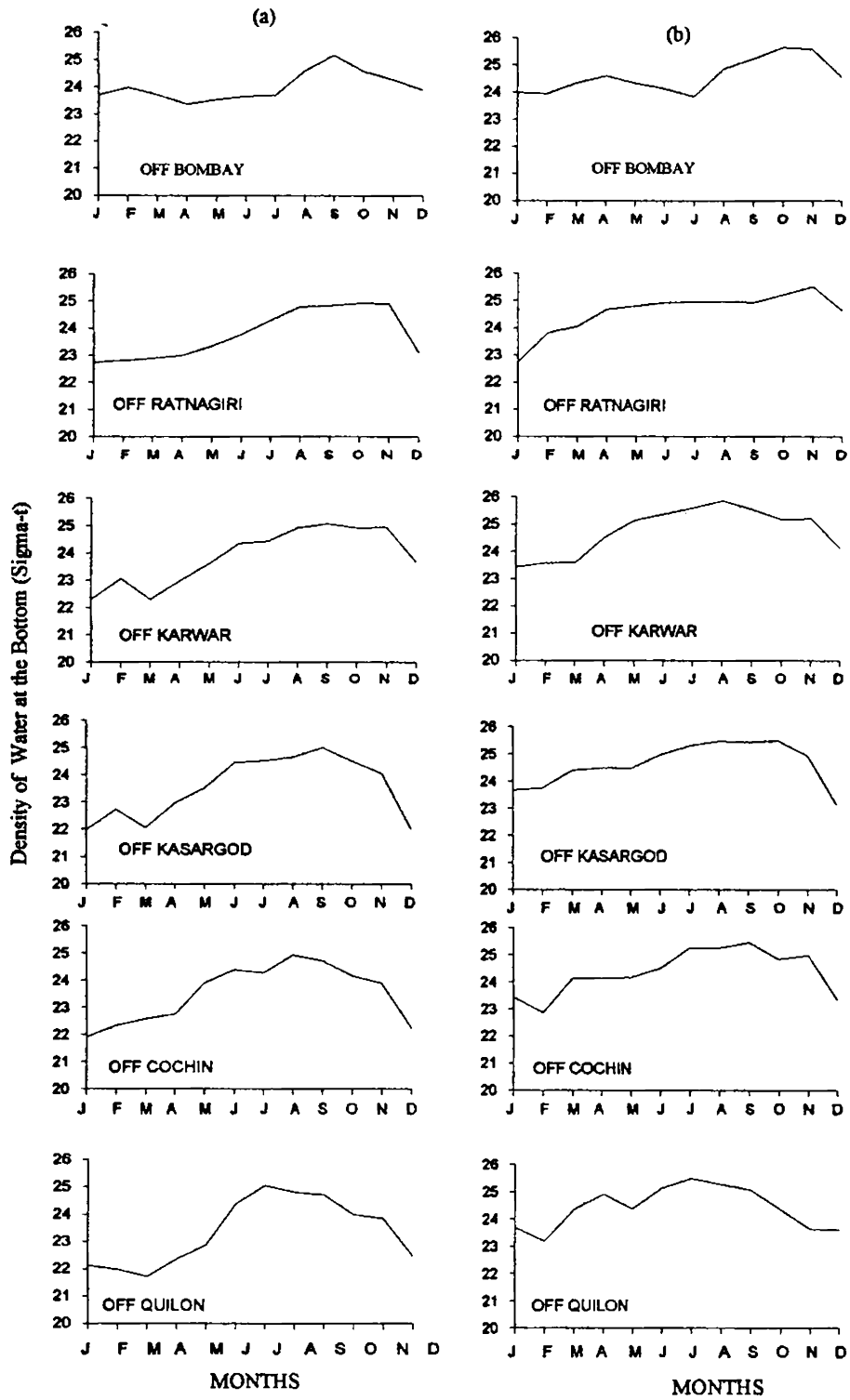
Fig.3.16. Seasonal variation of density at the bottom water (a) at SD50 (b) at SD100.

TABLE: 3.1. Observed annual variation in temperature, Salinity, Density and Sound
Speed at the Bottom Water

Study Areas	Temperature ($^{\circ}$C)		Salinity (PSU)		Density (kg/m^3)		Sound Speed (m/s)	
	SD50	SD100	SD50	SD100	SD50	SD100	SD50	SD100
Off Quilon	09	10	1.0	0.8	3.0	2.0	23	27
Off Cochin	08	09	1.0	1.0	2.5	2.0	20	26
Off Kasaragod	09	09	1.5	1.5	3.0	2.5	20	26
Off Karwar	08	09	1.5	1.0	2.5	2.0	20	24
Off Ratnagiri	06	08	1.0	1.0	1.5	2.0	15	20
Off Bombay	03	05	0.5	0.5	1.0	1.5	08	13

SD50 – at water depth of 50m
SD100 – at water depth of 100m

The analysis shows that both at SD50 and SD100 off the west coast of India the annual variations of temperature and salinity and hence that of density and sound speed are much larger at the bottom rather than at the surface. This is caused by a variety of factors, mainly upwelling and downwelling and to a lesser extent due to the presence of high saline Arabian waters and low saline Bay of Bengal Waters. Moreover, the intensity of these factors varies seasonally and spatially. It can be seen that the annual variations of temperature and sound speed are maximum in the four southern stations compared to those of the two northern stations as the process of upwelling and sinking are more dominant at the southern locations. The large fluctuations of temperature and salinities at the bottom modify the properties of sediments and this aspect is dealt in Chapter 6.

CHAPTER 4

LABORATORY MEASUREMENTS OF SOUND SPEED
IN MARINE SEDIMENTS

Several seafloor instruments are available for measuring geoacoustic and geo-technical properties and the details are discussed in Chapter1. These are mostly shallow water systems, although seafloor acoustic measurements have even been made in deep water using a submersible (Hamilton et al., 1963, 1970) or a modified piston corer (Shirley and Anderson, 1975; Fu *et al.*, 1996). Measuring acoustic signals from small explosive charges with sonobuoys, Hall (1996) estimated sound speed profiles at the sea bottom in Australian northern shallow waters. Best et al. (1998) developed an instrument for the rapid acquisition of seafloor geophysical and geo-technical data. The system can measure compressional wave speed and attenuation down to 1m sub-bottom depth in sand and gravel and the speeds of horizontally and vertically polarised shear waves at the surface.

Accurate measurements of compressional wave speed (sound speed) in the laboratory is possible (room temperature, 1-atm pressure) with proper instrumentation. Hamilton and Bachman (1982) measured compressinal wave speed in sediments in the laboratory by a pulse technique (operating at about 200 kHz); estimated margins of error were ±3m/s in clays and ±5 m/s in sands.

Harker et al. (1991) made a series of sound speed and attenuation measurements in suspensions in the laboratory. The equipment used to determine the sound speed and attenuation in suspensions consists of a cylindrical cell with two piezoelectric transducers, one of which was the transmitter and the other the receiver, a Hewlett Packard function generator and a Tektronix digital storage oscilloscope. Temperature measurements were made with platinum resistance thermometer.

To determine sound speed, the time difference between the proper cycles of the transmitted and received signal was determined using the oscilloscope cursors in the storage mode and simply reading the time difference of the display. The path-length

between the external surfaces of transducers is measured using vernier calipers. Harker et al., (1991) used the sound speed/temperature values for pure water given by Del Grosso and Mader (1972), together with the sound speed at the specific temperature to yield the acoustic path length from the time difference and sound speed values. This method requires measurement of the time difference between corresponding cycles of two waveforms displayed, at different times, on a digital storage oscilloscope. Harker et al., (1991) reported the timing error related to the sampling frequency (20 MHz) of $\approx 0.05 \mu s$ associated with the determination of sound speed. The errors associated with the attenuation measurements are primarily those arising from physical measurement of peak to peak heights of the waveforms and the error in the physical measurement was estimated to be ± 5 mm. This corresponds to ± 1.2 np/m at a value of 277 np/m, and to ± 0.2 np/m at 12 np/m.

Richardson (1986) determined the spatial variability of surficial sediment geoacoustic properties from sediment samples collected using corer at eight continental shelf regions in the U.S., Italy and Australia. Sediment compressional wave speed and attenuation were measured at 1 cm intervals on sediments using pulse technique (operating at about 400 kHz). Time delay measurements were made through sediments and distilled water and the difference in time delay between distilled water and sediment samples were used to calculate sediment compressional wave speed.

Leroy et al. (1986) developed an experimental equipment to study the effect of pressure variation on sediment sound speed. They also included an appropriate heating system to study the effect of temperature variation in sediment sound speed. Sediments are introduced from one end by removing a closing piston. The physical force on the sediment is applied from this piston actuated by a hydraulic jack. The interstitial pressure can be varied by a separate water pressure circuit. Two acoustic probes are located on opposite sides of the cylinder and are used to measure sound speed from a few kHz to 50 kHz.

Courtney and Mayer (1993) have made high-resolution measurements of compressional wave speed and attenuation in the frequencies between 100 to 100 kHz.

The two pairs of ultrasonic transducers were imbedded directly into the core samples, a 2 μs, high voltage pulse was applied to the transmitter of each pair in turn. The compressional waveform transmitted across the core material was digitized at 20 MHz by a digital storage oscilloscope. Preliminary estimates of the compressional wave speed at each measurement position were made with a simple time-of-flight method. The separation between the transmitter and receiver of each pair was measured before and after the measurements with a vernier caliper of 0.00002 m. The transducer pair separations were recalibrated in a distilled water bath, using temperature corrected, tabulated values for the speed of sound in distilled water. Courtney and Mayer (1993) reported that sound speed determinations with this method are accurate and repeatable within 1 m/s.

Zhang and Yang (1999) reported laboratory measurements of sound speed and attenuation of the fluid mud samples. They used one transmitter and two receivers for measurements in a tank for the frequencies of 100 kHz, 150 kHz, 500 kHz, and 1500 kHz with 100 μs pulse duration of the signal. Their results showed good agreement with the Wood theory.

Since no instrument is available for measurement of sound speed of sediments a new instrument is developed and the details are discussed in this Chapter.

4.1. Development of the instrumentation

The block diagram of the instrumentation that is developed is shown in fig.1. The sediment velocimeter is an instrument that has been developed to obtain compressional wave speed in marine sediments. The speed of sound in the sediment sample is determined from the time delay between the transmitted and received signals at the transducer. The signal to be transmitted is generated using an oscillator and a gating circuit. Attenuation of the acoustic signal increases as frequency increases. Since one measure the time delay between the transmitted and received pulse trains, to achieve good accuracy in time delay
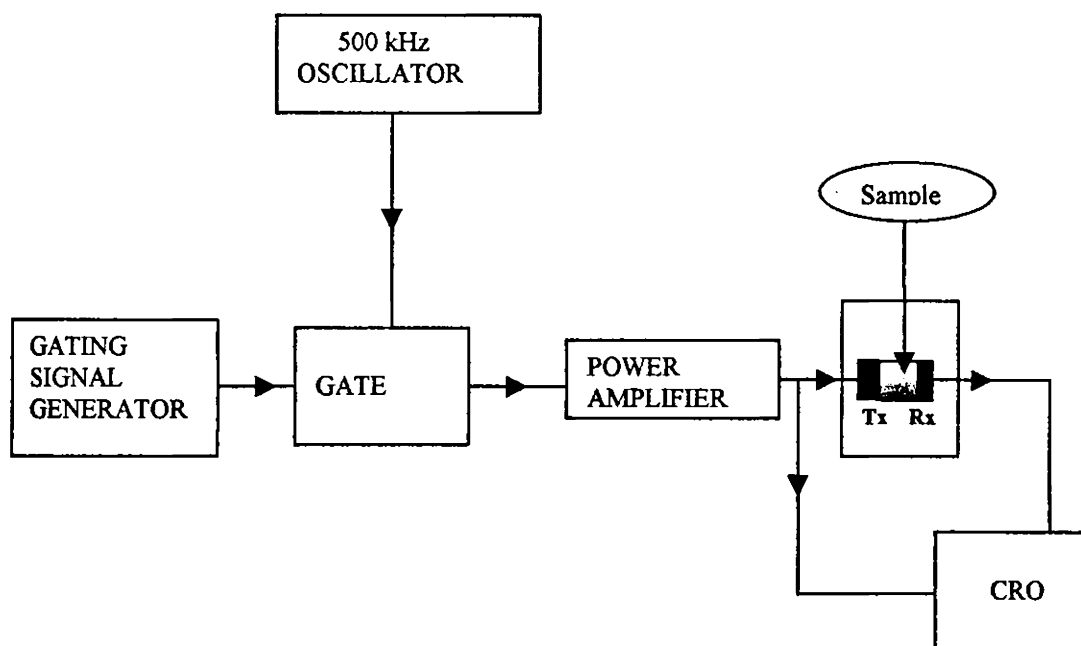
Fig. 4.1. Block diagram of sediment velocimeter.

measurements, the transmitted signal should have high frequency. So a compromise is made to have low attenuation and high accuracy. A frequency of 500 kHz was selected. A crystal oscillator generates a highly stable 1 MHz signal. Using a frequency divider, the 1 MHz signal is transformed to a 500 kHz square wave. One of the limitations of laboratory measurement of sound speed is generally been restricted to frequencies of 10-500 kHz and above, because sample dimensions selected must be much larger than the wavelength of the propagating signal (Fu et al., 1996).

A gating signal is generated to modulate the oscillator output. The pulse width and pulse repetition rate of the gating signal can be adjusted according to our requirements. Pulse width determines the number of cycles to be transmitted in a burst. Pulse repetition rate determines the time difference between repetitive bursts. Pulse width can be varied from 5 microseconds to 50 microseconds. Pulse repetition rate can be varied from 100 microseconds to 1 second.

The modulated signal is fed to a power amplifier, which drives the transmitter. The transmitter and the receiver are mounted on the ends of the sediment sample. Presence of air between the sediment sample and transducer causes impedance mismatch for acoustic transmission. Hence care should be taken to avoid the formation of air film in the gaps between the sample and the transducer. The presence of water in the gaps prevents the formation of air film and improves impedance matching.

The transmitted and received signals are viewed on a dual channel oscilloscope and the time delay between the two signals is measured. Knowing the distance of travel and the time delay, the sound speed in the particular sediment sample can be determined.

4.2. Calibration of Velocimeter

a) Correction for moulding material

When the two transducers are placed face to face touching each other, there is some 'time-delay' between the transmitted and received signals. Since the signal should traverse the moulding material cover before reaching the transducer crystal. Hence corrections are to be applied to the time delay measurements. The present set of transducers, when placed touching each other, a time delay of 8.4 microsecond is observed between transmitted and received signal. This value has to be deducted from the observed time delay to get actual travel time. Before making sound speed measurements in marine sediments, the calibration of the instrument is carried out as follows

b) Sound speed measurements in distilled water.

In order to calibrate the velocimeter, sound speed through distilled water at known temperature is measured at laboratory temperature of 26.1°C. The temperature measurements are carried out using a mercury thermometer having an accuracy of 0.1°C. The transducers are placed at different path lengths and the travel time through

the distilled water is noticed. The spacing between the transducers are measured using a vernier calipers having least count of 0.02 mm. The results are given in Table I.

Wilson (1960) derived an empirical relation giving the speed of sound in distilled water as a function of temperature at a pressure of one atmosphere from experimental data.

$$c = 1403 + 5t - 0.06t^2 + 0.0003t^3 \qquad (4.1)$$

where t is the temperature of the water in °C and c is in meters per second. Wilsons formula (1959,60) predicts sound speed in distilled water at 26.1 °C as 1498 meters per second. Average value of the three observations is 1483 meters per second, which shows a variation of about 15 meters per, second (1% variation).

TABLE 4.1. Sound speed measurements in distilled water.

Sl. No	Transducer separation (cm)	Observed travel time (μs)	Corrected travel time (μs)	Computed sound speed (m/s)	Difference in sound speed (Pred. – Mead.)
1	1.472	18.4	10.0	1472	26
2	2.216	23.2	14.8	1497	01
3	0.800	13.8	05.4	1481	17

4.2.1. Sound Speed Measurements in Metallic Blocks

The sound speed measurements are also carried out in aluminum and stainless steel blocks of different thickness and the results are shown in Table 4.2 and 4.3 respectively.

TABLE 4.2. Measurements through aluminum blocks.

Sl. No	Sample thickness (cm)	Observed travel time (μs)	Corrected travel time (μs)	Computed sound speed (m/s)
1	8.0	21.0	12.6	6349
2	5.0	16.2	07.8	6410

TABLE 4.3. Sound speed measurements through steel blocks.

Sl. No	Sample thickness (cm)	Observed travel time (μs)	Corrected travel time (μs)	Computed sound speed (m/s)
1	7.118	20.8	12.4	5740
2	5.020	17.6	8.8	5704

4. 2.2. Measurements of Compressional Wave Speed in Sediments

Sound speed through sediment samples is measured using this instrumentation. Sediment samples of known length (path length) is placed between the transducers and kept in standard seawater of known sound speed (V_1). The sound speed through core samples is then measured by comparison of the two different transit times in the sea water (t_1) and sediment samples (t_2) of same path length. The path length between the external surfaces of the transducers is recorded using vernier calipers. Sound speed in sediment (V_2), is computed using the relation (Harker et al., 1991).

$$V_2 = \frac{V_1 t_1}{t_2} \qquad (4.3)$$

Richardson (1986) measured sound speed in sediments by following similar method. Time delay measurements were made through sediments and a distilled water

reference with a dual time interval oscilloscope. Differences in time delay between distilled water and sediment samples were used to calculate sediment compressional wave speed.

In this study, measurements are carried out on different types of sediment samples at the laboratory temperature (27.5 °C). The seawater used for the measurements has salinity 35 PSU. The estimated sound speed using equation (1.1) of Mackenzie (1981) is 1540 m/s. The equation (Mackenzie, 1981), has a standard error estimate of 0.07 m/s and is accurate enough for practical computations of sound speed in seawater. The results of the measurements conducted in clayey and sandy sediments are shown in Table 4.4.

After the completion of acoustic measurements, sediment porosities are determined by weight loss of sediment dried at 105 °C for 48 hours. Values are corrected for pore water salinity (Chapter 1, Appendix I). Sediment mean grain size M(φ), bulk density, and dry density are determined by following the methods as described in Chapter 1.

4.3. *In Situ* Sediment Sound Speed

Laboratory sound speed must be corrected to *in situ* conditions for use in acoustic propagation studies. When a sediment sample is removed from the surface of the sea floor to the laboratory, the salinity of the water within the pore spaces remains the same and does not change from *in situ* to laboratory; therefore, the only changes in sound speed in the bottom water and pore water are due to the temperature and pressure changes. The effects of temperature and pressure changes on sound speed in the minerals in the sediment are insignificant (Hamilton, 1971). This shows that both water and sediment sound speed can be corrected from laboratory to *in situ* by making corrections for temperature and pressure.

Table 4.4. Sample location, water depth, porosity, bulk density, dry density, grain size, compressional wave speed, and velocity ratio.

Sample Location	Water Depth (m)	Sediment Type	Porosity (%)	Bulk densiy (gm/cm^{-3})	Dry density (gm/cm^{-3})	Grain Size (Mϕ)	Sound Speed (m/s)	Velocity Ratio
Gujarat	90	Sand	46.0	2.007	2.839	2.2	1644	1.068
Gujarat	70	Silty sand	69.0	1.551	2.718	3.3	1579	1.025
Gujarat	58	Clayey silt	68.1	1.577	2.554	6.5	1597	1.037
Bombay	83	Sand	59.4	1.739	2.790	1.9	1786	1.160
Bombay	73	Sand	57.9	1.763	2.786	2.4	1774	1.152
Bombay	77	Sand	44.2	2.010	2.796	1.6	1862	1.209
Bombay	80	Sand	59.1	1.842	2.740	1.8	1569	1.005
Bombay	78	Sand	57.9	1.752	2.683	2.0	1674	1.087
Bombay	75	Sand	46.9	1.898	2.672	1.8	1842	1.196
Bombay	65	Sand	37.3	2.121	2.775	1.9	1812	1.177
Bombay	70	Sand	56.0	1.746	2.672	1.8	1691	1.098
Panaji	113	Sand	49.8	1.906	2.783	2.2	1691	1.098
Panaji	35	Silty sand	45.0	1.943	2.699	2.8	1833	1.190
Karwar	320	Sandy silt	75.5	1.345	2.345	5.6	1577	1.024
Bhatkal	100	Sandy silt	64.7	1.595	2.769	4.9	1594	1.035
Mangalore	42	Sand	54.5	1.757	2.642	2.4	1760	1.143
Kasaragod	270	Silty sand	58.2	1.749	2.600	3.2	1652	1.073
Cochin	13	Clay	87.0	1.252	2.48	9.2	1469	0.954
Cochin	12	Clay	82.0	1.235	2.47	9.4	1475	0.958
Cochin	11	Clay	85.0	1.175	2.34	9.3	1456	0.945
Cochin	10	Clay	87.0	1.216	2.31	8.5	1506	0.978
Cochin	10	Clay	81.0	1.308	2.36	8.6	1506	0.978
Cochin	10	Silty clay	85.0	1.282	2.29	7.9	1625	1.055
Cochin	09	Silty clay	76.0	1.42	2.56	8.1	1513	0.982
Cochin	10	Silty sand	67.0	1.560	2.42	4.5	1669	1.084
Cochin	51	Sand	48.0	1.93	2.56	1.94	1886	1.225
Cochin	40	Sand	56.0	1.88	2.42	2.36	1763	1.145
Cochin	46	Sand	57.0	1.780	2.51	2.29	1725	1.120
Cochin	67	Sand	44.0	1.960	2.52	1.85	1825	1.185
Cochin	80	Sand	53.0	1.88	2.48	2.28	1813	1.177
Cochin	50	Sand	57.0	1.800	2.44	3.05	1669	1.084

Laughton (1957) demonstrated by laboratory tests that sound speed changes in saturated sediments due to hydrostatic pressure were about the same as in sea water. Shumway (1958) demonstrated that sound speed changes in saturated sediment due to temperature changes were about the same as in sea water. Hamilton (1963) measured sound speed *in situ* from a deep submersible and in the laboratory from core samples taken at the site of the *in situ* measurements and concluded that laboratory measurements could be corrected to *in situ* values by applying full corrections for temperature and pressure *in situ*, for speed of sound in sea water. Hamilton (1971) suggested to use the ratio of sound speed in sediment to sound speed in sea water. This ratio, is called "velocity ratio" is constant for a given sediment sample. Richardson (1986) reported this ratio is independent of sediment temperature, salinity and depth and therefore ideal for comparison to other geoacoustic properties. Bachman (1989) also reported that velocity ratio is constant for a given sediment sample: It is the same in the laboratory as it is at the seafloor at any water depth.

To determine *in situ* surface sediment sound speed, one simply multiplies the speed of sound in the bottom water at the desired location by the velocity ratio. In surficial sediment, grain size, grain density and porosity do not vary significantly with temperature and pressure (Hamilton, 1971). This method eliminates the need to correct for temperature and pressure differences, velocity ratio is a more convenient measure of surficial sediment sound speed than is sound speed in the laboratory. The applicability of this method was confirmed by Tucholke and Shirley (1979) in a study comparing *in situ* nose-cone velocimeter measurements of piston cores with laboratory sound speed corrected to *in situ* conditions. In this study, laboratory measured porosity, bulk density, dry density, grain size, compressional wave speed, and velocity ratios are given in Table 4.4.

4.4. Measured velocity ratio versus physical properties

In this section an attempt is made to establish empirical relationship between measured velocity ratio and physical properties of sediments. The data shown in Table 4.4 is used.

The fitted linear equation relating mean grain size, $(M\varphi)$ to measured velocity ratio (R_m) is

$$R_m = 1.8653 - 0.0246 M\varphi \qquad (4.4)$$

(σ = 2.79, coefficient of determination, r^2 = 0.669, standard error of estimate, s.e = 0.049)

This equation accounts 66.9.4 % of the variation in the velocity ratio.

The equation for density is

$$R_m = 0.6559 + 0.2562 \rho_{sat} \qquad (4.5)$$

(σ = 2.74, coefficient of determination, r^2 = 0.705, s.e =0.046)

which accounts 70.5 % of the variation in the velocity ratio

The equation for porosity (P) is

$$R_m = 1.3945 - 0.00499 P \qquad (4.6)$$

(σ = 14.44, coefficient of determination, r^2 = 0.741), s.e = 0.043).

This equation explains 74.1 % variation in the velocity ratio. Further discussions on velocity ratio are included in Chapter 5.

CHAPTER 5

INTER-RELATIONSHIPS AMONG PHYSICAL PROPERTIES AND GEOACOUSTIC PROPERTIES OF SEDIMENTS

&

PREDICTION OF SOUND SPEED AND ATTENUATION IN MARINE SEDIMENTS

In this chapter study on the relationships among physical properties of sediments, prediction of compressional wave sound speed and attenuation in sediments, comparison between measured sound speed with predicted sound speed, and relationships between velocity ratio and attenuation versus physical properties are included.

5.1. Relationship among physical properties of sediments

The main purpose of the study in this section is to establish relationships among various physical acoustic properties of marine sediments. These relationships are useful for predictions of acoustic characteristics using the more commonly available physical property measurements. The sediment samples are collected from the continental shelf of the eastern Arabian Sea extending from off Gujarat to south off Quilon. A total number of 109 sediment samples are collected from the continental shelf using sediment samplers (gravity corer and grab) during different cruises. Measurements of physical properties are carried out in the laboratory following the methods discussed in Chapter 1. Data from older measurements (30 samples) are also considered and combined with the new results after applying the required correction. Thus data from 139 sediment samples are considered in this study. The measured physical properties are bulk density, grain density, grain diameter, and porosity. Measurements of sound speed in sediments are available for 31samples only and attenuation measurements are not carried out. Therefore, compressional wave sound speed and attenuation in sediments are computed following Biot-Stoll Model and Haumeder model respectively.

5.1.1. Porosity versus Mean Grain Diameter

In natural marine sediments, porosity usually ranges between about 35% and about 90% (Hamilton and Bachman,1982). There is much scatter in the relationship between grain size and porosity is noticed because of a number of interrelated factors (Mitchell, 1976). The important factors for this scatter in the relationship are due to the difference in grain size, uniformity of grain size, grain shape, packing of grains and mineralogy of sediments (Hamilton,1974). Most of the authors suggested linear relationship between porosity and mean grain diameter. Hamilton (1974), and Hamilton and Bachman (1982) brought out separate equations for the sediments of continental shelf and slope, abyssal hill (pelagic), and abyssal plain (turbidite). Hamilton and Bachman (1982) suggested polynomial line fit for the shelf and slope sediments and linear fit for the other environments.

Porosity of the sediments considered in this study varies from 39 to 87% and grain size varying from 1 to 9 $M\varphi$ ($M\varphi$ =—$\log_2$ of grain diameter in mm). In general, porosity of sediments increases with decrease in grain size or increases with mean phi units, $M\varphi$ (Fig.5.1). In this study, polynomial curve fit is found to be the best fit (correlation coefficient = 0.80) for the data compared to linear and logarithmic curve fits.

$$P = 41.6911 + 6.50M\varphi - 0.237M\varphi^2$$
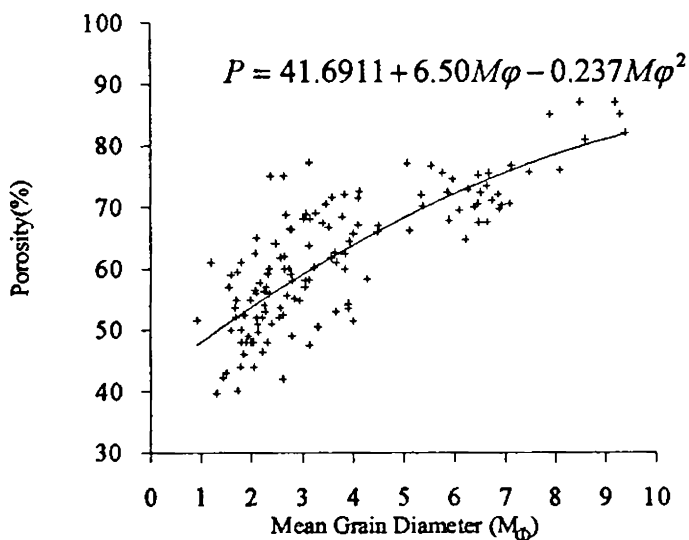
Fig. 5.1. Relationship between porosity and mean grain diameter.

The equation for the curve is found to be

$$P = 41.6911 + 6.50M\varphi - 0.237M\varphi^2 \qquad (5.1)$$

(correlation coefficient = 0.8, σ = 10.7)

where P is the porosity (%) and $M\varphi$ is the mean grain diameter in phi units. The estimated standard error (s.e) is 6.66 and coefficient of determination, r^2 = 0.64. This equation explains 64% of variation in porosity.

5.1.2. Bulk Density versus Porosity

The relationship of porosity to bulk density has been investigated by some authors (Hamilton et al., 1956, 1974; Nafe and Drake, 1957; Sutton et al., 1957; Shumway, 1960, Breslau, 1967; Akal, 1972, Murty and Muni, 1987) and are discussed in Chapter 1. All have shown a strong linear correlation. Theoretically this linearity only exists if the dry densities of mineral particles are the same for all marine sediments. The density of the sediment would then be the same as the density of the solid material at zero porosity, and the same as the density of the water at 100 % porosity. To check this linearity for measured values, the bulk density has been plotted as a function of the porosity for 139 samples and a regression line is fitted by computer and is illustrated in Fig. 5.2.
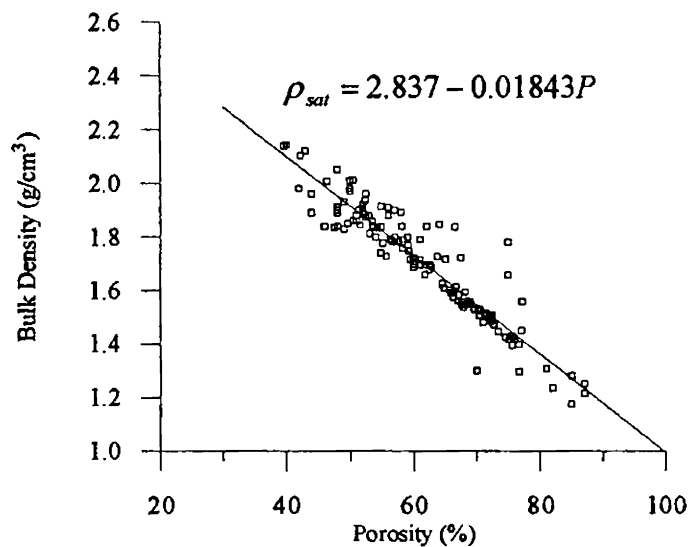
Fig. 5.2. Relationship between bulk density and porosity.

The equation for the straight line is found to be

$$\rho_{sat} = 2.837 - 0.01843P \qquad (5.2)$$

(correlation coefficient = 0.94, σ = 0.211)

where ρ_{sat} is the saturated bulk density and P is the porosity (%).

The estimated standard error (s.e) is 0.072 and coefficient of determination, $r^2 = 0.883$. This equation explains 88.3 % of variation in bulk density. The fitted equation shows that density of the sediment at zero porosity (i.e. the density of the solid material) would be 2.837 g/cm^3 which is slightly higher compared to the value given by Hamilton (1974). Hamilton reported that the density of mineral solids in sediments varies widely. He attributed these variations to the source material from which the sediments are derived. The presence of calcium carbonate content, clay minerals and the variations of quartz, feldspar and argonate crystals in the sediments are some other factors that influence grain density from one region to another (Murty et al., 1984)

5.1.3. Bulk Density versus Mean Grain Diameter
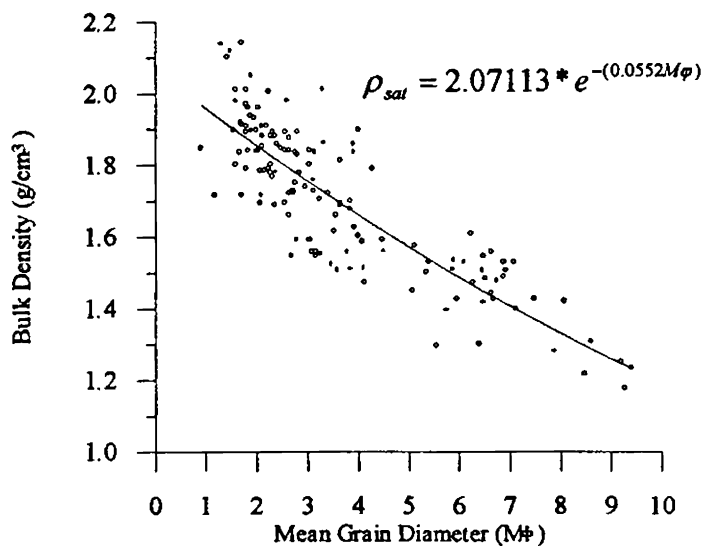
Fig. 5.3. Relationship between bulk density and mean grain diameter

73

The relationship between sediment bulk density and mean grain diameter of the sediment is shown in Fig.5.3 The best fitted exponential equation is given by:

$$\rho_{sat} = 2.07113 * e^{-(0.0552M\varphi)}$$ (5.3)

(correlation coefficient = 0.87, σ = 0.211)

where ρ_{sat} is the saturated bulk density and Mφ is the mean grain density.

The estimated standard error (s.e) is 0.109 and coefficient of determination, r^2= 0.754. This equation explains 75.4 % of variation in bulk density

5.2. Prediction of Sound Speed and Attenuation in Marine Sediments

The geoacoustic properties of marine sediments at the seafloor play a key role in bottom-interacting ocean acoustics. Sediments are usually inhomogeneous near the water-sediment interface and these inhomogeneties result in spatial variation of geoacoustic properties. It is practically very difficult to obtain accurate values of geoacoustic properties because direct measurements are costly and time consuming. However, it is comparatively easier and faster, to collect data on physical properties of sediments and to predict sound speed and attenuation using theoretical models. A promising approach in the prediction of acoustic wave speed and attenuation in marine sediments is the use of the Biot theory. The details are discussed in Chapter 2.

5.2.1. Prediction of compressional wave sound speed

Ogushwitz (1985) has shown that Biot-Stoll theory can be used to model sound speed and attenuation data for artificial and natural materials with porosities from 2% to 100%. Holland and Brunson (1988) made comparisons between Biot-Stoll Model predictions of compressional wave speed and compressional wave attenuation with *in situ* and laboratory measurements. They reported the model predictions showed excellent agreement with measured data. In this study Biot-Stoll model is considered for the prediction of compressional wave sound speed.

Model inputs

The Biot-Stoll model requires 13 geophysical sediment properties. Table 5.1 lists these parameters. These input values could be obtained by several methods including direct measurement, use of physical/empirical relationship to relate a measured property to the desired input property, or use of values found in the literature. The remainder of this section discusses empirical and theoretical methods of specifying values for the Biot model parameters.

Table. 5.1. Biot model parameters

Physical properties	Units
Pore fluid properties	
Fluid density, ρ_w	g/cm^3
Fluid bulk modulus, K_f	dyn/cm^2
Fluid viscosity, η	P
Grain Properties	
Grain bulk density, ρ_{sat}	g/cm^3
Grain density, ρ_s	g/cm^3
Grain bulk modulus, K_r	dyn/cm^2
Frame properties	
Structure factor, a'	
Porosity, n	
Permeability, k	cm^2
Pore size parameter, a	cm^{-1}
Dry frame bulk modulus, $K_{b\,real}$	dyn/cm^2
Dry frame Bulk modulus, $K_{b\,imaj}$	dyn/cm^2
Dry frame shear modulus, μ_{real}	dyn/cm^2
Dry frame shear modulus, μ_{imaj}	dyn/cm^2

Pore fluid density, ρ_w

In this study the pore fluid density, ρ_w is computed using the International Equation of State of Sea Water (Millero and Poisson, 1981) from near bottom temperature, salinity, and depth data.

Porosity, n

Porosity of the sediments was measured in the laboratory and corrected for the salt content of the pore water as described in Chapter 1.

Bulk density, ρ_{sat} and grain density, ρ_s

The bulk density and grain density of each sediment sample was measured in the laboratory by the weight-volume method using a pycnometer. The bulk density of saturated sediment varies with the density of the pore fluid and the effects of temperature and pressure changes on grain density of the minerals in the sediment are insignificant (Hamilton, 1971). All the measurements are carried out at about 27.5°C and the laboratory-measured values of bulk densities and grain densities are only considered in this Chapter.

Fluid viscosity, η

Viscosity of the pore fluid is not measured. In this study fluid viscosity at variable temperature is computed following Sverdrup et al., (1942) and Pradeep Kumar (1997) for a constant of salinity of 35 PSU.

Permeability, k

Sediment permeability is not measured. The permeability is related to the porosity and surface area of the grains. In this study the physical relationship of Kozeny–Carman (Carman, 1956; Holland and Brunson, 1988), which is given by

$$k = \frac{1}{K'S_o^2} \frac{n^3}{(1-n)^2},$$

(5.4)

where k is the permeability in cm^2, S_o is the specific surface of the particles in the sediment in cm^{-1}, K' is an empirical constant approximately equal to 5, and n is the porosity in decimal fraction. S_o can be defined analytically for a sphere as follows:

$$S_o = 6/d$$

(5.5)

76

where d is the diameter in cm and can be obtained from the mean grain size, Mφ.

Pore-size parameter, a

The pore-size parameter is introduced by Biot to describe the dependence of the viscous resistance to fluid flow on the size and shape of the pore. This parameter is not measured directly but computed by Kozeny-Carman relation following Hovem and Ingram (1979):

$$a = \sqrt{2[K'(k/n)]} \tag{5.6}$$

Bulk modulus of the pore fluid, K_f

Bulk modulus of the pore fluid varies with temperature. The fluid bulk modulus, K_f at different temperature t is obtained from the relation (Rajan, 1992),

$$K_f = C^2(t)\rho_w \tag{5.7}$$

where $C^2(t)$ is the sound speed in pore fluid at a temperature t and is the density of the pore fluid.

Grain bulk modulus, K_r

Bulk modulus of the sediment grains is not measured. A value of 4.0×10^{11} dyn/cm^2 is used for the sand sediments (Domenico, 1977). A value of 3.5×10^{11} dyn/cm^2 is used for the silty clay. No grain bulk modulus measurements of clays could be found in the literature. Stoll and Kan (1981) in their study used a value of 3.6×10^{11} dyn/cm^2 for soft sediment. The anelasticity of the sediment grains is negligible so that the imaginary part of the bulk modulus is considered as zero value (Holland and Brunson, 1988).

Structure factor, a'

The structure factor is a dimensionless term introduced in the Biot-Stoll theory to account for the nonviscous transfer of momentum from the fluid to the frame. Stoll

77

(1974) used the value $a' = 1.25$ for fine grained sands and $a' = 3.0$ for fine grained clays. Berryman (1980) in his study concluded that structure factor can be model theoretically by

$$a' = 1 - r_0(1 - 1/n),$$ (5.8)

where n is the porosity, and r_0 is a coefficient such that $r_0 \, \rho_w$ is the induced mass caused by the oscillation of solid particles in the fluid. The value of r_0 is restricted to the range $0 \leq r_0 \leq 1$. For spherical particles, $r_0 = 0.5$. In this study structure factor, a' is computed using Berrymans equation.

Frame moduli

The frame bulk modulus, K_b is not measured. Hamilton (1971a) derived the frame bulk modulus of the sedimentary materials from experimental data. He has given regression equations for natural sediments as follows.

For natural sands:

$$\log K_b = 2..70932 - 4.25391n$$ (5.9)

For natural silty clays:

$$\log K_b = 2.73580 - 4.25075n$$ (5.10)

here, the units of are 10^9 dyn/cm^2.

For a given value of K_b, the shear modulus μ can be determined from,

$$\mu = [3K_b(1 - 2\sigma)]/[2(1 + \sigma)]$$ (5.11)

where σ is the frame Poisson's ratio. Average values of Poisson's ratio appear to be about $\sigma = 0.2$ in granular sediments, $\sigma = 0.3$ for the silty clay and $\sigma = 0.5$ for soft sediments (Holland and Brunson, 1988).

78

The imaginary part of the frame shear modulus is descriptive of losses at grain-to-grain contacts and is related to the attenuation of shear waves. Its value can be obtained by

$$\mu_{imag} = \delta_s \mu / \pi, \qquad (5.12)$$

where δ_s is the logarithmic decrement for shear waves. A typical value of δ_s for many seafloor sediments appears to be 0.1 (Hamilton, 1976).

The imaginary part of the frame bulk modulus is descriptive of losses at grain-to-grain contacts and is related to the attenuation of compressional waves. Its value can be calculated in a similar way by a logarithmic decrement of longitudinal waves δ_e, analogous to the frame shear log decrement. The typical values of δ_e of seafloor sediments appear to be 0.1 and 0.01 for the granular sediments and for the silty clays.

The Biot-Stoll model (discussed in Chapter 2) is implemented on a personal computer and the program is written in FORTRAN language. The program computes the sound speed and attenuation of compressional and shear waves in sedimentary materials.

The following section contains discussions on the predicted values of compressional wave speed for those samples where laboratory measurements were carried out (described in Chapter 4). A comparison is also made between the laboratory-measured data against predicted compressional wave speed, where the geophysical inputs described in this section are employed.

5.2.3. Predicted sound speed versus measured data

The predicted values of compressional wave speed in sediments at 500 kHz are shown in Table. 5.2. The type of the selected sediments varies from very fine clay

Table 5.2. Predicted and measured compressional wave sound speed

Sediment Type	Porosity (%)	Dry density (gm/cm³)	Grain Size (Mφ)	Predicted Sound Speed (m/s)	Measured Sound Speed (m/s)	Difference in sound speed (m/s)	Difference in sound speed (%)
Sand	46.0	2.839	2.2	1761	1644	117	7.1
Silty sand	69.0	2.718	3.3	1663	1579	84	5.3
Clayey silt	68.1	2.554	6.5	1499	1597	-98	-6.1
Sand	59.4	2.790	1.9	1709	1786	-77	-4.3
Sand	57.9	2.786	2.4	1701	1774	-73	-4.1
Sand	44.2	2.796	1.6	1796	1862	-66	-3.5
Sand	59.1	2.740	1.8	1548	1569	-21	-1.3
Sand	57.9	2.683	2.0	1733	1674	59	3.5
Sand	46.9	2.672	1.8	1799	1842	-43	-2.3
Sand	37.3	2.775	1.9	1864	1812	52	2.9
Sand	56.0	2.672	1.8	1746	1691	55	3.3
Sand	49.8	2.783	2.2	1749	1691	58	3.4
Silty sand	45.0	2.699	2.8	1795	1833	-38	-2.1
Sandy silt	75.5	2.345	5.6	1544	1577	-33	-2.1
Sandy silt	64.7	2.769	4.9	1530	1594	-64	-4.0
Sand	54.5	2.642	2.4	1746	1760	-14	-0.8
Silty sand	58.2	2.600	3.2	1695	1652	43	2.6
Clay	87.0	2.48	9.2	1514	1469	45	3.1
Clay	82.0	2.47	9.4	1516	1475	41	2.8
Clay	85.0	2.34	9.3	1527	1456	71	4.9
Clay	87.0	2.31	8.5	1528	1506	22	1.5
Clay	81.0	2.36	8.6	1529	1506	23	1.5
Silty clay	85.0	2.29	7.9	1532	1625	-93	-5.7
Silty clay	76.0	2.56	8.1	1511	1513	-2	-0.1
Silty sand	67.0	2.42	4.5	1560	1669	-109	-6.5
Sand	48.0	2.56	1.94	1813	1886	-73	-3.9
Sand	56.0	2.42	2.36	1783	1763	20	1.1
Sand	57.0	2.51	2.29	1756	1725	31	1.8
Sand	44.0	2.52	1.85	1860	1825	35	1.9
Sand	53.0	2.48	2.28	1791	1813	-22	-1.2
Sand	57.0	2.44	3.05	1768	1669	99	5.9

to coarse sand (mean grain size Mφ varies from 9.4 to 1.6). Porosity of the sediments varies from 37 to 87%. The predicted sound speeds in clay sediments are much above the measured values. The disagreement between measured and predicted sound speeds for these samples may be due to the inadequacy of Biot's model. These sediments have mean grain size Mφ values around 9 and porosities in the range of 81 to 87%. For sediments at this range of porosity and grain size, the skeletal frame proposed by Biot may not be suitable and the sediment grains behave like suspensions (Murty and Pradeep Kumar, 1989).

It is noticed that in majority of sandy sediments, the predicted sound speeds are much below the measured values. The calcium carbonate content in these samples may be the reason for this. The sound speed generally increases with rise in calcium carbonate content (Sutton et al., 1957). Anderson (1974) reported that carbonate content significantly affects the predictability of sound speeds in shallow-water (<1500m) sediment samples. Murty and Muni (1987) reported calcium carbonate content in the range of 20 to 50 % in the sediments of the continental shelf off Cochin. Hashimi et al., (1981) reported that carbonate content increases from 21.9% off Cochin to 37.4% off Quilon and 71.4% off Tuticorin. In this study also, shells of marine organisms in considerable quantities are noticed in most of the sandy sediments and in some fine sediments. The calcium carbonate content in these sediments are not estimated in this study .

Ogushwitz (1985) has shown that Biot's model is sensitive to the frame modulii and when Hamilton's regression equations are used for the derivation of frame modulii, the estimated wave speeds fell below the measurements. This indicates that Hamilton's empirical relations used in this study for computing the frame modulii are also not adequate for carbonate rich sediments resulting in underestimation of the predicted values over measured ones (Murty and Pradeep Kumar, 1989). They reported that considering the experimental errors in measured data, it is reasonable to say that the estimates of the Biot theory agree within ± 3% of the measured data. Nobes (1989) reported that the errors in sound speed measurements in sediments were estimated of the order of ± 50m/s.
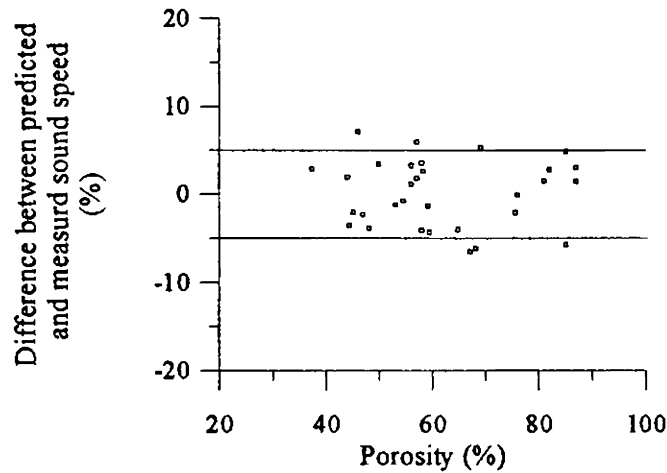
FIG.5.4. The percentage variation of difference between predicted and measured sound speed versus porosity. The solid lines represent ± 5% deviation from a perfect fit.

In order to understand the deviation from predicted sound speed to the measured sound speed, the percentage variation to the measured sound speed is computed. The standard deviation is estimated to be 3.77 %. The results (percentage variation) are plotted versus porosity (Fig.5.4). The solid lines represent ± 5% deviation from a perfect fit. It is observed that 81% of the sediment fall within this limit.

5.2.4. Prediction of compressional wave attenuation

A difficulty in the use of Biot-Stoll model is the problem of accurately determining the 13 geophysical inputs since many of the inputs cannot be directly measured (discussed in the previous section). The imaginary part of the frame bulk modulus is related to the attenuation of compressional waves and is calculated by a logarithmic decrement of longitudinal waves δ_e. The typical values of δ_e is 0.1 for the granular sediments and 0.01 for silty clay are chosen by most of the researchers and this may cause error in the computation when considering different types of sediments ranging from coarse sands to very fine soft clay.

Haumeder (1986) has shown that with the knowledge of the relaxation times, for a porous, fluid-filled material the response of the attenuating medium can be completely characterized (discussed in Chapter 2). Compared to Biot-Stoll model the later model does not considering logarithmic decrement of longitudinal wave δ_e for the computation of attenuation.

LeBlanc et al., (1992) proposed a relaxation-time model that combines the various dissipative energy loss mechanisms of sound in marine sediments into a single parameter. They used published experimental d ata on compressional wave attenuation in marine sediments and converted attenuation data to the relaxation time. Their study concluded that previous attenuation measurements support the use of relaxation time model.

In this study the equation of Haumeder (1986) which is derived based on Biot model is opted for computing compressional wave attenuation. Discussions on predicted compressional wave attenuation for the sediment samples of the eastern Arabian Sea, where the geophysical inputs described in the section 5.2.1 are employed.

Compressional wave attenuation is computed in those sediment samples that are considered for sound speed measurements in this study. The computed attenuation is given in Table 5.3. LeBlanc et al., (1992) suggested that the single most important geotechnical property that should correlate with attenuation is the mean grain size. They plotted measured attenuation in dB/m/kHz against the mean grain size diameter in phi units. The result is that data is widely scattered and also showed two separate groupings between high frequency (>200 kHz) data and Hamilton's low-frequency (<50 kHz) data by a large margin for the sediments in the range of 1 to 6 phi units (medium sand to coarse silt). This indicates that the assumption of linear frequency dependence with attenuation is not correct. On the other hand, if the linear dependency exist, there would not have been any grouping of data.

In this study compressional wave attenuation in dB/m is computed at 500 kHz and 40 kHz (Table 5.3.) for similar comparis on with the results of LeBlanc et al.,

Table 5.3. Predicted compressional wave attenuation

Sediment Type	Porosity (%)	Grain Size (Mφ)	Predicted attenuation at 500 kHz (dB/m)	Predicted attenuation at 40 kHz (dB/m)
Sand	46.0	2.2	581.3	13.3
Silty sand	69.0	3.3	264.9	7.3
Clayey silt	68.1	6.5	44.3	1.3
Sand	59.4	1.9	848.6	19.8
Sand	57.9	2.4	596.6	14.0
Sand	44.2	1.6	825.6	18.9
Sand	59.1	1.8	881.8	20.6
Sand	57.9	2.0	739.4	17.3
Sand	46.9	1.8	718.4	16.5
Sand	37.3	1.9	550.8	12.5
Sand	56.0	1.8	830.1	19.3
Sand	49.8	2.2	611.8	14.1
Silty sand	45.0	2.8	351.1	8.1
Sandy silt	75.5	5.6	41.2	2.0
Sandy silt	64.7	4.9	. 122.0	3.4
Sand	54.5	2.4	532.9	12.5
Silty sand	58.2	3.2	313.0	7.6
Clay	87.0	9.2	14.9	0.4
Clay	82.0	9.4	13.2	0.2
Clay	85.0	9.3	14.4	0.2
Clay	87.0	8.5	9.7	0.8
Clay	81.0	8.6	18.0	0.4
Silty clay	85.0	7.9	20.0	1.0
Silty clay	76.0	8.1	22.4	0.5
Silty sand	67.0	4.5	114.8	3.6
Sand	48.0	1.94	628.5	14.5
Sand	56.0	2.36	485.7	11.6
Sand	57.0	2.29	543.2	12.9
Sand	44.0	1.85	599.2	13.8
Sand	53.0	2.28	516.7	12.2
Sand	57.0	3.05	311.2	7.6

(1992). The computed attenuation is converted to dB/m/kHz and plotted against mean grain diameter in phi units (Fig. 5.5a). In this study also, it is seen that the data points showed separate groupings similar to LeBlanc's et al.,(1992) observations. It is also noticed in both studies (LeBlanc et al., 1992 and this study) for the mean grain size above 8 phi units (fine silts and clay) the separation of grouping of data disappears and only scattered data is seen.

At high porosity (> 80%), the sediment behaves like suspensions and the assumption of linear dependency can be considered. Urick (1948) measured absorption coefficient in suspension at 1 and 3 MHz and shown that the linearity of the absortion of sound with concentration is in agreement with theory. He reported that this linearity holds good only at low concentrations where particle interactions can be neglected.
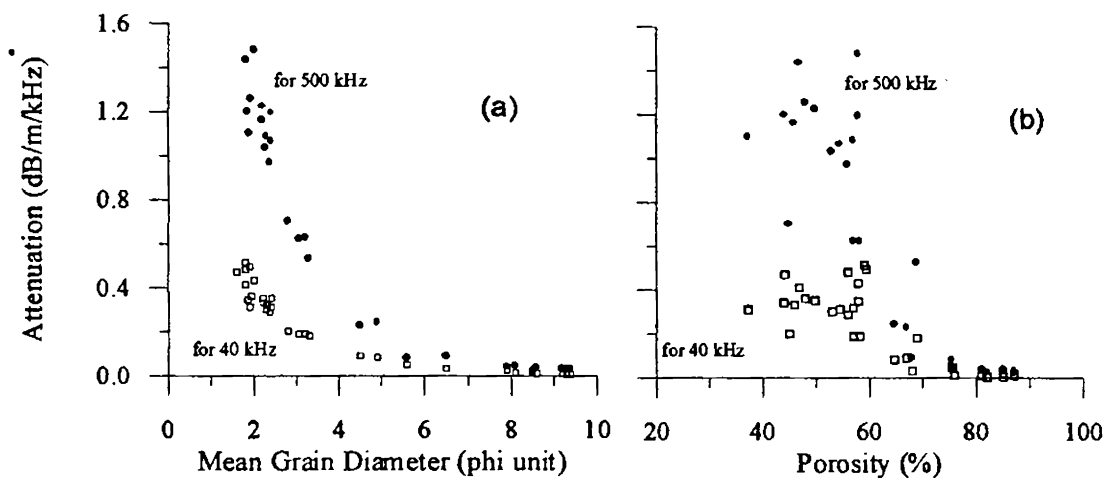
FIG.5.5. Computed attenuation in dB/m/kHz versus (a) mean grain size in phi units and (b) porosity (%).

Computed attenuation in dB/m/kHz is plotted against porosity in Fig.5.5b. The data shows more scattering compared to the data in Fig.5.5a. Here also the separate grouping of data is observed and the separation is not distinguishable in sediments having porosity of 60% or above. The predicted values of compressional wave attenuation is compared with the measured values available in the frequency range of 40 kHz and 500 kHz. In this study the predicted compressional wave attenuation varies

between 300 and 900 dB/m at 500 kHz in sandy sediments and varies between 10 and 50 dB/m in silt and clay sediments. At 40 kHz, attenuation is predicted below 20 dB/m in sandy sediments where as < 1dB/m is predicted in silt and clay sediments. Literature (Hamilton,1980; Stoll, 1985; and Kibblewhite, 1989) also indicates variation within this range and agrees well with the predicted attenuation values.

5.3. Velocity ratio versus physical properties

Sound speed and compressional wave attenuation in 139 sediment samples are computed using Biot-Stoll model and the equation of Haumeder (1986) respectively. The selected frequency is 100kHz and temperature is 27.5°C. The sound speed is converted to velocity ratio by dividing with sound speed in seawater at 27.5°C and its relationships with physical properties are estimated and are shown in Fig. 5.6.

Fig. 5.6. Velocity ratio versus (a) mean grain size, (b) bulk density, and (c) porosity

The equation relating mean grain size, $(M\varphi)$ to velocity ratio (R) is

$$R = 1.22493 - 0.0295 M\varphi$$
(5.13)

$(\sigma = 0.66$, coefficient of determination, $r^2 = 0.804$, s.e $= 0.029)$

This equation accounts 80.4 % of the variation in the velocity ratio (Batchman, 1989; Sanders, 1990).

The equation for density (ρ_{sat}) is

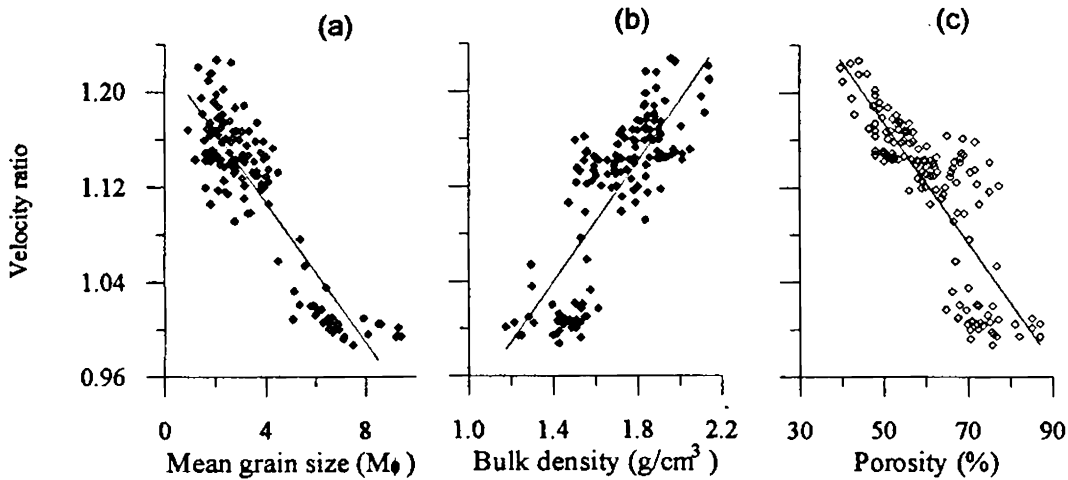$$R = 0.6834 + 0.2541\rho_{sat}$$

(5.14)

(σ = 0.66, coefficient of determination, r^2 = 0.653, s.e = 0.038)
which accounts 65.3 % of the variation in the velocity ratio

The equation for porosity (P) is

$$R = 1.4284 - 0.0051P$$

(5.15)

(σ = 0.66, coefficient of determination, r^2 = 0.678, s.e = 0.038)

This equation explains 67.8 % variation in the velocity ratio. To compute *in situ* surface sediment sound speed, one has to multiply the speed of sound in the bottom water at the desired location by the velocity ratio. Bachman (1989) studied the relationship between laboratory measured velocity ratio and physical properties. He suggested least-squares regression relationships between velocity ratio and mean grain size, porosity, and bulk density. These equations respectively explain 91.6 %, 88.0, and 86.4% of the variation observed in the velocity ratio.

5.4. Attenuation versus physical properties

Compressional attenuation in the sediment is a critical model input with significant control over the computed transmission loss (Ajaykumar, 1992). Estimates or measurements of the attenuation coefficient in sediments of the continental shelf of India are not available, and hence published results for other areas are normally used as guidelines in this regard. The published relationships between compressional wave attenuation and sediment porosity/mean grain size diameter are usually based on measurements (Hamilton, 1972, 1974, 1976). Attenuation in sediments is highly frequency dependent and also varies with sediment type and is related to porosity and mean grain diameter. Hamilton (1980) compiled all the available measured data and

showed that compressional wave attenuation (in dB/m/kHz) increases with porosity at the lower end (from 39 to about 55%) and then decreases very rapidly with increase of porosity. Similar increase is noticed in coarse sand to medium sand (mean grain size, from 0 to about 4.5 Mφ) and decreases exponentially with the increase of grain size. Hamilton (1972, 1980) separated the data set into four sections and fitted separate regression equations for each set. In this study an attempt is made to understand the relationships of compressional wave attenuation versus physical properties. The estimated attenuation in dB/m at 100kHz is converted to dB/m/kHz and the relationship between mean grain size, and porosity are illustrated in Fig. 5.7.
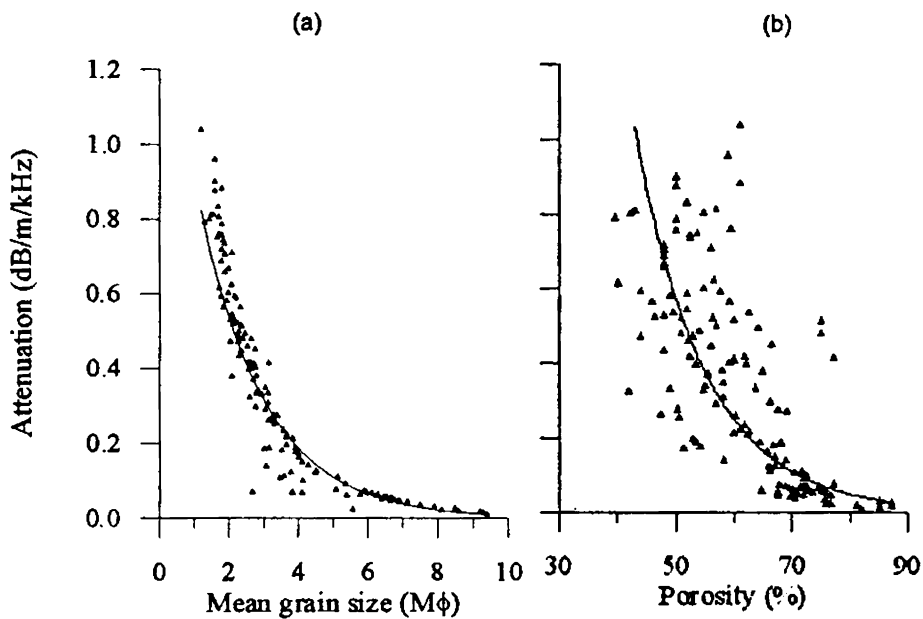
Fig. 5.7. Attenuation versus (a) mean grain size, and (b) porosity

The best fit equation (correlation coefficient = 0.96) for mean grain size is estimated and is given by:

$$\alpha = 1.5622 * e^{(-0.5327 M\varphi)} \qquad (5.16)$$

($\sigma = 0.28$, coefficient of determination, $r^2 = 0.923$, s.e = 0.092)

where α is the attenuation in dB/m/kHz , Mφ is the mean grain size diameter. The equation explains 92.3 % of the variation in attenuation.

The equation (correlation coefficient = 0.81) for porosity is given by:

$$\alpha = 37.7597 * e^{(-0.0837P)} \qquad (5.17)$$

(σ = 0.28, coefficient of determination, r^2 = 0.656, s.e = 0.244)

where α is the attenuation in dB/m/kHz , P is the porosity (%).The equation explains 65.6 % of the variation in the attenuation.

The regression equations indicate that the attenuation decreases exponentially with increase of mean grain size in phi units and porosity for the entire range of mean grain size and porosity considered. Similar trend is reported by Hamilton for high porosity ((>55%) and silt and clays (> 4Mφ) The increase of attenuation noticed by Hamilton (1972, 1980) in medium and fine sands is not observed here. LeBlanc (1992) also reported similar trend showing the increase of attenuation in medium and fine sand at low frequency (<50 kHz). In order to check this, attenuation is computed at 1 kHz for the same data set and no trend showing the increase of attenuation in sand is noticed (not shown). However, in Fig. 5.7 (a), decrease of attenuation with decrease of mean grain size (in phi units) is noticed for some sediment samples.

Measurements carried out by many workers (discussed above) reported a decrease of attenuation with decrease of mean grain size in phi units (in sands). Model suggested by BSM and Haumeder (1986) do not show this trend. This matter has to be investigated further whether it maybe due to the effect of the properties of sediments considered or due to the inadequacy of equations suggested in those models.

CHAPTER 6

SEASONAL VARIATION OF GEOACOUSTIC PROPERTIES
OF SEDIMENTS - OFF THE WEST COAST OF INDIA

The effect of temperature on sound speed and attenuation in marine sediments was discussed in section 2.3, chapter 2. In this chapter the effect of variation of temperature of the bottom water off the west coast of India (discussed in chapter 3) on sound speed and attenuation in sea floor sediment is presented.

6.1. Effect of temperature on sound speed in sediments: laboratory measurements

A few cases of laboratory studies on the effect of temperature on sound speed in water-saturated sediments have been reported (Sutton *et al.*, 1957; Shumway, 1958; Leroy *et al.*, 1986). This information on laboratory measurements of sound speed as a function of temperature is helpful in estimating *in situ* sound speeds and also in understanding the complexities of acoustic propagation in mixtures of solid particles and fluid. In order to study the effect of temperature on compressional wave sound speed in sediments, laboratory measurements are carried out on selected sediment samples at different temperatures and the details are discussed below.

Sound speed measurements are carried out on four sediment samples using the sediment velocimeter following the method discussed in chapter 4. Sediment sample of known length (path length) is placed between the two transducers and kept in standard seawater of known sound speed. The sound speed through core samples is then measured by comparison of the two different transit times in the sea water and sediment samples of same path length During measurements, constant temperature in sediment and standard seawater was maintained by continuous stirring of the standard seawater. Temperature at the time of measurement is noticed using mercury thermometer having an accuracy of 0.01 °C. Shumway (1958) reported that water sample or water saturated sediment in equilibrium with atmosphere may develop visible bubbles when heated. These air bubbles within sediment can interfere greatly with the sound speed measurement. Considering this, measurements are carried out at the lowest temperature and were continued as the temperature was raised to room temperature

gradually. Temperatures lower than that of the room were achieved by placing the sample and standard seawater in a refrigerator. Measurements were continued as the temperature was increased gradually to room temperature.

Sound speed measurements are carried out in four sediment samples A, B, C, and D and results are illustrated in Fig.6.1. Sample A and B are sandy sediments (% of sand is >80) where as sample C and D are silty sands (% sand is <80). It is seen that in all sediment samples considered here, sound speed increased linearly with temperature. For samples A and B a variation of 79 and 114 m/s in sound speed is observed when temperature varied between 5 and 29 °C. The corresponding variation was about 84 m/s for sample C and 77 m/s for sample D. Leroy *et al.* (1986) reported a variation of about 150 m/s in sound speed for sands for a temperature variation of 60°C (5 to 65°C). His results indicate that the maximum variation in sound speed is observed between 5 and around 30 °C. The present experiments clearly indicate that temperature variability in the water column can influence the compressional wave speed profile at the sea bottom interface.

In a related study, Rajan and Frisk (1991, 1992) studied the variation of the compressional wave speed profile with season due to temperature fluctuations in the pore water. The variability of pore water temperature with season was computed using a one-dimensional theory for heat transfer across the water/sediment interface and this was then combined with Biot-Stoll model for the sediments to determine the changes in compressional wave speed profile. Rajan and Frisk reported a variation in sediment sound speed of 30m/s, for a change in temperature of 11 °C for sands of porosity 50% in the Gulf of Mexico. Their results indicated that the influence of temperature variation in water column is felt to substantially greater depths in the sediment and cause variation in sound speed gradient within the sediment column.

Yamamoto (1995) studied sound speed and density fluctuations in the sediments of five shallow water sites and five deep-water sites at Tokyo Bay. He noticed that in sediments the density fluctuations are proportional to the sound speed fluctuations and the density fluctuations are usually much larger than the sound speed fluctuations. In
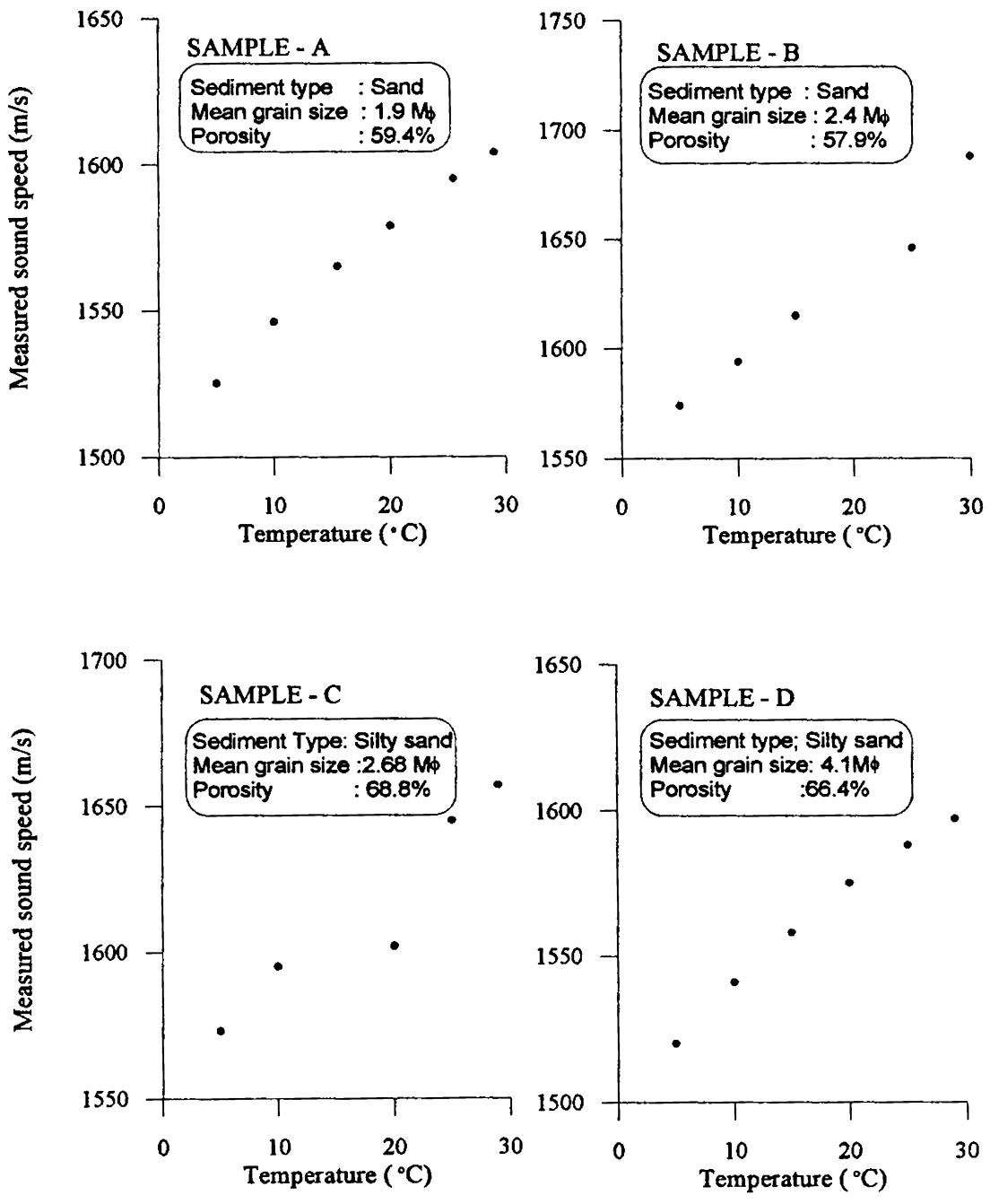
Fig.6.1. Measured values of sound speed in sediments with temperature

another study Yamamoto (1996) showed that the density fluctuations is the dominant mechanism for scattering from a sediment volume.

Murty and Naithani (1996) made a case study on the effect of sound speed gradients in sediment column on bottom reflection loss (BRL). They considered three types of sediments namely, silty clays, clayey silts and sand-silt-clay and showed that there exists an inverse relation between BRL (a measure of sound energy lost in to the seabed) and sound speed gradient. In these sediments BRL increases with decrease of sound speed gradient in sediment.

Pradeep Kumar (1997) reported seasonal variation in sound speed and attenuation due to bottom temperature fluctuation of the order of 11 °C in the water column off Cochin. He reported annual variation of 27 m/s in sound speed at 76 m water depth. The annual variation noticed in attenuation was of about 0.6 dB/m and 0.02 dB/m at 20 kHz and 2 kHz respectively. In the following section, the studies made on the seasonal variation of sound speed and attenuation in sediments at the sea bottom interface are presented for few locations in the shelf off west coast of India.

6.2. Seasonal variation of sound speed and attenuation in sediments at the sea bottom/water interface

The propagation of acoustic energy in shallow water is strongly influenced by the geoacoustic properties of sediments. These properties depend on the physical properties of the sediment material, the overburden pressure, and sediment temperature. In this study, the data on seasonal variation in bottom water temperature (discussed Chapter 3) is considered and the corresponding change in the compressional wave speed and attenuation in sediment is estimated. As discussed in chapter 2, Biot-Stoll Model (BSM) and Haumeder (1986) model is used to compute sound speed and attenuation in sediments respectively. BSM predicts sound speed in sediment as functions of frequency. Hovem and Ingam (1979) reported that the small sound speed dispersion predicted by the theory seems to be confirmed experimentally. The dispersion in sound speed is mainly caused by a decrease in the effective density at

higher frequencies (Hovem, 1980). Hovem showed that in normal compressional wave dispersion is negligible at low frequencies and very small dispersion is noticed at high frequencies (~50 m/s between 1 kHz and 1 MHz).

Sediment samples are collected from the respective study areas mentioned in Chapter 3. These samples represent surficial sediments and were analysed in the laboratory for their physical properties (bulk density, dry density, mean grain size, and porosity). The heat flow across the water/sediment interface results in the variation of the density and viscosity of the pore fluid (density of bottom water) with season. It is known that bulk density of the saturated sediment varies with the density of pore fluid. The effects of temperature and pressure changes on grain density of the minerals in the sediment are insignificant (Hamilton, 1971). Porosity of saturated sediment does not vary with season. In this study the variation in bulk density of the sediment and pore fluid viscosity with season are incorporated in the computation of sound speed and attenuation. The computation is carried out at 100 kHz and the results are illustrated in Figs.6.2 to 6.7.

6.2.1. Off Quilon

Figs. 6.2.a and   .b show the computed sound speed and attenuation in sediment at SD50. The bottom is sandy with mean grain size 2.29 in phi units and of porosity 57.4 %. Annual variation of 22 m/s in sound speed (between 1755m/s in January and 1777m/s in July) is noticed in sediment corresponding to a variation in bottom water temperature of 9 °C. Similarly, compressional wave attenuation indicated annual variation of 5.70 dB/m (46.74 to 52.44 dB/m). It can be clearly seen that the variation in sound speed and attenuation in sediment follows the thermal variation (Fig. 3.14) and varies approximately linearly with pore water temperature.

At SD100 the bottom is sandy (Figs. 6.2.c and   .d) having physical properties similar to the sediment at 50m location. Annual variation of 26 m/s in sound speed (from 1796 to 1822 m/s) is noticed with maximum in December and minimum in July for a temperature variation of 10°C. Attenuation indicated a variation of 5.23 dB/m

OFF QUILON

DEPTH: 50 m

(a)

(b)

SEDIMENT TYPE: SAND

MEAN GRAIN SIZE: 2.29 M

POROSITY　　　　: 57.40 %

DEPTH: 100 m

(c)

(d)

SEDIMENT TYPE : SAND
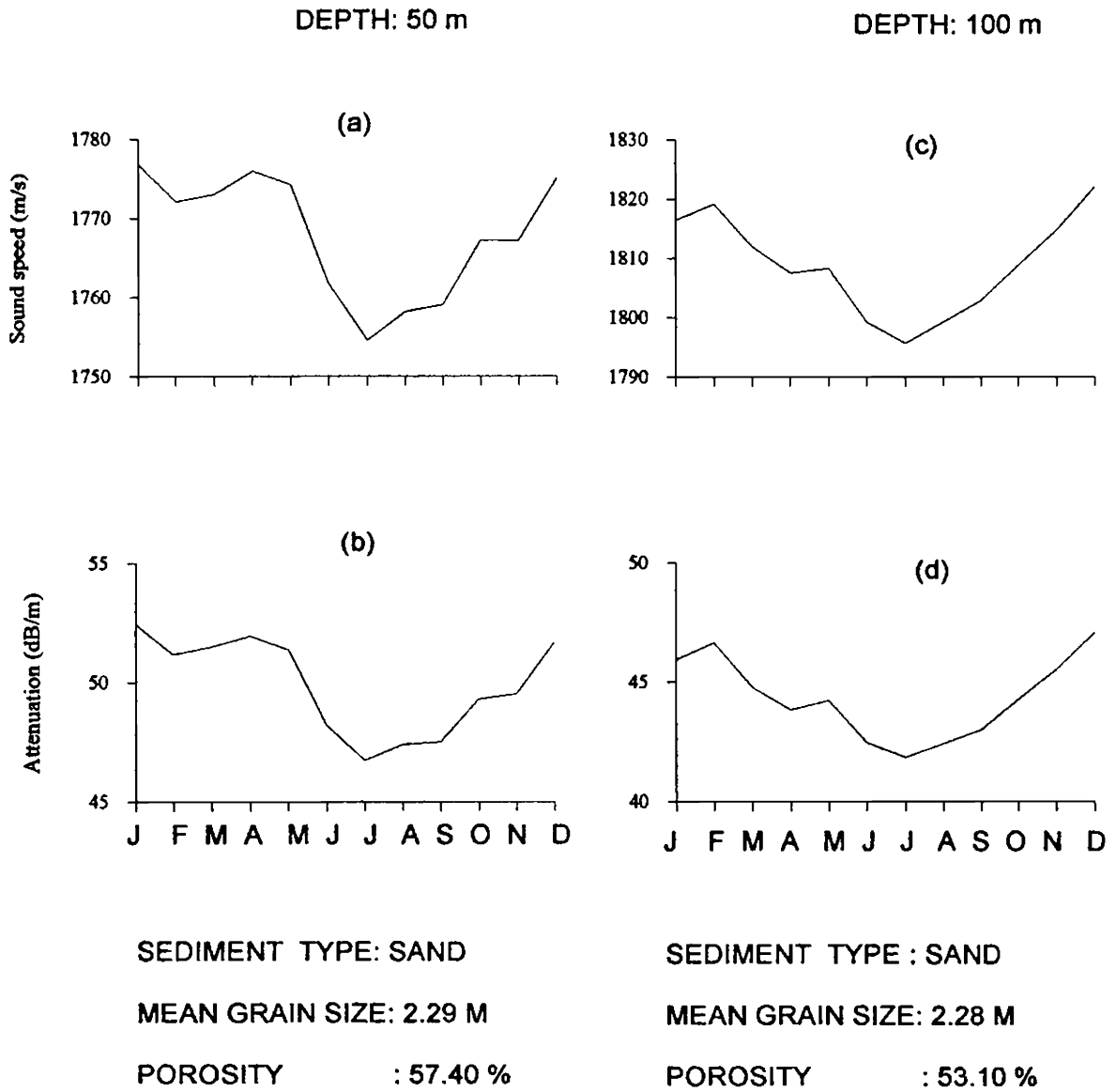
MEAN GRAIN SIZE: 2.28 M

POROSITY　　　　: 53.10 %

Fig. 6.2. Seasonal variation of sound speed and attenuation in sediments
at SD50 and SD100, off Quilon.

almost similar to that of SD50. Compared to the sediments at SD50, sound speed in sediments at SD100 is slightly higher, mainly due to the difference in porosity of the sediments. The sediment at SD100 is less porous (less water content and hence more rigid) compared to the sediment at SD50. At both locatons, sediment is sandy and having almost uniform grain size. Hamilton (1972a) reported that at any given particle size in sediments, porosity is a measure of packing. The number of interparticle contacts in sands depend on grain size and density of packing. At the same grain size, dynamic rigidity increases with decreasing porosity in sands because of more interparticle contacts with denser packing. Dynamic rigidity is a measure of resistance (friction and interlocking between grains) to shearing forces, which tend to move grains (Hamilton, 1972a, b). The main reason for higher values of sound speed noticed in sediments at SD100 could be the lower porosity resulting denser packing compared to the other.

6.2.2 Off Cochin

Annual variation in bottom water of about 8 and 9 °C temperatures are noticed at SD50 and SD100 respectively. Sandy sediments are noticed at both stations where as the sediment at SD50 is finer and more porous than the sediment at SD100. At SD50 (Figs. 6.3.a and   .b) a variation of about 19 m/s (1878 to 1859 m/s) in sound speed is noticed. Attenuation showed a variation of 5.31dB/m. Maximum values are noticed during December to February and minimum in August.

At SD100, sound speed varied from 1878 to 1855 m/s (a variation of 23 m/s) and attenuation showed a variation of 6.2 dB/m (Figs. 6.3.c and   .d). The maximum values of sound speed and attenuation are noticed during December to February and minimum in September.

6.2.3. Off Kasaragod

The sediment at SD100 is finer and having high porosity compared to the sediments at SD50. At both the study area annual variation of 9 °C is observed which resulted in a

OFF COCHIN

DEPTH: 50 m

DEPTH: 100 m
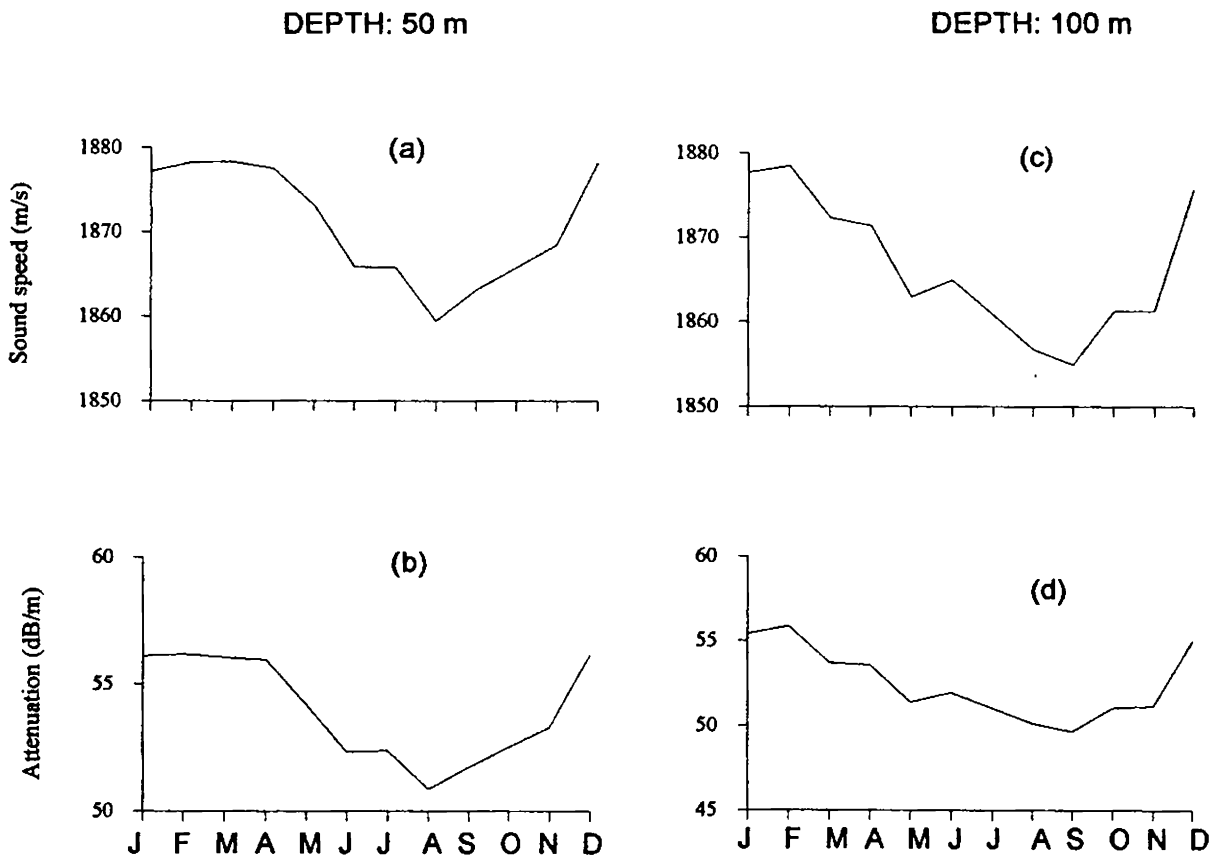
SEDIMENT TYPE: SAND

MEAN GRAIN SIZE: 3.05 M

POROSITY   : 57.40%

SEDIMENT TYPE: SAND

MEAN GRAIN SIZE: 1.85 M

POROSITY   : 45.60 %

Fig. 6.3. Seasonal variation of sound speed and attenuation in sediments
at SD50 and SD100, off Cochin.

variation of about 22 m/s in sound speed (1788 m/s in February and 1766 in September) in sediment at SD50 (Fig. 6.4a). Similarly attenuation varied between 33.29 and 30.02 dB/m and a variation of 3.27 dB/m is observed (Fig. 6.4b). At SD100, annual variation of 24 m/s in sound speed (1760 m/s in December and 1736 m/s in October) and annual variation of 1.53 dB/m in attenuation (between 17.38 dB/m in October and 18.91 dB/m in December) is noticed (Figs. 6.4c and   d). Compared to the sediments at SD50, less attenuation is noticed in sediments at SD100. The reason for the lower value of attenuation in the sediment may be due to the loose packing of finer material at high porosity.

6.2.4. Off Karwar

Very coarse sand with mean grain size of 0.93 Mφ is seen at SD50 location where as fine sand with mean grain size 4.09 Mφ is noticed at SD100. A variation of 20 m/s in sound speed and 11.98 dB/m in attenuation is noticed (Figs. 6.5a and   b) at SD50 (annual variation of temperature is 8 °C) where the maximum values are noticed in April and the minimum in November. Compared to SD50, the sediment at SD100 is finer and lower values of sound speed and attenuation is found. The sound speed varied between 1628 m/s in February and 1601 m/s in September (Fig. 6.5c) at SD100. Attenuationin sediment (Fig. 6.5d) showed annual variation of about 1.24 dB/m (varied between 15.85 and 14.64 dB/m). The lower values of attenuation at 100m sediment is related to the higher porosity (67%) and finer grain size compared to the sediment at 50m location.

6.2.5. Off Ratnagiri

At both locations silty sand sediments are noticed. At SD50 the sediment is finer and highly porous compared to the sediments at SD100. Compared to study areas in the southern locations, a lower annual variation of temperature (6 °C) is noticed. Correspondingly, sound speed in sediment showed lesser variation of about 18 m/s (varies between 1564 and 1582m/s) with maximum in April and minimum in

OFF KASARAGOD

DEPTH: 50 m

DEPTH: 100 m

SEDIMENT TYPE: SILTY SAND

MEAN GRAIN SIZE: 2.94 M

POROSITY   : 54.75 %

SEDIMENT TYPE: SAND

MEAN GRAIN SIZE: 3.15 M
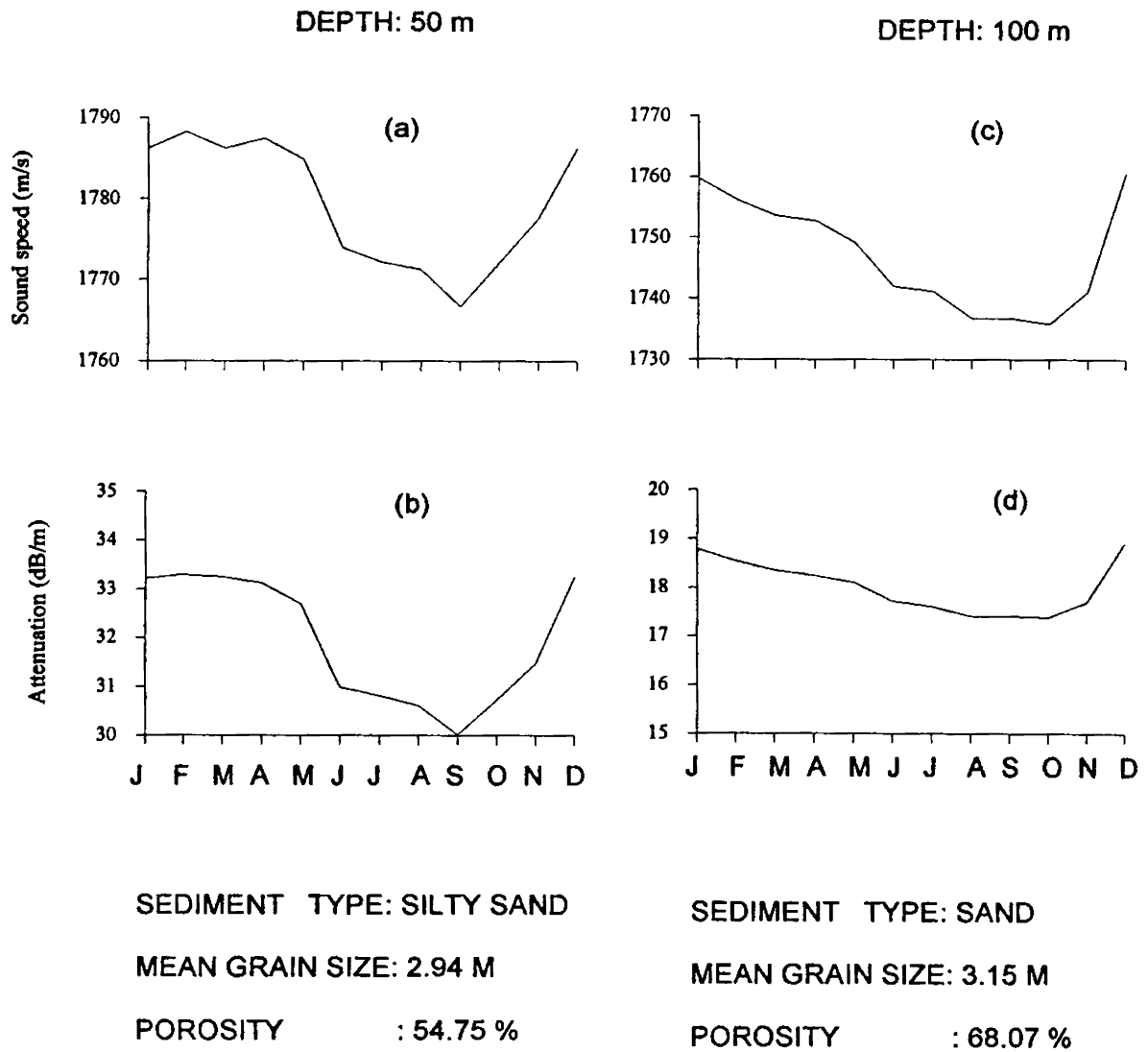
POROSITY   : 68.07 %

Fig. 6.4. Seasonal variation of sound speed and attenuation in sediments
at SD50 and SD100, off Kasaragod.

OFF KARWAR

DEPTH: 50 m

DEPTH: 100 m
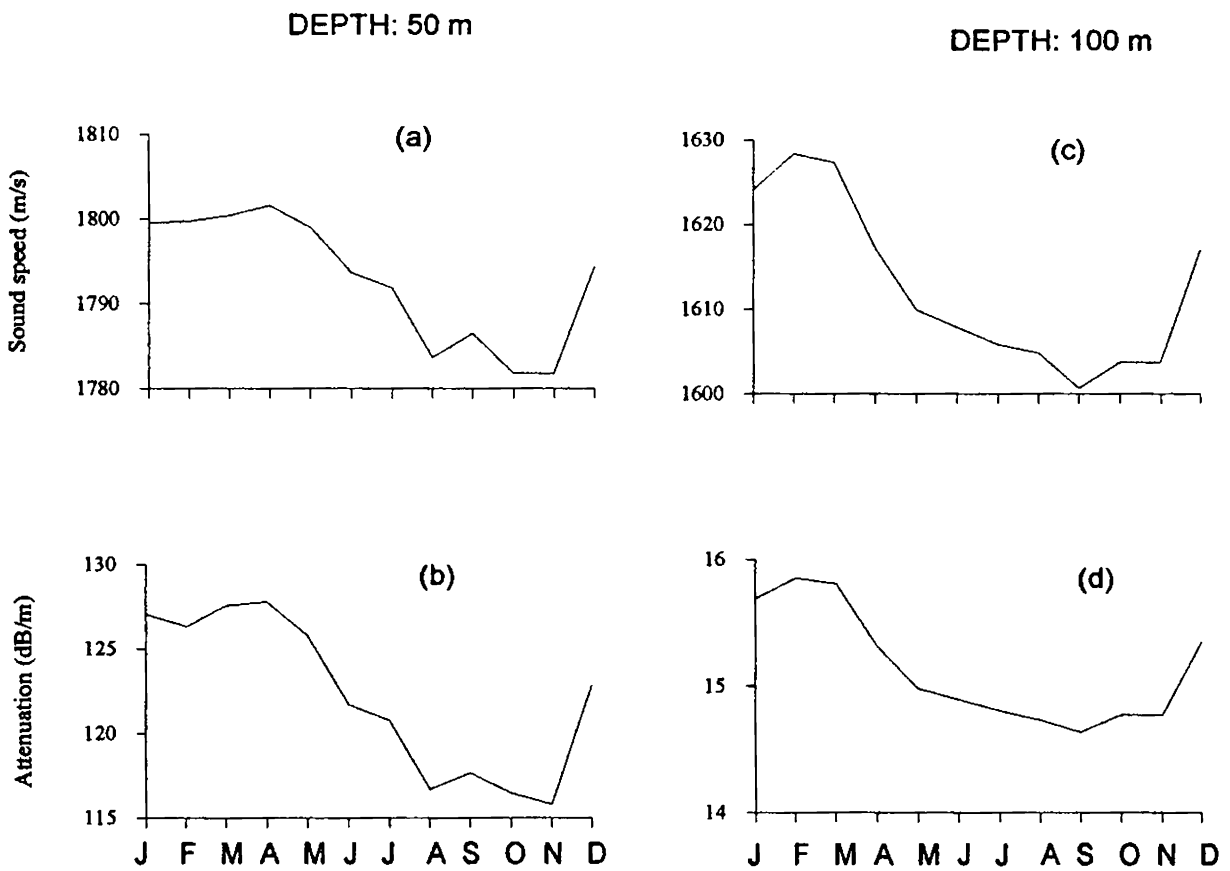
SEDIMENT TYPE: SAND

MEAN GRAIN SIZE: 0.93 M

POROSITY   : 51.56 %

SEDIMENT TYPE: SITY SAND

MEAN GRAIN SIZE : 4.09 M

POROSITY   : 67.11 %

Fig. 6.5. Seasonal variation of sound speed and attenuation in sediments
at SD50 and SD100, off Karwar.

OFF RATNAGIRI

DEPTH: 50 m

(a)

(b)

DEPTH: 100 m

(c)

(d)

SEDIMENT   TYPE: SILTY SAND

MEAN GRAIN SIZE: 5.38 M

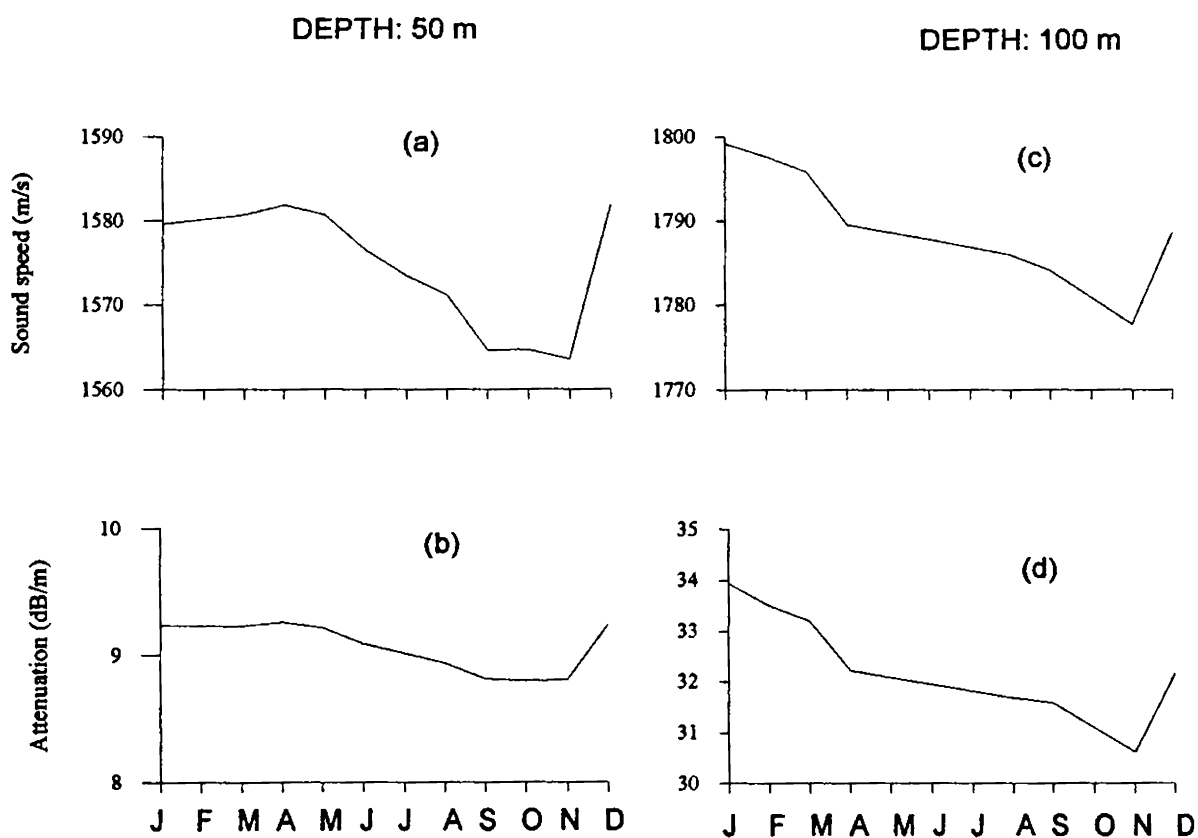POROSITY   : 70.21 %

SEDIMENT TYPE: SILTY SAND

MEAN GRAIN SIZE: 2.84 M

POROSITY   : 55.07 %

Fig. 6.6. Seasonal variation of sound speed and attenuation in sediments
at SD50 and SD100, off Ratnagiri.

October/November (Fig. 6.6a). The attenuation showed a variation of 0.46 dB (Fig. 6.6b).

At SD100, annual variation of 8 °C in bottom temperature is noticed corresponding to a variation of 21 m/s in sound speed with maximum value in January and minimum in November (Fig. 6.6c). Attenuation values are relatively higher compared to the sediments at SD50 and showed an annual variation of 3.32 dB/m (Fig. 6.6d). The higher values of attenuation at Sd100 is due to the coarser grain size and lower porosity compared to the sediment at SD50.

6.2.6. Off Bombay

The lowest annual variation in bottom water temperature among the study areas is noticed off Bombay where the process of upwelling and sinking are not prominent compared to southern locations. Annual variation of 3 °C and 5 °C in bottom temperature is noticed at SD50 and SD100 respectively. Highly porous clayey sediment is noticed at SD50. Sound speed in these finer sediment indicated lowest variation (Fig. 6.7a) of 10 m/s (between 1520 and 1530 m/s) corresponding to the annual variation of 3 °C in temperature. Attenuation values are also very low, varied between 2.64 and 2.74 dB/m in the annual cycle (Fig. 6.7b). The maximum values are noticed in July and minimum in September.

Coarser sand is noticed at SD100 location with porosity 51%. An annual variation of 12 m/s in sound speed is noticed with maximum value of 1873 m/s in July and a minimum value of 1861 m/s in November (Fig. 6.7c). Attenuation in this sediment varies between 77.71 dB/m in July and 73.76 dB/m in November (Fig. 67d).

At SD50, the sound speed in sediment observed in the range of 1520 to 1530 m/s is the lowest value noticed in this study variation (Fig. 6.7a). This indicates that these sediments (clay with porosity 79 % and grain size 8Mφ) are having low sound speed values compared to the sound speed in bottom water. In bottom water the annual variation of temperature is very small and sound speed varied between 1532 and 1541

OFF BOMBAY

DEPTH: 50 m

(a)

Sound speed (m/s)

1540
1530
1520
1510

(b)

Attenuation (dB/m)

3.0
2.5
2.0

J F M A M J J A S O N D
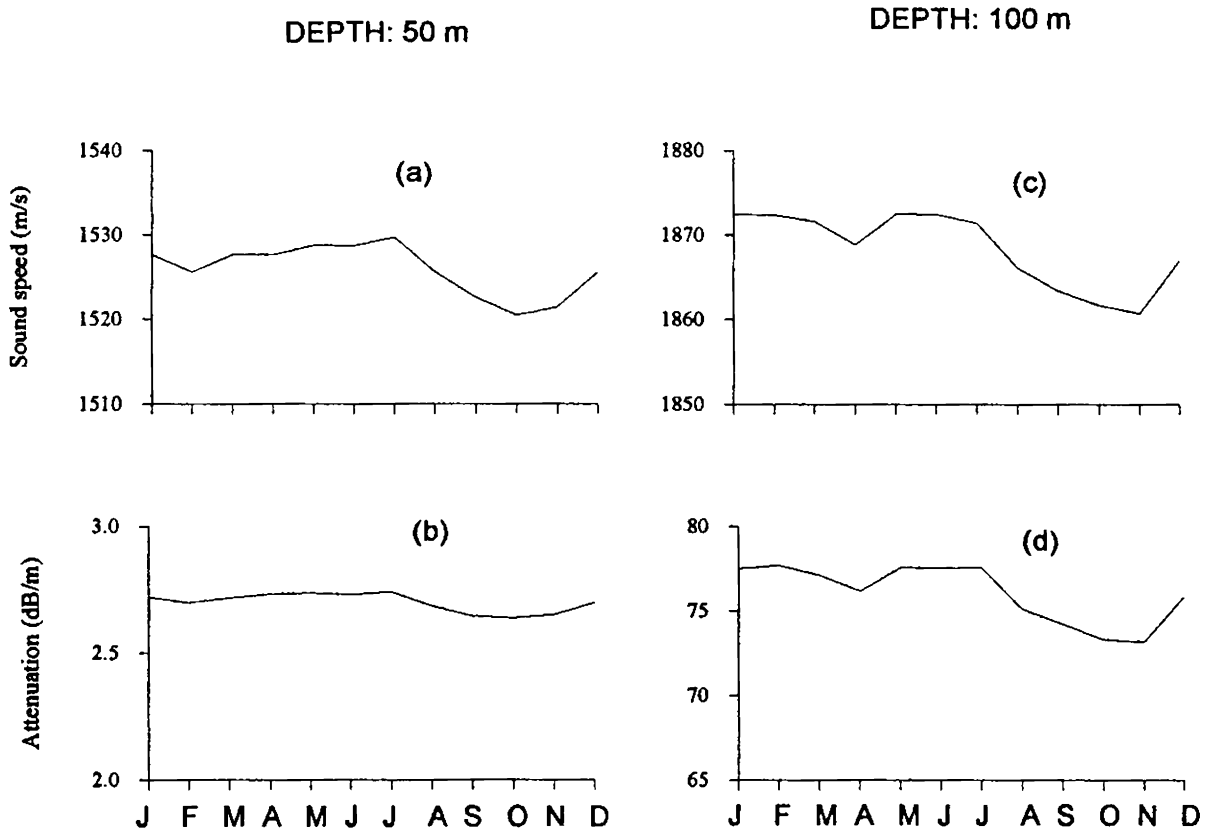
SEDIMENT   TYPE: CLAY

MEAN GRAIN SIZE: 8.0 M

POROSITY   : 79.0 %

DEPTH: 100 m

(c)

1880
1870
1860
1850

(d)

80
75
70
65

J F M A M J J A S O N D

SEDIMENT   TYPE: SAND

MEAN GRAIN SIZE: 1.29

POROSITY   : 51.0%

Fig. 6.7. Seasonal variation of sound speed and attanuation in sediments
at SD50 and SD100, off Bombay

m/s annually variation (Fig. 3.14). This indicates that in general, sound speed in bottom water at SD50 is higher than that of the sediment underlying and may result in the formation of a sound channel in surficial sediments which is analogous to that in the oceanic water masses. Hamilton (1970a, 1980) reported that in Central Pacific, deep-sea silt-clay surficial sediments have sound speeds less than that in the water overlying the bottom. Hamilton reported the existence of a sound channel in Central Pacific at water depths 4000-6000 m and he estimated the height of these channels should vary between 15 and 60 m. The height of this channel depends on the velocity ratio and on the sound speed gradient within the sediment layer (Hamilton, 1980).

Shirley and Anderson (1975) reported the existence of sediment with low sound speed layers in sediments than the overlying water in the deep sea of Guiana Basin. They observed that high porosity (71.8 to 78.5%) values of the samples are consistant with the low sound speed values measured. This low sound speed in sediment is due to high porosities, balance between water and mineral compressibilities (or bulk moduli) and densities, plus low rigidities and low mineral frame bulk moduli (Hamilton, 1971; Hamilton and Bachman, 1982).

Murty and Pradeep Kumar (1986) reported the distribution of similar type of sediments near the coast off Bombay. The seismic profile data collected over this area indicated a minimum layer thickness of 15 m lying over a sandy sub-bottom layer. This clearly indicates the possibility of the existence of sound channels in the surficial sediments, off Bombay. However, this requires further detailed investigation.

CHAPTER 7

SUMMARY OF RESULTS AND CONCLUSIONS

Sediments with different physical properties cover the bottom of the ocean and knowledge of the physical and geoacoustic properties is essential for understanding the propagation of sound through the sediment. It is within this surficial zone (upper 50 cm of sediment) that the most active and rapid diagenic changes in sediment properties are noticed. For high frequency acoustic applications, geoacoustic properties of the upper tens of centimeters must be known where as for low frequency applications surficial geoacoustic properties provide the initial conditions used for prediction of depth gradients of sediment physical properties. Accurate values, including variability, of surficial sediment properties are therefore required for geoacoustic models covering the wide range of frequencies of interest in studies related to underwater acoustics.

Obtaining accurate values of geoacoustic properties, however, is not an easy process, as direct measurements are expensive and time consuming and hence alternative methods have to be selected. In this study two alternative methods are considered to infer the geoacoustic properties of surficial sediments. One method is to relate, empirically, the geoacoustic properties of a sediment to its physical properties (such as porosity, grain size and density) which takes advantage of the fact that sediment geophysical properties are easily measurable than geoacoustic properties. Another method also relates geoacoustic properties to physical properties based on physical principles and a single comprehensive theory of porous media proposed by Biot. Stoll latter applied the Biot's theory to marine sediments and popularly known as Biot-Stoll Model (BSM).

Estimates or measurements of geoacoustic properties of sediments of the Indian Ocean are not available. Hence estimates/relationships derived for sediments of other areas (e.g. Atlantic and Pacific Oceans) and different environment are normally considered by researchers for studies related to geoacoustic properties of sediments of the Indian Ocean which may not be adequate. This study brought-out the inter-relationships among physical and geoacoustic properties of sediments off the west coast of India. These relationships derived from the present study can be utilised in bottom

interacting ocean acoustics and other related studies, as it is useful for the estimation of geoacoustic characteristics of sediments using more commonly available physical property measurements.

7.1. Relationship among the physical properties of sediments

The data on physical properties of 139 sediment samples collected from the continental shelf off Gujarat to south off Quilon are considered in this study. These sediment samples are collected from the continental shelf using sediment samplers (gravity corer and grab) during different sea trials. Sediment type showed variation from coarse sand to clay. Measurements of physical properties are carried out in the laboratory following standard methods. In these sediments porosity varies from 39 to 87% and mean grain size varies from 1 to 9 $M\varphi$. The empirical relations among porosity, mean grain size, bulk density of these sediments are derived and discussed with the results of other oceans.

Most of the earlier studies suggested linear relationship between porosity and mean grain diameter. For the data set (porosity versus mean grain size) considered in this study a polynomial curve fit is found to be the best fit. In general, porosity of sediments increases with increases with mean phi units, $M\varphi$.

T
551.75
PRA

The relationship between porosity and bulk density showed linear correlation. Theoretically this linearity only exists if the dry densities of mineral particles are the same for all marine sediments. The density of the sediment would then be the same as the density of the solid material at zero porosity, and the same as the density of the water at 100 % porosity. The regression equation shows that density of the sediment at zero porosity (i.e. the density of the solid material) would be 2.837 g/cm^3 which is slightly higher compared to the values given for other oceans. The presence of calcium carbonate content, clay minerals and the variations of quartz, feldspar and argonate crystals in the sediments are some factors that influence grain density from one region to another. In this study the relationship between bulk density and mean grain diameter

indicated an exponential curve fit and the bulk density of the sediment decreases with mean grain size in phi units.

7.2. Measurement of sound speed in sediments

During the course of this study, a new instrumentation 'sediment velocimeter' is developed to measure compressional wave sound speed in sediments. This velocimeter operates at 500 kHz. The speed of sound in marine sediment is determined from the time delay between the transmitted and received signals at the two transducers kept on either side of the sediment sample and computation is carried out following Richardson (1986) and Harker et al., (1991). The instrumentation is calibrated by measuring sound speed in distilled water and the velocimeter is used for measuring sound speed in different types of marine sediments.

7.3. Velocity ratio versus physical properties

Laboratory measured sound speed must be corrected to *in situ* conditions for use in acoustic propagation studies,. The ratio of sound speed in sediment to sound speed in sea water is called "velocity ratio" is constant for a given sediment sample. It is the same in the laboratory as it is at the seafloor at any water depth. To determine *in situ* surface sediment sound speed, one has to simply multiply the speed of sound in the
. bottom water at the desired location by the velocity ratio. In surficial sediments, grain size, grain density and porosity do not vary significantly with temperature and pressure. This "velocity ratio" method eliminates the need to correct for temperature and pressure differences, velocity ratio is a more convenient measure of surficial sediment sound speed than is sound speed in the laboratory. The applicability of this method was confirmed by Tucholke and Shirley (1979) in a study comparing *in situ* nose-cone velocimeter measurements of piston cores with laboratory sound speed corrected to *in situ* conditions. The interrelation between velocity ratio and physical properties of sediments is studied. Equations relating velocity ratios and physical properties (porosity, mean grain size and density) are derived. In this regard, the relation between laboratory measured velocity ratios versus physical properties are studied. Velocity ratios of 31 sediment samples are measured and a linear regression relation is found to

be the best fit for the data. The relationship between computed velocity ratio versus physical properties for 139 sediment samples is also presented.

7.4. Prediction of compressional wave sound speed and attenuation in sediments

Previous studies have examined the physics of Biot's formulation in the laboratory and the results generally appear to confirm the accuracy of the theory. Since some of the model input parameters are difficult to acquire even under controlled laboratory settings, its usefulness in generating geoacoustic models for field applications has been in question. In this study BSM is applied for the sediments and only a few of the model inputs were directly measured.

The predicted sound speeds in clay sediments are seen above the measured values. These sediments have mean grain size Mφ values around 9 and porosities in the range of 81 to 87%. In sediments at this range of porosity and grain size, the skeletal frame moduli proposed by BSM may not be suitable and the sediment grains behave like suspensions. Hence the disagreement between measured and predicted sound speeds in clay samples may be due to the inadequacy of BSM to contain sediments of these properties.

In most of sandy sediments, the predicted sound speeds are below the measured values. The calcium carbonate content in these samples may be a reason for this. The sound speed generally increases with rise in calcium carbonate content in the sediment. The calcium carbonate content in sediments is not estimated in this study. BSM is sensitive to the frame modulii for the prediction of sound speed in sediments. In earlier studies it is reported that when Hamilton's regression equations are used for the derivation of frame modulii, the predicted sound speeds fell below the measurements (Ogushwitz, 1985). This indicates that Hamilton's empirical relations used in this study for computing the frame modulii are not adequate for carbonate rich sediments resulting in underestimation of the predicted values over measured ones.

The study on the deviation from predicted sound speed to the measured sound speed in sediments indicated that 81% of the sediment fell within the limit of ± 5% deviation from a perfect fit.

7.5. Prediction of compressional wave attenuation

A difficulty in the use of BSM is the problem of accurately determining the 13 geophysical inputs since many of the inputs cannot be directly measured. The imaginary part of the frame bulk modulus is related to the attenuation of compressional waves and is calculated by a logarithmic decrement of longitudinal waves. The typical values of 0.1 for the granular sediments and 0.01 for the silty clay are chosen by most of the researchers and this may cause error in the computation when considering different types of sediments ranging from coarse sands to very fine soft clay. Therefore, BSM is not considered for the prediction of compressional wave attenuation in sediments. However, the equations of Haumeder which is derived from Biot theory is considerd in this study.

Haumeder has shown that with the knowledge of the relaxation times, for a porous, fluid-filled material the response of the attenuating medium can be completely characterized. Compared to BSM the later model does not considering logarithmic decrement of longitudinal wave for the computation of attenuation. Relaxation times are expressed entirely in terms of flow parameters and with knowledge of the relaxation time, the response of the attenuating medium can be completely characterized and hence the equation of Haumeder is opted for computing compressional wave attenuation in this study.

Many authors suggested a linear dependency between frequency and attenuation. In order to study the dependency of attenuation with frequency, compressional wave attenuation (dB/m) is computed for the frequencies 500 kHz and 40 kHz. The computed attenuation values agreed well with the published results. The computed attenuation is converted to dB/m/kHz and plotted against mean grain diameter in phi units. The result is that data is widely scattered and also showed two

separate groupings. If the linear dependency exist, there would not have been any grouping of data.

It is also noticed in this study that sediments with mean grain size 8 phi units and above (fine silts and clay) the separation of grouping of data disappears and only scattered data is seen. At high porosity (> 80%), the sediment behaves like suspensions and the assumption of linear dependency can be considered. This linearity holds good where particle interactions can be neglected at low concentrations of sediment in suspension.

Computed attenuation in dB/m/kHz is also plotted against porosity. The data shows more scatter compared to attenuation versus mean grain size. Here also the separate grouping of data is observed and the separation is not distinguishable in sediments having porosity of 60% or more.

7.6. Relationship between the physical properties and geoacoustic properties of sediments

Compressional wave sound speed and attenuation in sediments are computed using BSM and the equation of Haumeder respectively. The sound speed is converted to velocity ratio by dividing with sound speed in seawater and relationships with physical properties are derived. Attenuation in sediment is highly frequency dependent and also varies with sediment type and is related to porosity and mean grain diameter. The estimated attenuation in dB/m at 100kHz is converted to dB/m/kHz and the relationships between mean grain size, and porosity are derived.

The regression equations indicate that attenuation decreases exponentially with increase of mean grain size in phi units and porosity for the entire range of mean grain size and porosity considered. Similar trend is reported by Hamilton for high porosity ((>55%) and in silt and clays (> 4Mφ) The increase of attenuation with the increase of grain size in phi units noticed by Hamilton (1972, 1980) in sands (< 4Mφ) is not observed in this study. In few sediments of the data set considered in this study the computed attenuation at 1kHz showed a decrease of attenuation with decrease of mean

separate groupings. If the linear dependency exist, there would not have been any grouping of data.

It is also noticed in this study that sediments with mean grain size 8 phi units and above (fine silts and clay) the separation of grouping of data disappears and only scattered data is seen. At high porosity (> 80%), the sediment behaves like suspensions and the assumption of linear dependency can be considered. This linearity holds good where particle interactions can be neglected at low concentrations of sediment in suspension.

Computed attenuation in dB/m/kHz is also plotted against porosity. The data shows more scatter compared to attenuation versus mean grain size. Here also the separate grouping of data is observed and the separation is not distinguishable in sediments having porosity of 60% or more.

7.6. Relationship between the physical properties and geoacoustic properties of sediments

Compressional wave sound speed and attenuation in sediments are computed using BSM and the equation of Haumeder respectively. The sound speed is converted to velocity ratio by dividing with sound speed in seawater and relationships with physical properties are derived. Attenuation in sediment is highly frequency dependent and also varies with sediment type and is related to porosity and mean grain diameter. The estimated attenuation in dB/m at 100kHz is converted to dB/m/kHz and the relationships between mean grain size, and porosity are derived.

The regression equations indicate that attenuation decreases exponentially with increase of mean grain size in phi units and porosity for the entire range of mean grain size and porosity considered. Similar trend is reported by Hamilton for high porosity ((>55%) and in silt and clays (> 4Mφ) The increase of attenuation with the increase of grain size in phi units noticed by Hamilton (1972, 1980) in sands (< 4Mφ) is not observed in this study. In few sediments of the data set considered in this study the computed attenuation at 1kHz showed a decrease of attenuation with decrease of mean

grain size (in phi units). However, measurements carried out by many workers reported a decrease of attenuation with decrease of grain size in phi units (in sands). Results of the model suggested by Haumeder (1986) and BSM do not indicate this trend. This matter has to be investigated further in detail whether it is due to the difference in the properties of sediments considered or due to the inadequacy of equations suggested by Haumeder/BSM.

7.7. Seasonal variation of temperature, salinity, density and sound speed in water at the sea bottom – off west coast of India.

The bottom temperature and its seasonal variation have profound influence in modifying the acoustic properties of sediments. Most of the earlier studies on the temperature and salinity in the Arabian Sea are mainly confined to the upper layers of the water column. In this study six areas are selected and brought out certain aspects of the seasonal variability of temperature, salinity, density and sound speed in the continental shelf along the West Coast of India. At each study area, two stations are selected in such a way that the maximum depths at these stations are 50m and 100m.

The present study shows that at the study areas (at 50m and 100m stations) the annual variation of temperature and salinity and hence density and sound speed is much larger at the bottom rather than that of at the surface. This is caused by a variety of factors, mainly upwelling and downwelling and to a lesser extent due to the presence of high saline Arabian Sea waters and low saline Bay of Bengal waters. Moreover, the intensity of these factors varies seasonally and spatially. It can be seen that the annual variations of temperature and sound speed are maximum in the four southern stations compared to those of the two northern stations, as the processes of upwelling and sinking are more dominant at the southern locations. The large fluctuations of temperature and salinity at the bottom modify the properties of sediments. It is hypothesized that heat flow from the bottom of the water column into the sediment affects the sediment pore water temperature, there by influencing the temperature structure and thus the compressional wave speed and attenuation in the sediments.

Since this heat flux varies with season, the effect on sediment compressional wave speed and attenuation also changes seasonally.

The heat flow across the water/sediment interface results in the variation of the density and viscosity of the pore fluid (density of bottom water) with season. It is known that bulk density of the saturated sediment varies with the density of pore fluid. The variation in bulk density of the sediment and pore fluid viscosity with season is incorporated in the computation of sound speed and attenuation. The computation is carried out at 100 kHz.

It is also noticed that the variation of sound speed and attenuation in sediment follows the thermal variation and varies approximately linearly with pore water temperature. Corresponding variations in sound speed and attenuation in sediments are noticed in an annual cycle. The minimum variations are noticed in sediments off Bombay.

At 50m, depth off Bombay clay sediments (porosity 79 % and grain size 8Mφ) with sound speed less than that of the overlying water is noticed throughout the year. In an annual cycle sound speed at bottom of the water column varies between 1532 and 1541 m/s where as in sediment sound speed varies between 1520 and 1530 m/s. Based on the results of seasonal variation of temperature and sound speed in bottom water and sediment at 50m depth, off Bombay, a possibility of the formation of a sound channel in surficial sediments which is analogous to that in the oceanic water masses is indicated. However, this requires further detailed investigation.

7.8. Future scope of the work

The present study is mainly restricted to the sediments of continental shelf between off Gujarat and Quilon. More sediment samples and including samples from other area of the continental shelf of India will provide completeness of this study. The samples collected using grab and gravity corer generally represent surficial sediment of the study area.

Information below the sea floor can be estimated by using these surficial properties as the initial conditions and knowledge of gradients or by collecting sediment samples below the seafloor from corer/bore hole in addition to methods ranging from *in situ* probes in sediments to resonance technique and inversion technique. In this study, shear wave is not considered mainly due to the non-availability of data and measurement facility.

The compressional wave sound speed in sediment is likely to be influenced by the calcium carbonate content. This aspect is not included in the theoretical studies or establishing regression equations, as the carbonate content in sediment could not be estimated during this study. The modification of frame bulk moduli by including the effects of carbonate content will improve BSM model. Also both BSM and Haumeder model could not provide the results of 'observed decrease in compressional wave attenuation with decrease of grain size in phi units (in sands)'. The reason for this has to be studied further in detail.

In this study sound speed is measured at 500 kHz and attenuation measurements are not included. Attenuation in sediments strongly depends on frequency. More laboratory and *in situ* measurements of attenuation and sound speed in different types of sediment at the frequencies of interest are to be carried out to solve the complexities noticed in this study. Also *in situ* measurements of both sound speed and attenuation in sediments during different season would throw more light on the results presented in this study.

REFERENCES

Ajaikumar, M. P , (1992) Studies on sound propagation modelling in coastal seas – a ray theoretical approach. Ph. D Thesis, Cochin University of Science and Technology, Cochin, pp.148

Akal, T., (1972) The relationship between the physical properties of underwater sediments that affect bottom reflection. *Marine Geology*, 13, 251

Akal, T., (1980) Sea floor effects on shallow-water Acoustic propagation. In **Bottom Interacting Ocean Acoustics**, Edited by Kuperman, W.A, and Jensen, F.B, Plenum Press, New York

Akal, T., Stoll, R.D., (1995) An expendable penetrometer for rapid assessment of seafloor parameters,In **Oceans '95**, MTS/IEEE Proceedings

Akal, T,, Caiti, A. and Stoll, R.D., (1992) Seismo-acoustic waves for remote sensing in shallow-water sediments. In **European conference on underwater acoustics**, edited by M. Weydert, Elsevier Science Publishers, England

Ali, H. B., (1993) Oceanographic variability in shallow-water acoustics and the dual role of the sea bottom. *IEEE J. Ocean Engg.*, 18, 31

Anderson, R.S., (1974) Statistical correlation of physical properties and sound velocity in sediments. In **Physics of Sound in Marine Sediments**, edited by L.Hampton (Plennum, New York

Bachman, R.T., (1985) Acoustic and physical property relationships in marine sediments. *J.Acoust.Soc.Am*, 78, 616

Bachman, R.T., (1989) Estimating velocity ratio in marine sediment. *J.Acoust.Soc.Am*, 86, 2029

Bachman, R.T. and Hamilton, E.L., (1976) Density, porosity, and grain density of samples from deep sea drilling project site 222 (Leg 23) in the Arabian sea. *J.Sediment. Petrol.* 46, 654

Badri, M, and Mooney, H.M., (1987) Q measurements from compressional waves in unconsolidated sediments. *Geophysics*, 52, 772

Banse, K., (1968) Hydrography of the Arabian Sea shelf of India and Pakistan and effects on demersal fishes. *Deep-Sea Research*, 15, 45

Bell, D.W., (1979) Shear wave propagation in unconsolidated fluid saturated porous media. ARL-TR-79-31, Applied Res. Labs., Univ. of Texas, Austin

Bennet, R.H. and Lambert, D.N., (1971) Rapid and reliable techniques for determining unit weight and porosity of deep-sea sediments. *Mar. Geol.*, 11, 201

Berryman, J.G., (1980) Long wavelength propagation in composite elastic media.I. Spherical Inclusions. *J.Acoust.Soc.Am*, **68**, 1809

Best, A.L, Roberts, J.A., and Somers, M.L., (1988) A new instrument for making in-situ acoustic and geotechnical measurements in seafloor sediments. *J.Soc. for Underwater Technology*, **23**, 123

Biot, M.A., (1956a) Theory of propagation of elastic waves in a fluid-saturated porous solid.I. Low frequency range. *J.Acoust.Soc.Am*.**28**, 168

Biot, M.A., (1956b) Theory of propagation of elastic waves in a fluid-saturated porous solid.I. Low frequency range. *J.Acoust.Soc.Am*, **28**, 179

Biot, M.A., (1962) Generalised theory of acoustic propagation in porous dissipative media. *J.Acoust.Soc.Am*, **34**,1254

Bowles, F.A., (1997) Observation on attenuation and shear wave velocity in fine grained marine sediments. *J. Acoust. Soc. Am*, **101**, 3385

Bowman, L., March, R., Orenberg, P. and True, D., (1995) Evaluation of dropped versus static cone penetrometers at a calcareous cohesive site.In **Oceans '95**, MTS/IEEE Proceedings

Boyce, R.E., (1976) Sound velocity-density parameters of sediment and rock from DSDP drill sites 315-318 on the Line Island chain, Manihiki Plateau, and Tuamotu Ridge in the Pacific Ocean. In **Initial reports of Deep Sea Drilling Project** edited by Schlanger SO et al. (GPO, Washington DC)

Brekhovskikh, Yu. Lysanov., (1982) Fundamentals of ocean acoustics, Springer-Verlag, New York.

Brunson, B.A., and Johnson, R.K., (1980) Laboratory measurements of shear wave attenuation in saturated sands. *J.Acoust.Soc.Am*, **68**, 1371

Buckingham, M.J., (1997) Theory of acoustic attenuation, dispersion, and pulse propagation in unconsolidated granular materials including marine sediments. *J.Acoust.Soc.Am* , **102**, 2579.

Buckingham, M.J., (1998) Theory of compressional and shear waves in fluidlike marine sediments. *J.Acoust.Soc.Am*. **103**,288

Bullard, E.C., (1963) The flow of heat through the sea floor of the ocean. In **The Seas**, Interscience Publishers, New York

Carman, P.C., (1956) Flow of geases through porous media, Academic, New York

Chapman, N.R., Levy, S., Cabrera, Stinson, K. and Oldenburg, D., (1985) The estimation of the density, P-wave, and S-wave speeds of the top-most layer of

sediments, from water bottom reflection arrivals. . In **Ocean Seismo-Acoustics**, Edited by Akal T and Berkson JM, Plenum Press, New York

Chapman, N.R., Levy, S., Stinson. K Jones. I., Prager, B. and Oldenburg. D., (1985) Inversion of sound speed and density profiles in deep ocean sediments. *J.Acoust.Soc.Am.*, 79, 1441

Chari, T.R., (1978) Instrumentation problem related to determination of geotechnical properties of ocean sediment. *IEEE J. Ocean Engg*, OE-3

Chen, C.T. and Millero, F.J., (1977) Speed of sound in sea water at high pressures. *J.Acoust.Soc.Am.*, 62, 1129

Chotiros, N.P., (1995) Biot-model sound propagation in water-saturated sand. *J. Acoust. Soc. Am*, 97, 199

Clay. C.S. and Medwin. H., (1977) Acoustical Oceanography: Principles and applications. Wiley-Interscience Publication, Canada

Colborn, J.G., (1975) The thermal structure of the Indian Ocean. East-West Centre Press, University of Hawaii, pp173

Collins. J.A., Sutton, G.H. and Ewing, J.I., (1996) Shear wave velocity structure of shallow-water sediments in the East China sea. *J. Acoust. Soc. Am* 100,

Costley, R.D. and Bedford. A., (1988) An experimental study of acoustic waves in saturated glass beads. *J. Acoust. Soc. Am.*, 83, 2165

Courtney, R.C. and Mayer, L., (1993) Calculation of acoustic parameters by a filter-correlation method. *J. Acoust. Soc. Am*, 93, 1145

Courtney, R.C. and Mayer. L., (1993) Acoustic properties of fine-grained sediments from Emerald Basin: Toward an inversion for physical properties using Biot-Stoll model. *J. Acoust. Soc. Am*, 93, 3193

Darbyshire, M., (1967) The surface waters off the coast off Kerala, southwest India, *Deep-Sea Research*, 14, 295

Das, B.K., Srivastava, B., Kumar, J.P., Mistra, P.K. and Samadder, A.K., (1993) Index properties of sediments off Narsapur, east coast of India and their importance to off shore construction. *Ind. J. Mar.Sc*, 22, 123

Davis, A.M. and Bennel, J.D., (1986) Dynamic properties of marine sediments. In **Ocean Seismo-Acoustics**, Edited by Akal.T and Berkson.J.M., Plenum press, New York

Del Grosso, V.A. and Mader,C.W., (1972) Speed of sound in sea water samples. *J. Acoust. Soc. Am.*, 52, 961

Del Grosso, V.A., (1974) New equation for the speed of sound in natural waters (with comparisons to other equations). *J.Acoust.Soc.Am.*, 56, 1084

Dera, J., (1992) The transfer of mass, heat and momentum in the marine environment. In **Marine Physics**, PWN-Polish Scientific Publishers, Warszawa, Poland

Domenico, S.N., (1977) Elatic properties of unconsolidated porous sand reservoirs, *Geophysics*, 42, 1339

Duing, W (1970) **The monsoon regime of the currents in Indian Ocean.** East West Centre Press, Honolulu

Dunlop, J.I., (1992) measurement of acoustic attenuation in marine sediments by impedance tube. *J.Acoust.Soc.Am.*, 91, 460

Duykers, L.R.B., (1970) Relaxation in kaoline-water mixtures. *J.Acoust.Soc.Am.*, 47, 396

Elliott, A.J., Clarke, T. and Li, Z., (1991) Monthly distributions of surface and bottom temperatures in the northwest European shelf seas. *Continental Shelf Research*, 11, 453

Fofonoff, N.P. and Millard, Jr., R.C., (1984) Algorithms for computation of fundamental properties of sea water. *UNESCO Technical papers in marine science*, (Paris) 44, 46

Folk, R.C. and Ward, W.C., (1957) Brazos river bar: A study in significance of grain size parameters. *J. Sediment. Petrol.*, 27, 3

Frisk, G.V., (1995) A review of model inversion methods for infering geoacoustic properties in shallow water. In Full field inversion methods in ocean and seismoacoustics, Edited by Diachok et al., Kluwer Academic Publishers

Fu, S.S., Wilkens, R.H. and Frazer, L.N., (1996) Acoustic lance: New in-situ sea floor velocity profiler. *J. Acoust. Soc. Am.*, 99, 234

Gerard, R., Langseth Jr., M. G. and Ewing, M., (1962) Thermal gradient measurements in the water and bottom sediment of the western Atlantic. *J. Geophys. Res.*, 66, 589

Govem, J.M. and Ingram, G.D., (1979) Viscous attenuation of sound in saturated sand. *J.Acoust.Soc.Am.*, 66, 1807

Hall, M.V., (1996) Measurement of seabed sound speeds from head waves in shallow water, *IEEE J. Ocean Engg*, 21, 413

Hamilton, E.L., (1956) Low sound velocities in high-porosity sediments. *J.Acoust.Soc.Am., 28*, 16

Hamilton, E.L., (1963) Sediment sound velocity measurements made in situ from bathyscaphe Trieste. *J. Geophys. Res., 68*, 5991.

Hamilton, E.L., (1965) Sound speed and related properties of sediments from experimental Mohole (Guadalupe Site). *Geophysics,30*, 257

Hamilton, E.L., (1970a) Sound channels in surficial marine sediments. *J.Acoust.Soc.Am, 48,*1296

Hamilton, E.L., (1970b) Sound velocity and related properties of marine sediments, North Pacific. *J. Geophys. Res. 75*, 4423

Hamilton, E.L., (1971a) Elastic properties of marine sediments. *J. Geophys. Res. 76*, 579

Hamilton, E.L., (1971b) Prediction of *in situ* acoustic and elastic properties of marine sediments. *Geophysics* **36**, 266

Hamilton, E.L., (1972a) Sound attenuation in marine sediments, Research report, Naval Undersea Research and Development Center, San Diego, C.A

Hamilton, E.L., (1972b) Compressional wave attenuation in marine sediments. *Geophysics,* **37,** 620

Hamilton, E.L., (1974a) Prediction of deep-sea sediment properties: state of art. In **Deep-sea sediments, Physical and Mechanical Properties,** edited by A.L. Inderbitzen, Plenum, New York

Hamilton, E.L., (1974b) Geoacoustic models of the sea floor. In **Physics of Sound in Marine Sediments**, edited by L.Hampton,(Plennum Press, New York

Hamilton, E.L., (1976a) Sound attenuation as a function of depth in the sea floor. *J.Acoust.Soc.Am.59*, 528

Hamilton, E.L., (1976b) Attenuation of shear waves in marine sediments, *J.Acoust.Soc.Am,* **60,** 334

Hamilton, E.L., (1976c), Shear wave velocity versus depth in marine sediments: A review. *Geophysics,* **41,** 985

Hamilton, E.L., (1976d) Variations of density and porosity with depth in deep-sea sediments, *J.Sedim. Petrology,* **46,** 280

Hamilton, E.L., (1978a) Sound velocity-density relations in sea floor sediments and rocks. *J.Acoust.Soc.Am.,* **63,** 366

Hamilton, E.L., (1978b) Compressional wave attenuation in marine sediments. *Geophysics*, 37,620

Hamilton, E.L., (1979a) Vp/Vs and Poisson's ratios in marine sediments and rocks. *J.Acoust.Soc.Am*, 66, 1093

Hamilton, E.L., (1979b) Sound velocity gradients in marine sediments. *J.Acoust.Soc.Am*, 65, 909

Hamilton, E.L., (1980) Geoacoustic modeling of the sea floor. *J. Acoust. Soc. Am*, 68, 1313

Hamilton, E.L., (1985) Sound velocity as a function of depth in marine sediments. *J.Acoust.Soc.Am*, 78, 1348

Hamilton, E.L., Shumway, G., Menard, H.W. and Shipek. C.J., (1956) Acoustic and other physical properties of shallow water sediments off San Diego. *J. Acoust. Soc. Am*, 28, 1

Hamilton, E.L., Bucker,H.P., Keir, D.L. and Whitney, J.A., (1970) Velocities of compressional and shear waves in marine sediments determined *in situ* from a research submersible. *J. Geophys.Res.* 75, 4039

Hamilton, E.L., Batchman, R.T., Curray, J.R., and Moore, D.G., (1974) Sediment velocities from sonobuoys: Bay of Bengal, Bering Sea, Japan Sea, and North Pacific. *J. Geophys.Res.*, 79, 2653

Hamilton, E.L,. Moore, D.G., Buffington, E.C., Sherrer, P.L. and Curray, J.R., (1977) Sediment velocities from sonobuoys: Bengal Fan, Sunda Trench, Andaman Basin, and Nicobar Fan. *J. Geophys.Res.*, 82, 3003

Hamilton, E.L., Bachman, R.T., Curray, J.R. and Moore, D.G., (1977) Sediment velocities from sonobuoys: Bengal fan, Sunda trench, Andaman basin, and Nicobar fan. *J. Geophys. Res.* 82, 3003

Hamilton, E.L. and Bachman, R.T., (1982) Sound velocity and related properties of marine sediments. *J.Acoust.Soc.Am.*, 72, 1891

Hampton, L.D., (1985) Acoustic properties of sediments: An update. *Rev. Geophys.* 23, 49

Hareesh Kumar, P.V., (1994) Thermohaline Variability in the upper layers of the Arabian Sea. Ph. D Thesis, Cochin University of Science and Technology, Cochin, pp.109

Harker, A.H., Schofield, P., Stimpson, B.P., Taylor, R.G. and Temple, J.A.G., (1991) Ultrasonic propagation in slurries. *Ultrasonics*, 21, 427

Hashimi, N.H., Kidwai, R.M. and Nair, R.R., **(1978)** Grain-size & Coarse-fraction studies of sediments between Vengurla & Mangalore on the western continental shelf of India. *Ind. J. Mar.Sc,* **7,** 231

Hashimi, N.H., Kidwai, R.M. and Nair, R.R., **(1981)** Comparative study of the topography and sediments of the western & eastern continental shelves around Cape Comorin. *Ind. J. Mar.Sc,* **10,** 45

Hastenrath, S., and Lamb, P., **(1979)** Surface Climate and Atmospheric Circulation In **Climate Atlas of the Indian Ocean – Part I,** Wisconsin University Press, Madison

Haumeder, M.V., **(1986)** Low frequency anomalies in the reflection behavior of marine sediments. In **Ocean Seismo Acoustics,** Edited by Akal T, Berkson J.M, Plenum Press, New York

Holland, C.W. and Brunson, B.A., **(1988)** The Biot-Stoll sediment model: An experimental assessment. *J.Acoust.Soc.Am.* **84,** 1437

Hovem, J.M., **(1979)** The nonlinearity parameter of saturated marine sediments. *J.Acoust.Soc.Am,* **66,** 1463

Hovem, J.M., **(1980)** Attenuation of Sound in Marine Sediments. In **Bottom-interacting Ocean Acoustics,** Edited by Kuperman. W.A and Jensen F.B, Plenum Press, New York

Hovem, J.M. and Ingram, G.D. **(1979)** Viscous attenuation of sound in saturated sand. *J.Acoust.Soc.Am,* **66,** 1807

Jacobson, R.S., Slor Jr., G.G. and Dorman, L.M., **(1981)** Linear inversion of body wave data-Part II: Attenuation versus depth using spectral ratios. *Geophysics,* **46,** 152

Jacobson, R.S., Slor Jr., G.G. and Bee, M., **(1984)** A comparison of velocity and attenuation between the Nicobar and Bengal deep sea Fans. *Geophysics,* **89,** 6181

Johannessen, O.M., Subbaraju, G. and Blindheim, J., **(1981)** Seasonal variation of the oceanographic conditions off the west coast of India during 1971-75. *Fiskeri Dir. Skr. Ser.,* **18,** 247

Johnson, D. L. and Plona, T.J., **(1982)** Acoustic slow waves and the consolidation transition. *J.Acoust.Soc.Am* , **72,** 556

Johnston, D.H., Toksoz, M.N. and Timur, A., **(1979)** Attenuation of seismic waves in dry and saturated rocks, II. Mechanisms, *Geophysics,* **44,** 691

Joseph, P.V., **(1990)** Warmpool over the Indian Ocean and monsson onset. *Tropical Oceans Global Atmosheric Newsletter,* **53,** 1

Khadge, N.H., (1992) Geotechnical properties of deep sea sediments from Central Indian Ocean basin, *Ind. J. Mar.Sc* ,21, 80

Kibblewhite, A.C., (1989) Attenuation of sound in marine sediments; A review with emphasis on new low-frequency data. *J.Acoust.Soc.Am.*, **86**, 716

Kimuro, M. and Shimizu., (1989) A new method of simply measuring acoustic properties for marine sediments and basic experiments. *J.Acoust.Soc.Japan*, **45**, 274

Krumbein, W.C. and Pettijohn. F.J., (1938) In **Manual of sedimentary petrology,** Appleton Century Crafts, New York

Kudo, K. and Shima, E., (1970) Attenuation of shear waves in soil. **Bull. Earthquake Res. Inst.,** Univ. Tokyo, **48,** 145

LeBlanc, L.R., (1992) Acoustic characterization of marine sediments using a chirp sonar. *J.Acoust.Soc.Am*, 91, 106

LeBlanc, L.R., Panda, S. and Schock, S.G., (1992) Sonar attenuation modeling for classification of marine sediments. *J.Acoust.Soc.Am,* 91, 116

Leroy, C.C., (1969) Development of simple equations for accurate and most realistic calculation of the speed of sound in sea water. *J.Acoust.Soc.Am,,* 46, 216

Leroy, C.C., Daupleix, J.M. and Longuemard., (1986) Relationship between the acoustical characteristics of deep sea sediments and their physical environment. In **Ocean Seismo-Acoustics,** Edited by Akal, T. and Berkson, J.M.., Plenum Press, New York

Leurer, K. C., (1997) Attenuation in fine-grained marine sediments: extension of the Biot-Stoll model by the "effective grain model" (EGM). *J.Acoust.Soc.Am*, 62,1465

Levitus, S., (1982) Climatological Atlas of the World Ocean. US Government Printing Office, Washington DC

Mackenzie, K.V., (1981) Nine-term equation for sound speed in the oceans. *J.Acoust.Soc.Am,,* **70,** 807

Mathew, B., (1983) Studies on upwelling and sinking in the seas around India. Ph. D Thesis, University of Cochin, pp159.

Mathews, J.E., (1980) Heuristic physical property model for marine sediments. *J.Acoust.Soc.Am*, **68,** 1361

McCann, C., (1969) Compressional wave attenuation in concentrated clay suspensions. *Acoustica*, **22,** 352

McCann, C. and McCann, D.M., (1969) The attenuation of compressional waves in marine sediments. *Geophysics*, **34**, 882

McCann, C. and McCann, D.M., (1985) A theory of compressional wave attenuation in noncohosive sediments. *Geophysics*, **50**, 1311

McDonal, F.J., Angona, F.A., Mills, R.L., Sengbush, Van Nostrand, R.G. and White, J.E., (1958) Attenuation of shear and compressional waves in Pierre Shale. *Geophysics*, **23**, 421

McLeroy, E.G. and DeLoach, A., (1968) Sound speed and attenuation from 15 to 1500kHz, measured in natural sea floor sediments. *J.Acoust.Soc.Am*, **44**, 1148

Medwin, H., (1975) Speed of sound in water: A simple equation for realistic parameters. *J.Acoust.Soc.Am.*, **58**, 1318

Millero, F.J. and Poisson, A., (1981) International one-atmopshere equationof the state of sea water. *Deep-Sea Research*, **28A**, 625.

Mitchell, J.K., (1976) In **Fundamentals of Soil Behaviour**, A Wiley-interscience publication, New York

Mitchell, S.K. and Focke, K.C., (1980) New measurements of compressional wave attenuation in deep ocean sediments. *J.Acoust.Soc.Am*, **67**, 1582

Mitchell, S.K. and Focke, K.C., (1983) The role of seabed attenuation profile in shallow water acoustic propagation. *J.Acoust.Soc.Am*, **73**, 466

Mohan, M., (1985) Geohistory analysis of Bombay High region, *Marine and Petroleum Geology*, 2,350

Monin, A.S., Kamenkovich, V.M. and Kort, V.G., (1977) In **Variability of the oceans**. A Wiley-interscience publication, New York

Morrton, R.W., (1975) Sound velocity in carbonate sediments from the Whiting basin, Puerto-Rico. *Marine Geology*, **19**, 1

Murty, G.R.K. and Pradeep Kumar, T., (1986) Geoacoustic modelling of the continental shelf off Bombay. *Research report*-7/86

Murty, G.R.K. and Pradeep Kumar, T., (1987) Acoustic reflectivity characteristics of sediments of the continental shelf off Visakhapatnam. *J. Acoust. Soc. Ind*, NSA-87

Murty, G.R.K. and Muni, M.M., (1987) A study of some physical properties of sediments of the backwaters and the adjoining continental shelf off Cochin, India. *Marine Geology*, **77**, 121.

Murty, G.R.K. and Pradeep Kumar, T., (1988) Influence of variable bottom sediment characteristics on shallow water sound propagation. *J. Acoust. Soc. Ind.,* **XVI**, 316

Murty, G.R.K. and Pradeep Kumar, T., (1989) Biot-Stoll sediment model - an experimental assessment for predicting compressional sound speed in sediments. *J. Acoust. Soc. Ind.,* **XVII**, 222

Murty, G.R.K. and Pradeep Kumar, T., (1990) On the applicability of sound speed models to marine sediments of the continental shelf off Cochin: An experimental assessment. *J. Acoust. Soc. Ind.,* **XVIII**, 92

Murty, G.R.K. and Naithani, S., (1996) Effect of sound speed gradients of sediments on bottom reflection loss and caustics- a case study. *J. Acoust. Soc. Ind.,* **XXIV**, I-10.1

Murty, K.R.G.K., Murty, G.R.K., and Muni, M.M., (1984) Marine geoacoustic studies on the continental shelf off Cochin. *Research Report-7/84.*

Murty, P.G.K., (1986) Studies on thermal structure in the seas around India. Ph. D Thesis, Cochin University of Science and Technology, Cochin, pp.100

Muthukrishniah, K., Reji, Z., Murty, G.R.K. and Nair, P.V., (1995) Relationship between geophysical and geotecechnical properties of marine sediments using Biot-Stoll model. *Marine Georesources and Geotechnology,* **13**, 243

Nafe, J.E. and Drake, C.L., (1957) Variation with depth in shallow and deep water marine sediments of porosity, density and the velocities of compressional and shear waves. *Geophysics,* **22**, 523

Nafe, J.E. and Drake, C.L., (1963) Physical properties of marine sediments. In **The sea,** Interscience Publishers, New York

Nair, R.R. and Pylee, A., (1968) Size distribution and carbonate content of the sediments of the western shelf of India. *Bull. National Institute of Sciences,* India, **38**, 411

Null, J.M., Bourke, R.H. and Wilson, J.H., (1996) Perturbative inversion of geoacoustic parameters in a shallow water environment. *IEEE J. Oceanic Eng.,* **21**, 480

Nobes, D.C., (1989) A test of a simple model of the acoustic velocity in marine sediments. *J.Acoust.Soc.Am,* **86**, 290

Noble, A., (1968) Studies on sea water off the north Canara coast. *Jour. of Mar. Bio. Assn. India,* **10**, 197

Ogushwitz, P.R., (1985a) Applicability of Biot theory. I Low-porosity materials. *J.Acoust.Soc.Am.,* **77**, 429

Ogushwitz, P.R., (1985b) Applicability of Biot theory. II. Suspensions. ,J.Acoust.Soc.Am., 77, 441

Ogushwitz, P.R., (1985c) Applicability of Biot theory. III. Wave speeds versus depth in marine sediments. J.Acoust.Soc.Am, 77, 453

Orsi, T.H., Dunn, D.A., (1990) Sound velocity and related physical properties of fine-grained abyssal sediments from the Brazil basin (South Atlantic Ocean). J.Acoust.Soc.Am, 88, 1536

Owen, T.E. and Pantermuhl, P.J., (1990) A new seismo acoustic probe for sea bed measurements, In Ocean Technology Conference (OTC-6233).

Pankajakshan, T. and Ramaraju, D.V., (1987) Intrusion of Bay of Bengal waters into Arabian Sea along the west coast of India during north east monsoon. In Contributions in marine sciences (Dr. S.Z.Qasm's 60th birthday felicitation volume)

Paropakari, A.L., (1979) Distribution of organic carbon in sediments of the North Western continental shelf India. Indian J Mar.Sci., 8,127

Patil, M.R., Ramamithram, C.P., Varma, P.U., Nair, C.P. and Myrland., (1964) Hydrography of the west coast of India during the pre-monsoon period of the year 1962. Part I – Shelf waters of Maharashtra and southwest Sourashtra coasts. Jour. of Mar. Bio. Assn. India, 6, 151.

Pillai, N.V., Vijayarajan, P.K. and Nandakumar, A., (1980) Oceanographic investigations off the southwest coast of India. FAO/UNDP Report, FAO, Rome

Pond, S. and Pickard, G.L., (1986) In Introductory dynanical oceanography, Pergamon press, Great Britain, pp329.

Pradeeep Kumar, T., (1997) Seasonal variation of relaxation time and attenuation in sediment at the sea bottom interface. Acustica, 83, 461

Pradeep Kumar, T. and Murty, G.R.K., (1993) The effect of seasonal variation of temperature on compressional sound speed at the water/sediment interface and bottom raflection loss. J.Pure and Applied Ultrasonics, 15, 64

Prasanna Kumar, S. and Prasad, T.G (1999) Formation and spreading of Arabian Sea high-salinity water mass. J. Geophys. Res., 104, 1455

Rajan, S.D., Lynch, J.F. and Frisk, G.V., (1987) Perturbative inversion methods for obtaining bottom geoacoustic parameters in shallow water. J.Acoust.Soc.Am, 82, 998

Rajan, S.D. and Frisk, G.V., (1991) The effect of seasonal temperature fluctuations in the water column on sediment compressional wave speed profiles in shallow water. In

Ocean Variability & Acoustic Propagation. Edited by Potter J and Warn-Varnas A, Kluwer Academic Publishers, Netherlands

Rajan, S.D. and Frisk, G.V., (1992) Seasonal variation of the sediment compressional wave speed profile in the Gulf of Mexico. *J.Acoust.Soc.Am*, **91**, 127

Rajan, S.D., (1992) Determination of geoacoustic parameters of the ocean bottom-Data requirements. *J. Acoust. Soc. Am.*, **92**, 2126

Ramamirtham, C.P. and Jayaraman, R., (1960) Hydrographic features of the continental shelf waters off Cochin during the years 1958-59. *Jour. Mar. Bio. Assn. India*, **2**, 155

Ramamurty, S,. (1963) Studies on the hydrological factors in the North Kanara coastal waters. *Ind. Jour. Fisheries*, **10**, 79.

Ramasastry, A.A. and Myrland, P., (1959) Distribution of temperature, salinity and density in the Arabian Sea along the South Malabar Coast (South India) during the post-monsoon season. *Indian Jour. of Fisheries*, **6**, 223

Ratcliffe, E.H., (1960) The thermal conductivity of ocean sediments. *J.Geophys.Res.*, **65**, 1535

Richardson, M.D., Young, D.K. and Briggs, K.B., (1983) Effects of hydrodynamic and biological processes on sediment geoacoustic properties in Long Island Sound, USA. *Mar. Geol.* **52**, 201

Richardson, M.D., (1986) Spatial variability of surficial shallow water sediment geoacoustic properties. In **Ocean Seismo-Acoustics**, Edited by Akal T and Berkson JM, Plenum Press, New York

Schreiber, B.C., (1960) Sound velocities in deep sea sediments by a resonance method. *Geophysics* -- Part 1, **25**, 451

Schreiber, B.C., (1968) Sound velocities in deep sea sediments. *J. Geophys. Res.*, **73**, 1259

Schulthesiss, P.J., (1981) Simullaneous measurement of P and S wave velocities during conventional laboratory sediment testing procedure. *Marine Geotechnology*, **4**, 343

Sclater, J.G., Corry, C.E. and Vacquer, V., (1969) *In situ* measurement of the thermal conductivity of ocean floor sediments. *J.Geophys.Res.* **74**, 1070

Sharma, G.S., (1966) Thermocline as an indicator of upwelling. *Jour. Mar. Bio. Assn. of India*, **3**, 8

Sharma, G.S., (1968) Seasonal variation of some hydrographic properties of the shelf water off west coast of India. *Bulletin of National Institue of Sciences*, **38**, 263

Sharma, G.S., (1978) Upwelling off the southwest coast of India. *Ind. Jour. Mar. Sc.*, **7**, 207

Shetye, S.R., Shenoi, S. S.C., Gouveia, A.D., Michael, G.S., Sundar, D. and Nampoothiri. G., (1991) Wind-driven upwelling along the western boundary of the Bay of Bengal during the southwest monsoon. *Continental shelf Research*, **11**, 1397

Shetye, S.R., Gouveia, A.D., Shenoi, S. S.C., Sundar, D., Michael, G.S., Almeida, A.M. and Santanam. K., (1990) Hydrography and circulation off the west coast of India during the Southwest Monsoon 1987. *Jour. Mar. Res.*, **48**, 359

Shirley, D. J, and Anderson, A.L., (1975) *In situ* measurement of marine acoustical properties during coring in deep water. *IEEE Transactions on Geoscience Electronics*, **4**,163

Shumway, G., (1958) Sound velocity vs temperature in water-saturated sediments. *Geophysics*, **23**,494

Shumway, G., (1960a) Sound speed and absorption studies of marine sediments by a resonance method. Part 1. *Geophysics*, **25**, 451

Shumway, G., (1960b) Sound speed and absorption studies of marine sediments by a resonance method. Part 1. *Geophysics*, **25**, 659

Smith, D.T., (1986) Geotechnical characteristics of the sea bed related to seismo-acoustics. In **Ocean Seismo-Acoustics**, Edited by Akal.T and Berkson.J.M., Plenum press, New York

Spiesberger, J.L. and Metzger, K., (1991) New estimates of sound speed in water. *J.Acoust.Soc.Am.,*_89, 1697

Stoll, R.D. and Bryan, G.M., (1970) Wave attenuation in saturated sediments. *J.Acoust.Soc.Am.*,47, 1440

Stoll, R.D., (1974) Acoustic waves in saturated sediment. In **Physics of Sound in Marine Sediments**, edited by L.Hampton (Plennum, New York

Stoll, R.D., (1977) Acoustic waves in ocean sediments. *Geophysics*, **42**, 715

Stoll, R.D., (1978) Experimental studies of attenuation in sediments. *J.Acoust.Soc.Am*, **64**, 5143(A)

Stoll, R.D., (1979) Experimental studies of attenuation in sediments. *J.Acoust.Soc.Am*, **66**, 1152

Stoll, R.D., (1980) Theoretical aspects of sound transmission in sediments. *J.Acoust.Soc.Am*, **68**, 1341

Stoll, R.D., (1985) Marine sediment acoustics. *J.Acoust.Soc.Am*, **77**, 1789

Stoll, R.D., Bryan, G.M., and Bautista, E., (1994) Measuring lateral variability of sediment geoacoustic properties. *J.Acoust.Soc.Am*, **96**, 427

Stoll, R.D., Bautista, E., and Flood, R., (1994) New tools for studying seafloor geotechnical and geoacoustic properties. *J.Acoust.Soc.Am*, **96**, 2937

Sutton, G.H., Berchemer, H. and Nafe, J.E., (1957) Physical analysis of deep-sea sediments. *Geophysics*, **22**, 779

Sverdrup, H.U., Johnson, M.W. and Fleming, R.H., (1942) The oceans; their physics, chemistry and general biology, Prentice-Hall, Englewood Cliffs, NJ

Thomas, P.R. and Pace, N.G., (1980) Broad band measurement of acoustic attenuation in water-saturated sands. *Ultrasonics*, **18**,13

Toksoz, M.N., Johnston, D.H. and Timur, A., (1979) Attenuation of seismic waves in dry and saturated rocks, 1. Laboratory measurements, *Geophysics*, **44**, 681

Tucholke, B.E. and Shirley, D.J., (1979) Comparison of Laboratory and *in situ* compressional wave velocity measurements on sediment cores from the western north Atlantic. *J. Geophys. Res.*, **84**, 687

Tucholke, B.E., (1980) Acoustic envirinment of the Hatteras and Nares Abyssal plains, Western North Atlantic Ocean, determined from velocity and physical properties of cores. *J.Acoust.Soc.Am*, **68**, 1376

Tosaya, C and Nur, A., (1982) Effects of diagenesis and clays on compressional velocities in rocks. Res. Letter, *Geophysics*, **9**, 5

Tullos and Reid., (1969) Seismic attenuation in Gulf coast sediments. *Geophysics*, **34**, 516

Han, D. and Nur, A, and Morgan, D., (1986) Effects of porosity and clay content on wave velocities in sand stones. *Geophysics*, **51**, 2093

Turgut, A. and Yamamoto, T., (1990) Measurements of acoustic wave velocoties and acoustic attenuation in marine sediments. *J.Acoust.Soc.Am* **87**, 2376

Urick, R.J., (1948) The absorption of sound in suspensions of irregular particles. *J.Acoust.Soc.Am*, **20**, 283

Urick, R.J., (1982) In Sound propagation in the sea. Peninsula Publishing, California

Uscinski, B.J., Macaskill, C. and Ewart, T.E., (1983) Intensity fluctuations, Part I: theory, Part II: comparison with the Cobb experiment. *J.Acoust.Soc.Am*,74, 1474

Venkateswarlu, P.D., Chatterjia, P., Sengupta, B.J., Brahmam, C.V. and Kar, Y.C., (1989) Shallow seismic investigations for placer minerals off Gopalpur (Orissa), east coast of India. *Ind. J. Mar.Sc*, 18, 134

Vidmar, P.J. and Foreman, T.L., (1979) A plane wave reflection loss model including sediment rigidity, *J.Acoust.Soc.Am*, 66, 1830

Wilson, W.D., (1960) Equation for the speed of sound in sea water. *J.Acoust.Soc.Am*, 32, 1357

Wingham, D.J., (1985) The dispersion of sound in sediments. *J.Acoust.Soc.Am*, 78, 1757

Winkler, K.W. and Nur, A., (1982) Seismic attenuation: Effects of pore fluids and frictional sliding. *Geophysics*, 47, 1

Wood, A.B., (1941) A Textbook of Sound, MacMillan, NewYork

Wood, A.B. and Weston, D.E., (1964) The propagation of sound in mud. *J.Acoust.Soc.Am*, 14, 156

Wyrtki, K., (1971) Oceanographic Atlas of the International Indian Ocean Expedition, US Government Printing Office, Washington DC

Wyllie, M.R.J., Gregory, H.R. and Gardner., (1956) Elastic waves in heterogeneous and porous media. *Geophysics*, 21, 41

Yamamoto, T., (1995) Velocity variabilities and other physical properties of marine sediments measured by crosswell acoustic tomography, *J.Acoust.Soc.Am*, 98, 2235

Yamamoto, T., (1996) Acoustic scattering in the ocean from velocity and density fluctuations in the sediments. *J.Acoust.Soc.Am*, 99,866

Zhang, S. and Yang, T.M.A.Z., (1999) Geoacoustic model and acoustic reflection properties of fluid mud layer in Changjiang estuary and Hangzhou Bay. *Chinese Journal of Acoustics*, 18, 1

Zhou. J., Zhang, X. and Rogers, P.H., (1987) Effect of frequency dependence of sea-bottom attenuation of the optimum frequency for acoustic propagation in shallow water. *J.Acoust.Soc.Am*, 82, 287